Environment Canada | Environnement Canada

Acoustic Measurement of Sediment Transport

C.K. Jonys

SCIENTIFIC SERIES NO. 66
(Résumé en français)

INLAND WATERS DIRECTORATE,
CCIW BRANCH,
BURLINGTON, ONTARIO, 1976.

Environment Canada
Environnement Canada

Acoustic Measurement of Sediment Transport

C.K. Jonys*

*Dr. Jonys is no longer with the Department of Fisheries and the Environment.

SCIENTIFIC SERIES NO. 66
(Résumé en français)

INLAND WATERS DIRECTORATE,
CCIW BRANCH,
BURLINGTON, ONTARIO, 1976.

Cat. No. En: 36-502/66

ISBN 0-662-00474-4

Contract No. 07KX.KL210-6-4526
THORN PRESS LIMITED

Contents

Contents (cont.)

Tables

Illustrations

Illustrations (cont.)

Illustrations (cont.)

Abstract

This report combines three studies on the acoustic method of sediment bed-load measurement in gravel-bearing rivers. The results of laboratory work, a theoretical feasibility study and a summary of the observations and analysis of a field investigation program are presented.

Laboratory experiments were carried out to verify some acoustical aspects of impact noise in water for application in the development of a theoretical relationship between the noise generated by riverbed pebble collisions and bed-load transport rates. Underwater pebble noise was simulated by rolling ceramic balls on a bed of similar balls in a large laboratory flume. Sound was measured with a stationary hydrophone located in the water above the pebble bed.

Specific information was obtained on the interparticle collision frequency delineating the limit of transition from impact to continuous type of sound; the applicability of theoretical relationship in the determination of total sound pressure levels owing to impact sources; the acoustic directivity of pebble collision noise; the sound field characteristics surrounding pebble collision sources; the effect of pebble velocity on the generated sound pressure level; and the spectrum characteristics of the pebble collision generated noise.

An idealized relationship is formulated between the rate of bed-load transport and the sound pressure level which is generated by interparticle collisions and measured with an omnidirectional hydrophone located at a finite distance above the riverbed. The transfer function shows the rate of bed-load transport to be dependent not only on the observed sound pressure level but also on at least six other variables that must be determined independently of the acoustic observations.

In field experiments, underwater sound samples were recorded in two gravel-bearing rivers during periods with and without bed-load movement. Also, samples of artificially generated interparticle collision noise by different sizes of gravel pebbles were recorded. Flow velocities and bed-load transport were measured as well. The purpose of the observations was to obtain field data for the study of the feasibility of the acoustic method for bed-load measurement.

The sound samples recorded in the field were analyzed for pressure spectrum in one-third octave or one-octave bands between frequencies from 50 Hz to 30 kHz. The pressure spectra exhibited no distinguishing features for positive identification of pebble collision generated noise. The absence of the gravel noise component in the spectra was attributed to masking by high levels of background noise owing to turbulence below 500 Hz, and water droplets and air bubble sources above 500 Hz.

Résumé

Le présent rapport comprend trois études sur une méthode acoustique de mesure du charriage des sédiments dans des rivières porteuses de gravier. Il fournit les résultats des expériences effectuées en laboratoire, une étude des possibilités théoriques d'application de la méthode et un aperçu des observations et des analyses faites dans le cadre d'un programme de mesures sur le terrain.

On a effectué des expériences de laboratoire dans le but de vérifier certains aspects d'ordre acoustique du bruit engendré par les chocs dans l'eau, et de pouvoir ainsi établir une relation théorique entre le bruit produit par les collisions de galets du fond d'une rivière et les débits de charriage. Ces bruits sous l'eau ont été simulés à l'aide de billes en céramique roulant sur un lit de billes semblables dans un grand canal vitré de laboratoire. Le son a été mesuré à l'aide d'un hydrophone immobile placé dans l'eau, au-dessus du lit de galets.

On a ainsi obtenu des informations particulières sur la fréquence des collisions de particules limitant la zone de transition entre le type de son dû à un choc et le son continu; sur la possibilité d'utiliser la relation théorique pour déterminer les niveaux de pression sonore totaux engendrés par les collisions; sur la directivité acoustique du bruit produit par les collisions entre galets; sur les caractéristiques du champ sonore entourant les sources de ces collisions; sur l'effet que la vitesse des galets exerce sur le niveau de pression sonore engendré par ces collisions; et sur les caractéristiques spectrales du bruit engendré par les collisions entre galets.

Une relation idéale est établie entre le débit de charriage et le niveau de pression sonore produit par les collisions entre particules et mesuré à l'aide d'un hydrophone omnidirectionnel placé à une distance donnée au-dessus du lit de la rivière. La fonction de transfert montre que le débit de charriage dépend non seulement du niveau de pression sonore observé, mais aussi d'au moins six autres variables qui doivent être déterminées indépendamment des observations acoustiques.

Lors des mesures sur le terrain, on a enregistré des échantillons de sons produits sous l'eau dans deux rivières porteuses de gravier, au cours de périodes avec et sans charriage, ainsi que des échantillons de bruits dus à des collisions entre particules engendrées artificiellement par des galets de dimensions différentes. On a également mesuré la vitesse d'écoulement et le débit de charriage. Le but de ces mesures était d'obtenir sur le terrain des données qui permettent d'étudier la possibilité d'appliquer la méthode acoustique de mesure du charriage.

On a analysé des échantillons sonores enregistrés sur le terrain pour le spectre des pressions situées dans des bandes de fréquences d'un-tiers d'octave ou d'une octave s'étalant de 50 Hz à 30 kHz. Les spectres de pressions ainsi obtenus n'ont révélé aucune caractéristique qui permette d'identifier de façon certaine le bruit engendré par les collisions entre galets. L'absence dans les spectres d'une composante des bruits dus aux galets, a été attribuée à un phénomène de masquage par des bruits de fond de hauts niveaux imputables à une turbulence en dessous de 500 Hz et, à des sources sonores produites par des gouttelettes d'eau et des bulles d'air au-dessus de 500 Hz.

CHAPTER 1

Laboratory Experiments

INTRODUCTION

Background

A variety of techniques has been developed for routine sediment transport measurements and has provided much useful engineering information. The accuracy of these methods, however, has seldom been adequate, and new techniques have continually been sought to improve the reliability of these measurements. The measurement of gravel transport rates is especially difficult because gravel is transported at high flow velocities only and moves intermittently in time and space.

In the search for better bed-load measurement methods, it has been recognized that the sound generated by moving particle collisions might serve as a parameter indicative of bed-load transport rates. The acoustic concept for bed-load measurement appears to have originated with Mühlhoffer (1933). Since that time numerous other attempts to measure bed load with hydrophones have been made, which are described by Bradeau (1951), Juniet (1952), Smoltczyk (1955), and Bedeus and Ivicsics (1963). Recently, Johnson and Muir (1969) carried out a laboratory study and concluded that "interparticle collision sound could yield continuous measurement of coarse sediment particles moving as bed-load."

Attempts to use the hydrophone for bed-load measurement in Canada are reported by Hollingshead (1969, 1971) and Samide (1971). Only limited success was achieved. The instrument used assisted in the qualitative recognition of the beginning of the movement of bed particles, but was incapable of yielding quantitative transport information.

Activities to adapt the hydrophone technique as a standard sediment measurement instrument were initiated by the Sediment Survey Section, Water Survey of Canada, Department of the Environment, in 1971. A hydrophone system was acquired and tests were carried out in a towing tank by Tywoniuk (1971). Field observations were carried out also by Tywoniuk and Warnock (1973) during the 1972 spring runoff.

None of the past attempts to adapt the acoustic approach for practical bed-load measurement was successful. All were limited in scope and instrumentation, and their results were inconclusive. Some of the difficulties occurred because the feasibility of the method had never been systematically explored.

The research development program undertaken at Canada Centre for Inland Waters investigated the feasibility of hydrophone measurement of bed-load transport. It consisted of instrument development and laboratory, theoretical and field studies. The results of the experimental investigation carried out in the laboratory are presented in this Chapter. The results of the theoretical and field study parts of the general investigation are covered in Chapters 2 and 3. The instrument development work is summarized by White (1975).

General Considerations

The development of an acoustic technique for bed-load measurement can be approached from several directions. These can be distinguished by the parameters chosen to represent the information on the sound produced by the sediments; the methods of measurement employed to obtain the acoustic information; and the techniques of analysis and interpretation of this information.

Throughout this investigation, it was considered that the sound parameter most indicative of the movement of sediments is the acoustic power of the noise produced by the riverbed pebble collisions. The acoustic power of a collision source depends to a great degree on the force of impact that generates it. Because this force is related to the momentum of the moving pebbles, it depends on their mass and velocity. But the rate of sediment transport is also a function of the mass and velocity of the particles and therefore must be related, in some way, to the acoustic power of the noise which the particle collisions make.

The determination of the acoustic power radiated by a source is very difficult. Even when a source produces continuous sound its acoustic power cannot be measured directly, but must be estimated from measurements of sound pressure levels (SPL) considering also the acoustics of the environment in which the measurements are made.

To date, no attempts have been made to measure the acoustic power of moving riverbed pebbles, mostly because of the presence of a number of complicating factors affecting the observations and analysis of acoustic information in natural rivers. The collision of two pebbles generates sound which exhibits transient characteristics and differs from continuous sound. The interparticle collisions can occur over large areas of the riverbed and simultaneously produce sound at many locations and at different distances from an observation point. The power generated by the collisions differs because of natural variations in particle sizes, their mechanical properties and impact velocities. The power transmitted from collision positions to the observation hydrophone may be affected by the directivity characteristics of the pebble. In addition, high levels of background noise may exist in a river which can mask the sound generated by the bed pebbles.

To provide a model for the assessment of the feasibility of the acoustic concept for bed-load measurement and to provide guidance for the development of a practical measurement technique, an attempt was made to establish a theoretical relationship between a readily measurable sound parameter and the bed-load discharge. The basis of the model development was the measurement of sound pressure levels at a finite distance from the riverbed with a non-directional hydrophone.

In the development of the model, generally accepted acoustic theories were employed. Because of the uniqueness of the underwater environment and the proximity of the observation hydrophone to the source, however, some assumptions related to the nature of the pebble sound and its behaviour in water had to be verified experimentally. The results of the laboratory experiments carried out in support of the theoretical study of the acoustic bed-load measurement approach are presented in this Chapter.

Objectives and Scope

The specific objectives of the experiments were the following:

1) to observe the variation of sound pressure levels with the number of rolling pebbles,
2) to determine the minimum frequency of interparticle collisions for the pebble-generated sound to be continuous,
3) to verify the applicability of accepted continuous sound analysis principles for estimating sound pressure levels owing to multiple collision sources,
4) to investigate the effect of the velocity of rolling pebbles on the sound level produced by impact with stationary bed pebbles,
5) to determine the extent and characteristics of the acoustic fields above a bed of sound-generating pebbles in water,
6) to obtain information on the acoustic directivity of the sound-radiating pebbles, and
7) to measure the spectrum of the sound generated by rolling pebbles.

The laboratory work was limited in scope and was carried out under ideal conditions. All experiments were performed in still water, and gravel noise was simulated by gravity-induced movement of pebbles. No attempt was made to verify the applicability of the laboratory results to natural rivers. It was assumed, however, that the acoustic factors investigated were relatively independent of the environmental factors so that the experimental results would be valid under both ideal and natural conditions.

THEORETICAL BACKGROUND

Sediment-Generated Sound

Although acoustic measurement of bed-load transport was suggested at least 40 years ago, Johnson and Muir were the first to make quantitative observations of bed-load generated sound in a laboratory flume. Their results showed that a relationship between the noise and the sediment discharge existed only in the lower range of sediment transport rates, and that the hydrophone signal became insensitive to additional increases in bed-load discharge as the rates of transport increased.

There may be several reasons for the noise saturation tendency with increasing bed-load discharges. Among these is the possible reduction of acoustic power generated by the interparticle collisions. At higher velocities, when particle saltation occurs, the trajectory of the particle paths becomes elongated and their angles of collision with the stationary bed are decreased, reducing the change of particle momentum upon collision. Because momentum changes determine the force of collision, the impact-generated acoustic power is also reduced.

The occurrence of saltation of the moving particles can also decrease the number of interparticle collisions. In the limit, when all moving sediments are suspended by the flow and collisions with the stationary bed do not occur, no sound is generated at all.

A reexamination of the experimental results presented by Johnson and Muir indicated that the loss of acoustic sensitivity with increasing sediment discharge rates may also be due to the multiple sound source effect. Although the acoustic data reported by the authors were given in terms of electrical output of their measurement system and not in the accepted acoustic units, it was determined from their results that the average microphone output increased by a constant for each doubling of the measured rate of bed-load transport. If doubling of the transport rate is assumed to double the number of sound sources, the observation agrees with theoretical results obtained when the number of sound sources is doubled. As shown by Beranek (1971), if more than one source contributes to the total sound at a point, the total rms pressure p for continuous sound tones of different frequencies is given by

$$p = \sqrt{p_1^2 + p_2^2 + p_3^2 + \ldots p_n^2} \tag{1}$$

where p_1, p_2 and p_n are the rms magnitudes of the pressures contributed by the individual sources. When all sources produce equal p_i at a point the relationship can also be expressed as

$$SPL = SPL_1 + 10 \log n \tag{2}$$

where SPL[1] represents the sound pressure level in decibels owing to n sources when each source contributes a sound pressure level of SPL_1. Equation (2) indicates that as the number of sources increases, the increment in SPL owing to the addition of each new source decreases, and that doubling of the number of sources increases the SPL by a constant 3 dB regardless of the initial number of sources.

The sound generated by the collisions of two gravel pebbles, as illustrated in Figure 1, possesses highly transient characteristics. It can influence the acoustic determination of bed load because the measurement and analysis of impulsive sounds differ from those for continuous sound.

In the measurement of bed load each pebble collision constitutes a pulse source, and the frequency of collisions, or the number of sources, is one of the parameters related to the sediment discharge. If the pebble-generated sound is continuous it should be possible, in principle and under certain conditions, to determine the frequency of collisions from theoretical considerations. This may not be possible, however, throughout the full range of collision frequency values. As indicated by Beranek, impulsively generated sound in air exhibits quasi-steady characteristics and may be considered as continuous only if the frequency of impulses exceeds 10 Hz. In water, this limiting frequency value has not been determined.

Sound Fields and Source Directivity

The existing methods to determine acoustic power of an individual sound source are of two categories and depend on the sound field at the location of SPL observations. The sound fields vary with distance from the source and are affected by the nature of the enclosure around the source.

Generally, three distinct acoustic fields, illustrated in Figure 2, are associated with a sound source. In the near field, which is immediately adjacent to the source, the SPL exhibits large variations because fluid particle velocities have tangential components relative to the direction of the pressure wave travel. In the free field part of the far field, the SPL decreases by 6 dB for each doubling of the range from the source. In the reverberant field, sound waves that are reflected from the boundaries of an enclosure are superimposed on the incident waves from the source, and the SPL again exhibits large variations.

---

[1] By definition $SPL = 20 \log \frac{p}{p_o}$ in dB, where p = rms sound pressure and p_o = reference pressure of 1 μbar.

The role of the sound fields in the measurement of bed-load noise is twofold. First, only the incident sound waves, arriving directly from the sources to the observation point in the flow, can be considered in the theoretical determination of the total SPL owing to the individual pebble collisions. This requires that no contributions originate from the reflected waves and, therefore, is possible only if the observation point is in the far field part of the free field. Secondly, because of wave divergence, identification of near-bed sound sources and, hence, of the pebble noise should be possible by SPL observations at different distances from the bed.

The extent of the different sound fields in rivers is not known. For example, it is not known if the reverberant field owing to the pebble noise is affected by the proximity of the free surface, which provides an excellent reflective boundary.

The acoustic directivity of a source describes the spatial distribution of the energy radiated by the source and can greatly affect the measurement of the acoustic power which a sound source generates. A directive source emits the acoustic energy into one or more specific directions. To determine the acoustic power of such a source, observations of SPL are required at a number of positions in the surrounding space. A non-directive source, on the other hand, radiates the acoustic energy uniformly into the space which surrounds it, and the power of the source can be determined from a single observation of SPL at a known distance from the source.

In principle, the directivities of individual riverbed pebbles influence the observed SPL at any position in the flow. It is most likely that their directivities will be random, however, in which case their individual effects would be impossible to assess. In the development of the theoretical model of bed-load transport, it was therefore considered that particle directivity would not be important if it could be shown that either the individual particles are non-directive and radiate the acoustic energy hemispherically above the bed or that the random directivities of individual pebbles, because of their numbers, are statistically averaged and produce an equivalent uniform directivity.

Background Noise

The background noise present in river water is a key factor in determining the feasibility of the acoustic bed-load measurement technique because it has the potential to mask the pebble-generated noise.

The effects of background noise in the measurement of pebble-generated noise in rivers are illustrated in Figure 3. Range r represents the distance of the observation point from the riverbed when the total depth of flow is d. Background noise level variations are represented by curves B_1 and B_2, and curve S, taken from Figure 2, is

the level of sound generated by the source-pebble collisions. Curves B_1 and S intersect at r_1, and the background noise masks the source sound when the range exceeds r_1. Curves B_2 and S intersect at r_2 and show that the observation range in the free field is limited by the reverberation field at r and not by the background noise. Obviously, measurement of SPL owing to riverbed pebbles is possible only in the ranges between r_n and r_1 if B_1 is present, or between r_n and r_r if B_2 is present.

A number of independent sound sources contributing to the background noise in oceans have been identified by Wentz (1962). On the basis of a classification presented by Urick (1967), various possible sound sources in rivers with gravel transport are listed in a chart in Figure 4. Not all of the sources identified on the chart, however, may be contributing to the observed sound at any time or location, and the contributions of individual sources may differ greatly, with one or two sources dominating and masking the effects of all the others.

A component of the background noise that is always present is the noise of the equipment used in the acoustic measurements. It determines the minimum value of noise which can be detected by the instrument and limits noise observations to levels above this value.

The most probable background noise sources are the ambient and the platform noise components owing to turbulence and bubbles in the flow, surface splash and possibly the impact of the suspended sediment particles on the hydrophone sensor. The propulsion machinery noise can occur if observations are made from a ship whose engines are used to maintain stationary position in the flow.

The sources of background noise least likely to contribute to the noise level in a gravel-transporting river are the thermal, wave, biological and man-made components of the ambient noise. Generally, thermal noise levels are very low relative to other sources. Wave-produced noise has frequencies below those of interest, and it is unlikely that biological sources could exist in the violent flow of a stream. Also, precipitation noise can be observed only during rainfall periods.

The identity and characteristics of background noise sources are of interest because they provide information for minimizing their effects on the identification and measurement of pebble-generated sound. For example, it may be found that a high level of sound is produced by platform noise. Steps can then be taken to reduce or eliminate this source by redesigning the equipment. Similarly, the location of the hydrophone above the moving bed particles may be influenced by the proximity of the individual background noise sources.

Most importantly, however, the identity of background noise sources can assist in the identification of the gravel-generated noise because generally, all sound sources exhibit individual spectral characteristics.

It must be expected that riverbed pebble noise also exhibits a characteristic spectrum. Yet its identification may still present difficulties. If curves S and B_1 in Figure 3 represent the source and background sound pressure levels in a band of frequencies from f_1 to f_2, the background noise will mask the pebble noise when the range of observation is greater than r_1. The same sound contained in a band of different frequencies from f_3 to f_4 may be represented by the signal and background noise curves S_2 and B_2. The observed SPL of both components is shown to have decreased from those observed in the f_1 to f_2 band, but the background noise no longer masks the signal noise, and identification and observations of the pebble noise are possible throughout the entire free field except near the source.

EXPERIMENTAL DETAILS

Program

The laboratory experiments were in two categories: 1) those intended to verify some acoustic aspects of the pebble collision generated sound including its transmission underwater and sound field characteristics and 2) those aimed at disclosing the sound spectrum of potential ambient noise sources present under natural conditions.

In the first category, all experiments were quantitative. Sound was generated by pebbles rolling over an inclined bed of identical pebbles. The variables that were controlled included the number of rolling pebbles; the slope of the ramp, and hence, the velocity of the pebbles; and the position of the hydrophone relative to the stationary bed. Average pebble velocities were measured and broad-band recordings were made of the sound produced by pebble collisions from which SPL and frequency spectrum information could be obtained.

The experiments in the second category were qualitative. Attempts were made to simulate flow noise around the hydrophone by towing it in the CCIW tank.

A complete summary of all laboratory experiments is given in Table 1.

Experimental Equipment and Procedures

Rolling Pebble Tests

Noise generated by moving particles was simulated with nearly spherical Porox type silica-base porcelain balls, 40 mm in diameter, normally used for industrial grinding purposes. The manufacturer's specified density of the balls was 2403 kg/m^3.

Table 1. Summary of Laboratory Experiments

Test group	Date	Number of tests	Test type	Measurement system		Test function*							Remarks
				Hydrophone	Recorder	A	B	C	D	E	F	G	
1	April 5, 1973	4	Rolling pebbles	Ithaco	Uher			✓	✓				Preliminary
2	April 25-26, 1974	15	Rolling pebbles	Ithaco	Uher	✓	✓	✓	✓			✓	
3	April 25-26, 1974	2	Rolling pebbles	Ithaco	HW 5600	✓			✓			✓	
4	April 25-26, 1974	6	Rolling pebbles	Gould	HW 5600	✓						✓	
5	April 25-26, 1974	9	Rolling pebbles	ITC	HW 5600	✓	✓	✓	✓			✓	
6	April 25-26, 1974	2	Towing tank	ITC	HW 5600					✓	✓		
7	October 20-22, 1974	74	Rolling pebbles	Ithaco	Uher	✓	✓	✓					
8	December 17, 1974	9	Rolling pebbles	ITC	HW 96		✓	✓	✓			✓	
9	December 17, 1974	10	Rolling pebbles	Ithaco	HW 96		✓	✓	✓			✓	

*Test function code: A - acoustic wave transmission
B - rate of collision effect
C - SPL vs transport rate
D - spectral characteristics
E - extraneous noise
F - CCIW towing tank noise
G - instrument comparison

The stationary bed was 7 balls wide and 59 balls long. The balls were attached by glue to a 12-mm thick foam rubber pad which was attached to the floor of a U-shaped wooden trough. The sides of the trough, intended to prevent the loss of particles over the edge of the ramp, were also lined with foam rubber and prevented generation of sound by collision with the rolling balls. The dimensions of the pebble ramp are given in Figure 5.

The ramp with the stationary balls was placed in 1.20 m of water in the wind-wave flume of the hydraulics laboratory at CCIW. Only two different slopes of the ramp (24° and 27°) could be employed in the experiments because of restrictions imposed by the maximum depth of water in the flume and by the minimum slope of the ramp over which the balls could roll without stopping.

Collision sound was generated when one or more of the ceramic balls were allowed to roll, under the action of gravity, down the stationary ball platform. In some preliminary tests, the rolling balls were injected individually or in pairs. In the majority of tests, however, the balls were arranged on a foam rubber pad immediately above the first row of the stationary balls and held in place by a vertical gate; they were released by manually removing the gate. Up to 25 balls could be injected for observation.

The positions of the ramp in the flume and the position of the hydrophone relative to the ramp, shown in Figures 6 and 7 and Table 2, were preselected depending on the purpose of the experiment.

Table 2. Summary of Rolling Pebble Experiments

Test group	Number of tests	Hydrophone position*	Ramp		Number of rolling pebbles†
			Position*	Slope angle θ	
1	3	Z_4	C	24°	52, 50
2	15	Z_4	D	23.8°	1,3,6,9,12,14,15,16,18,19
3	2	Z_4	D	23.8°	9
5	6	Z_4	D	23.8°	1,3,6,9,12,15
7	9	Z_4	D	27.1°	1,3,6,9,12,15
10	74	Z_1, Z_2, Z_3	A,Ba,Bb	$24^{\circ}, 27^{\circ}$	1,3,9,5,10,15,20,25
11	9	Z_2	A	23.8°	5,10,15,18,20,25
12	10	Z_2	A	23.8°	5,10,15,20,25

*Hydrophone and ramp positions are indicated in Figures 5 and 7.
†At least one test was made with each of the number of rolling pebbles indicated.

Acoustic observations were made using three different hydrophone systems. The performance of these systems is described by White and also in Appendix A. Hydrophone sensitivities employed in noise recordings are summarized in Table 3.

Table 3. Summary of Hydrophone System Sensitivities

Test group	Date	Hydrophone	Hydrophone sensitivity* (dB)	Gain (dB)
1	April 5, 1973	Ithaco	-64	0
2	April 25-26, 1974	Ithaco	-64	0
3	April 25-26, 1974	Ithaco	-64	0
4	April 25-26, 1974	Ithaco	-64	0
5	April 25-26, 1974	Gould	-58	-9
6	April 25-26, 1974	Gould	-58	-9
7	April 25-26, 1974	ITC	-63	-9
8	April 25-26, 1974	ITC	-63	-9
9	April 25-26, 1974	ITC	-63	-9
10	October 21-22, 1974	Ithaco	-64	0
11	December 17, 1974	ITC	-63	0
12	December 17, 1974	Ithaco	-64	0

*Hydrophone sensitivity is given in decibels re 1 V/μbar.

In a typical rolling pebble experiment, broad-band recording of sound was obtained immediately prior to the injection of the pebbles until they came to rest in the recovery basket at the foot of the ramp. The signal was also passed through the Ithaco signal conditioning apparatus and recorded on a paper chart. Preselected positions of the rolling balls on the ramp were marked on the chart during the recording to determine the position of the sound source from the hydrophone.

Frequency analysis of the recorded signal was made using the Ithaco filter system in one-third octave or one-octave bands.

Towing Tank Tests

To isolate platform noise, the hydrophones were towed at velocities up to 2.7 m/s through still water in the CCIW towing tank. Because of the relatively high level of noise produced by the towing carriage, recordings were made also of the carriage-generated noise alone, with the hydrophone stationary near the midpoint of the towing tank.

RESULTS AND ANALYSIS

Sound Level Variation

The variation of SPL with the number of sound-generating pebbles was determined by observing the SPL at the time when the centre of the group of N_B rolling balls was located directly under the hydrophone. The centre of the group of pebbles was considered to be the acoustic centre of the sound. No attempt was made to apply a range correction for the particles moving at edges of a group because the maximum number of pebbles used in experiments increased the range of edge particles by only 5%, and this increase was not considered to be significant and warrant correction.

The experimental results, showing the variation of a broad-band SPL with the number of rolling particles N_B and obtained with hydrophone ranges of 0.30 m and 0.325 m, are presented in Figures 8a and 8b.

The reproducibility of SPL measurements for any N_B was within a band of 3 dB in any one group of observations and within 5 dB between different groups using the same hydrophone. In view of the nature of the acoustic environment and of the sound-generating sources, this was considered to be satisfactory.

The results show that the relationship between SPL and N_B is nonlinear and that the rate of change of SPL with N_B ($\Delta SPL/\Delta N_B$) is very large at low N_B and decreases as N_B increases. Because this trend agrees qualitatively with the multiple source effect, the experimental results were compared with theoretical results obtained from equation (2), assuming N_B to represent the number of sources n. The theoretical curve was chosen to equal the observed SPL at $N_B = 25$. An equivalent SPL_1 for $N_B = 1$ was then calculated from equation (2) and used in the determination of SPL for different N_B values. For the Ithaco and ITC hydrophones, the SPL values at $N_B = 25$ were 47 dB and yielded equivalent one pebble SPL_1 values of 33 dB and 30 dB, respectively.

The theoretical and experimental results were found to correspond when N_B was greater than 12 or 15. Below these N_B values, the theoretically predicted sound pressure levels were higher than those observed experimentally.

The discrepancy between theoretical and experimental results at low N_B is possible for a number of reasons. Foremost is that rolling pebbles produce impact type of sound, but equation (2) is applicable to continuous sound sources. The chart recording the acoustic record shown in Figure 9a indicates that during the passage of one pebble from the top to the bottom of the ramp, all 59 collisions with stationary pebbles were detected. The chart recorder, however, may not have had the response to record the peak values of the collision noise and the measured SPL was below

the true average value. For 9 rolling balls, the noise record chart in Figure 9b indicates that the contributions of individual collisions were integrated into continuous sound.

It is also possible that the force of collisions between particles was not constant and that at the time of an observation, the measured SPL at low N_B was below the true mean value.

Nevertheless, the experiments confirm that a relationship exists between the number of rolling particles and the SPL which they produce. Furthermore, except at low N_B, this relationship appears to have the same functional form as the theoretical relationship for multiple continuous sources given in equation (2).

Collision Frequency and Equivalent SPL

In the development of the theoretical relationship between the rates of sediment transport and the level of noise produced by the pebbles, it was necessary to consider the frequency of sound-producing collisions, and also the level of sound generated by a single collision.

The frequency of collisions was determined from

$$F_c = \frac{N_B \bar{V}_p}{D} \tag{3}$$

where F_c is the frequency of particle collisions in hertz, N_B is the number of pebbles in the group, $\bar{V}_p$ is the average velocity of the group of rolling pebbles, and D is the diameter of the pebbles. Equation (3) is based on the experimental observation that a rolling pebble collides only once with each stationary pebble in its path.

The equivalent sound pressure level SPL_{eq} owing to one collision per second was calculated from

$$SPL_{eq} = SPL - 10 \log F_c \tag{4}$$

where SPL represents the total measured sound pressure level owing to a source-producing sound by collision at a frequency of F_c.

The experimental results are presented in Figures 10a and 10b. Although the data points show scatter, the results indicate that SPL_{eq} tends to become a constant as F_c increases. For the Ithaco hydrophone, the observed SPL_{eq} values fall in a band of 5 dB when F_c is greater than 60 Hz. For the ITC hydrophone, the scatter band for $\bar{V}_p$ = 0.29 m/s and F_c between 60 Hz and 180 Hz is only 3 dB. The results also show that SPL_{eq} decreases from the values in the constant range as F_c decreases from about 40 Hz.

With the measurement and recording systems used in this investigation, it appears that continuous sound analysis techniques become applicable when the frequency of particle collisions exceeds 50 Hz. Although this value is considerably greater than the minimum of 10 Hz suggested by Beranek, it nevertheless indicates that the concept of an equivalent sound pressure level and continuous sound analysis methods can be used in estimating the total contributions of multiple collisions such as occur among riverbed pebbles.

Pebble Velocity Effects

As shown in Figure 10b, group 7 tests with $\bar{V}_p$ = 0.31 m/s produced SPL_{eq} values below those from group 11 tests where the $\bar{V}_p$ was 0.29 m/s. Further analysis of data from group 10 tests, using identical N_B = 9 for comparison and presented in Table 4, also indicates that SPL_{eq} values decreased with the increase in the average pebble velocity $\bar{V}_p$.

Table 4. Sound Pressure Level Variation with Average Pebble Velocity

$\bar{V}_p$ (m/s)	F_c (Hz)	SPL (dB)	SPL_{eq} (dB)
0.29	65.25	51	33
0.35	78.25	49	30

Although the available experimental data are very limited and must be verified for other pebble velocities, the results confirm previously discussed reasons for the decrease in the acoustic power with increasing particle velocity.

Sound Field Characteristics

The characteristics of the sound fields generated by rolling pebbles were investigated by observing SPL at six positions from a fixed point on the stationary pebble ramp. The distances of the hydrophone to this point varied from 0.15 m to 4.80 m, with each new position approximately double in distance from the previous. The hydrophone was located at a depth of 0.67 m below the surface of water for the range of 0.15 m and at 0.53 m for all other observations.

The results, summarized in Figure 11, include observations of SPL generated by N_B values of 1, 3 and 9 on a ramp slope of 24°. The ordinate axis represents SPL

values relative to an arbitrary reference level. This permitted the superimposition of sound data from different N_B for the composite result.

All individual data points are contained within a band of 6 dB up to r/r_o value of 4.2, which represents an actual range r of 1.26 m. Furthermore, the data band lines have a negative slope of 6 dB per doubling of the range of observation. For r/r_o values larger than 4.2, the observed SPL fall above the upper band line.

The results indicate that an acoustic free field, illustrated in Figure 2, was established in the still water up to a range of 1.26 m from the centre of the group of the noise-generating pebbles. Above this range, the reduction of the slope from 6 dB per octave indicates that reverberation effects owing to the reflection of sound waves from the boundaries of the enclosure were being detected. Furthermore, the results suggest that the pebble-generated sound is, on the average, non-directional because only the spherical or hemispherical radiation of the pressure waves from the source could produce an attenuation of 6 dB for each doubling of the range.

Pebble Sound Spectrum

The characteristics of the frequency spectrum of the ceramic balls used in the laboratory experiments were determined from numerous recordings of sound generated by groups of pebbles rolling down the test ramp. The results presented in this section, however, were taken from test groups 11 and 12 only because similar results were obtained from other tests.

In test groups 11 and 12, sound recordings were made using the Ithaco and ITC hydrophones and a Honeywell 96 tape recorder. Sound data were determined with the hydrophones located at a range of 0.30 m to the centre of a group of rolling pebbles. The number of pebbles N_B in the tests was varied from 5 to 25. Spectral information was obtained by playing back the recorded broad-band (0.05 - 40 kHz) signal through every second of the one-third octave passbands of the Ithaco filter in a range from 0.05 kHz to 10 kHz.

The results of the tests, presented in Figures 12a to 12d, show the variation of the pressure spectrum level (PSL) with frequency. The PSL represents the effective SPL of the signal contained in a band 1 Hz wide, as determined from equation (5):

$$PSL = SPL_b - 10 \log \Delta f \tag{5}$$

where SPL_b is the sound pressure level in the one-third octave band and Δf is the band width in hertz centred on a frequency f_o and determined from

$$f_o = \sqrt{f_1 f_2} \tag{6}$$

where f_1 and f_2 are the high and low pass frequencies of the filter band.

From the spectrographs which cover the frequencies from 50 Hz to 10 kHz, the pebble noise spectra were found to be continuous. Yet a substantial difference was found to exist between the spectra determined by the Ithaco and the ITC hydrophones. The spectrographs obtained with the Ithaco hydrophone show a maximum of about 140 Hz as well as a secondary peak of about 560 Hz. In addition, there appears to be a small increase of PSL from the general trend of the spectrum curve in the vicinity of 2.24 kHz. The ITC hydrophone results, however, show that the maximum PSL occurs in the 140-Hz to 220-Hz frequency band, and that the peak is much more gradual and less pronounced than the peak determined from Ithaco hydrophone measurements. Furthermore, only one secondary peak at about 3550 Hz was found with the ITC hydrophone.

No attempt was made to resolve the discrepancy between the results obtained by the two hydrophones. Measurements, however, were made with the hydrophones deliberately positioned at identical locations relative to the water surface, flume boundaries and pebble ramp. The method of pebble injection and the average pebble velocity were also identical. Hence, it is unlikely that the differences were due to experimental errors. Yet it is possible that the Ithaco hydrophone output is affected by the variations of its sensitivity with signal frequency because of placement of the sensor in the hollow of the lead weight.

Generally, the spectrographs show that PSL increases with N_B, but that the forms of the spectrographs, produced by different N_B and determined by the same hydrophone, are similar. The variations of PSL with N_B were evaluated for every frequency band where data were available. The relative variation of PSL with N_B in all frequency bands, obtained by superimposing data points from different bands, is given in Figure 13. The two lines are 3 dB apart and are sloping at 3 dB per octave (i.e., doubling of N_B). Although some data scatter is present, the majority of data points fall between the band lines indicating that doubling of the number of the rolling pebbles increased the PSL by a constant 3 dB when N_B was greater than 10. This confirms the theoretical result which can be obtained from equation (2) by substituting N_B for n. Furthermore, the results are independent of the frequency band - a condition which must be satisfied in pebble noise identification and measurement when background noise is present.

Towing Tank Test Results

To determine the characteristics of the platform noise that can be generated by the flow around the hydrophone and its underwater support system, both the Ithaco and ITC hydrophones were towed through still water in the CCIW towing tank.

The results with the Ithaco hydrophone were inconclusive. At velocities comparable with those at which gravel movement takes place in rivers the excessive noise generated by the towing carriage exceeded the upper limit of the instrument range and could not be interpreted.

The signal from the ITC hydrophone, however, was attenuated, and observations were made at velocities of 1 m/s and 3 m/s. In addition, the carriage noise spectrum was determined by the hydrophone stationary midway between the ends of the towing tank.

The results, presented in Figure 14, show that the observed PSL were identical for the towed and stationary hydrophone conditions. This indicates that the observed PSL were due to the noise of the towing carriage which masked all noise that could have been generated by the hydrophone platform.

For the Ithaco hydrophone, towing tests had been conducted by Tywoniuk at the current meter calibration station (no longer in operation) located in Calgary. His data were used in calculating the PSL at a towing velocity of 2.74 m/s and are presented, for reference, in Figure 15.

SUMMARY AND CONCLUSIONS

A series of experiments were undertaken to verify some theoretical aspects of impact-generated noise in an underwater environment. The results of the acoustic aspects of the study were intended for application in the development of a theoretical relationship between the noise generated by sediment particle collisions and the rate of bed-load transport.

All observations were made in still water with a free surface. Gravel collision noise was simulated by ceramic balls rolling under gravity on a bed of similar balls. The size of the moving and stationary balls was identical.

Observations were made using three different hydrophones, one of which was used for reference only. Recordings of the observed sound were made, at various times, on three types of tape recorders. Spectral analyses were made using one-octave or one-third octave passband filters. All acoustic observations were made in terms of sound pressure levels in decibels re 1 μbar.

From the results of the rolling pebble experiments the following conclusions were reached:

1) The sound pressure level at a point in water owing to noise generated by collision of pebbles increases with an increasing number of rolling pebbles in accordance with the theoretical function applicable for the determination of total SPL by a number of separate and continuous sound sources, provided that the number of rolling pebbles is greater than 10 or 15.
2) The multiple source function is not affected by the width of the frequency passband in the calculation of total SPL from contributions by individual pebble collisions.

3) An equivalent SPL generated by one pebble can be calculated from total SPL if the number of rolling pebbles exceeds 10 or 15.
4) With the instruments used, the frequency of pebble collisions above which the impact noise effects become unimportant and the sound assumes continuous characteristics was found to be about 50 Hz.
5) The acoustic directivity of the pebbles as sound sources appears to be omnidirectional or is averaged when multiple collisions take place.
6) A free field part of the far field was found to exist in the experimental environment up to about 1.5 m from the source.
7) The SPL generated by a collision is a function, among others, of the velocity of the pebble.
8) The ceramic pebbles generate a pressure spectrum which is continuous and has a maximum between 100 Hz and 300 Hz.

CHAPTER 2

Theoretical Feasibility Analysis

INTRODUCTION AND OBJECTIVES

Although the possibilities of the acoustic approach for bed-load measurement have been recognized long ago and the existence of a functional relationship between pebble impact noise and sediment transport has been indicated by experiment, no theoretical feasibility studies of the method have been reported to date. Previous studies, although limited in scope, have nevertheless identified some of the practical difficulties that have to be surmounted to ensure the feasibility of acoustic measurement of bed load. The foremost among these is that the acoustic power of riverbed pebbles cannot be measured directly; it must be determined by remote sensing of the sound waves transmitted through the water to the receiver.

As part of a general investigation of the acoustic bed-load measurement method, an attempt was made to develop an analytical model relating the rate of bed-load transport to some acoustic parameter measurable in a natural stream. An idealized model is developed and presented in this report. The model is based on general acoustics theory supplemented by experimental measurements presented in Chapter 1 to verify the applicability of the theory to impact-generated underwater noise.

The primary objective of this part of the study was to establish a theoretical transfer function between the sound pressure levels generated by the collisions of rolling bed particles and the rate of bed-load movement. The transfer function was intended to serve in the assessment of the practical feasibility of the acoustic approach and to assist in the identification of other sediment or flow parameters to be established or measured in conjunction with acoustic observations for bed-load transport measurement.

MODELLING CONCEPTS AND ASSUMPTIONS

The development of the acoustic bed-load transport function was based on a conceptual model designed to represent, as realistically as possible, the sediment movement and the behaviour of acoustic waves in an underwater environment. Because of the number and the diversity of variables and the statistical nature of the sediment transport phenomena, certain idealizations were assumed and incorporated into the model.

The Physical Model

A physical model, illustrated in Figure 16, was used to formulate a relationship between the rate of bed-load transport, the position of the hydrophone in the flow and the positions of sound-producing riverbed pebbles relative to the hydrophone.

In the model it is assumed that all particles are spherical and have a diameter D. The stationary pebbles on the riverbed are arranged in concentric rings around a central pebble located on a common vertical and at a distance r_o (or n_d pebble diameters) below the acoustic centre of the listening hydrophone. The horizontal radius distance to the centre of any of the rings is R (or n_x pebble diameters).

The particles in motion above the stationary bed are arranged in rows spaced, on the average, n_w particle diameters apart across the stream. The total width of a moving strip of bed load occupies a width of n_r pebble diameters. In the direction of the movement, the particles in each row are spaced as λ_s or n_s pebble diameters. The average particle velocity is represented by $\bar{V}_p$.

The particles are assumed to move by rolling or by jumping over an integral number n_j of stationary bed pebbles. When movement is by rolling n_j equals one. If the pebbles move by jumping n_j is greater than one. A moving particle collides with an individual stationary particle in its path only once, so that when the motion is by rolling, collisions occur with all consecutive particles. If jumping occurs collisions take place, on the average, with every n_jth bed particle. The pebbles move in a layer one diameter deep.

Assumptions Related to Pebble Sound

The development of the acoustic bed-load transfer function is based on the following assumptions:

1) Sound is generated by collision of moving particles with stationary particles only. It is considered that collisions between moving pebbles do not occur.
2) The location of a collision source is at the stationary bed particle.
3) All collisions generate equal acoustic power.
4) Collision-generated acoustic power is a nonlinear function of the average particle transport velocity.
5) The receiving hydrophone has omnidirectional characteristics.
6) The receiving hydrophone is located in the free field part of the acoustic far field.
7) Collision-generated sound has continuous frequency spectrum characteristics.

8) Sound attenuation between source and receiver is due to non-directional wave divergence and is negligible because of turbulence, velocity gradients, temperature variations, etc.

9) Multiple collision source sound pressure levels are additive in the same way as continuous sources if the frequency of collisions exceeds 50 Hz.

10) Background noise levels do not mask pebble-generated sound.

11) Moving and stationary pebbles are of identical size.

Assumptions 1, 4, 6, 7 and 9 are supported by experiments reported in Chapter 1.

ACOUSTIC BED-LOAD TRANSPORT FUNCTION

Bed-Load Transport Relationship

In the transport model, it is assumed that bed particles move downstream in rows separated by a distance λ_w, which can also be expressed by

$$\lambda_w = n_w D \tag{7}$$

where n_w = separation distance between rows (or the width of channel occupied by a row) in numbers of particle diameter D.

The rate of bed-load transport in the width λ_w can be given by

$$g_{ws} = f\, m \tag{8}$$

where f = the frequency of passage of the particles past a reference line and
m = mass of one particle.

The mass of a spherical pebble can be expressed by

$$m = \rho_s \frac{\pi D^3}{6} \tag{9}$$

where ρ_s = density of particle.

The passage frequency f depends on the average velocity of particles $\bar{V}_p$ and the spacing λ_s between particles in the direction of the movement as follows:

$$f = \frac{\bar{V}_p}{\lambda_s} \tag{10}$$

Substituting equation (10) into equation (8)

$$g_{ws} = \frac{m\bar{V}_p}{\lambda_s} \tag{11}$$

from which the rate of transport per unit width of channel can be determined by dividing by λ_w:

$$g_s = \frac{g_{ws}}{\lambda_w} = \frac{m\bar{V}_p}{\lambda_s \lambda_w} = \frac{fm}{\lambda_w} \tag{12}$$

Collision Frequency and Transport Rate

Because collision between stationary and moving bed particles is considered as the only sound-generating mechanism, the frequency of collisions can provide a measure of the frequency of the particle passage past a stationary reference particle or a row of particles. The frequency of collisions with the specific reference particle, however, depends not only on the frequency of particle passage but also on the occurrence of impact. The occurrence of impact depends on the length of the jump that the moving particles may experience between collisions.

The jump length λ_j between collisions can be expressed by

$$\lambda_j = n_j D \tag{13}$$

where n_j = length of jump in number of particle diameters.

The average frequency f_c^1 of collisions with a reference bed particle in the path of a moving row of particles can then be estimated from

$$f_c^1 = \frac{f}{n_j} \tag{14}$$

for a row of moving particles, contained in a width λ_w of the channel. The frequency of collision with any one of the stationary particles in the reference row perpendicular to the direction of motion is

$$f_c = \frac{f}{n_w n_j} \tag{15}$$

which, substituted in equation (12), yields

$$g_s = f_c \frac{n_j m}{D} \tag{16}$$

Equation (16) expresses the relationship between the rate of bed-load transport per unit width of channel and the frequency of collisions with any one stationary bed particle.

Frequency of Collisions - Sound Pressure Level Relations

To express the relationship between the number of collisions and the total sound pressure level at a point above the bed, a concentric arrangement of the stationary bed particles in rings around the vertical axis passing through the observation point is employed. The total number of pebbles in any circular ring i located at a radius of N pebble diameters from the centre can be estimated from

$$N_i = 2\pi N \tag{17}$$

When the width of the stream of moving particles is $n_r D$ and extends equal distances to

both sides of the ring and N is greater than $\frac{n_r}{2}$, the number of pebbles in the two segments of a ring i can be determined from

$$N_i = 2\pi N \left[1 - \frac{2 \cos^{-1}\left(\frac{n_r}{2N}\right)}{\pi}\right] \tag{18}$$

The total number of collisions per unit time in any ring or ring segment i can then be estimated from

$$F_i = f_c N_i \tag{19}$$

It has been demonstrated experimentally (see Chapter 1) that if the frequency of sound-producing collisions exceeds 50 Hz and all collisions occur at the same distance from the hydrophone, an equivalent sound pressure level SPL_{eq} owing to one collision per second can be determined theoretically from equation (20):

$$SPL_{eq} = SPL' - 10 \log F' \tag{20}$$

where SPL' = the observed sound pressure level generated by all collisions at a fixed range from the observation point and

F' = frequency of noise contributing collisions.

Assuming that SPL_{eq} is a function only of the average velocity of particles and hence, is a constant in a given flow situation, the sound pressure level contribution SPL_i at the hydrophone location owing to all collisions in a ring i at range r_i can be calculated from equation (21):

$$SPL_i = SPL_{eq} + 10 \log F_i - 20 \log \frac{r_i}{r_o} \tag{21}$$

where r_o = the distance between the hydrophone and the bed of the river and is used as the reference range.

The term $20 \log \frac{r_i}{r_o}$ represents the SPL attenuation on account of wave divergence. Equation (21) can also be expressed in terms of f_c and N_i:

$$\frac{SPL_i}{10} = \frac{SPL_{eq}}{10} + 2 \log r_o + \log \frac{f_c N_i}{r_i^2} \tag{22}$$

The total SPL at the hydrophone location is determined by addition of the squares of the rms pressures owing to contributions from each of the pebble rings. Since

$$SPL_i = 20 \log \frac{p_i}{p_o} = 10 \log \frac{p_i^2}{p_o^2}$$

$$\frac{p_i^2}{p_o^2} = \text{antilog} \frac{SPL_i}{10} = 10^{SPL_i/10} \tag{23}$$

where p_i = rms sound pressure owing to collisions in ring r_i and

p_o = reference pressure of 1 μbar.

An expression for the total sound pressure can then be obtained from

$$\frac{p_T^2}{p_o^2} = \sum_{i=1}^{i=k} \frac{p_i^2}{p_o^2} = \sum_{i=1}^{i=k} 10^{SPL_i/10} \tag{24}$$

or in terms of SPL by

$$SPL = 10 \log \frac{p_T^2}{p_o^2} = 10 \log \sum_{i=1}^{i=k} 10^{SPL_i/10} \tag{25}$$

where k = the number of noise-contributing pebble rings.

Substituting SPL_i from equation (22) into equation (25), an expression for the frequency of collisions with any one stationary bed pebble is given by equation (26):

$$f_c = \frac{10^{SPL/10}}{r_o^2 \cdot 10^{SPL_{eq}/10} \cdot \sum_{i=1}^{i=k} (N_i/r_i^2)} \tag{26}$$

Sediment Transport Transfer Function

The transfer function between the observed SPL and the rate of bed-load transport is obtained by substituting equation (26) into equation (16):

$$g_s = \frac{m\, 10^{SPL/10}}{r_o^2 D} \cdot \frac{n_j}{10^{SPL_{eq}/10} \sum_{i=1}^{i=k} (N_i/r_i^2)} \tag{27}$$

NUMERICAL SIMULATION

To show how various factors affect the acoustic measurements of pebble-generated noise, equation (26) was programmed for numerical simulation by computer. The parameters that were investigated were the distance of the hydrophone to the riverbed, the aerial concentration of moving pebbles, the effect of particle saltation, and the influence of the average particle velocity.

Hydrophone Range Effect

The effect of the distance of the moving bed from an omnidirectional hydrophone on the observed SPL is illustrated in Figure 17. The curves represent the computed SPL values owing to all collisions contained in an area of riverbed defined by a radius

of N pebble diameters. The rates of bed-load transport g_s are the same for all curves and were calculated assuming identical SPL_{eq}, and $n_j = n_s = n_w = 1$. The distance of the hydrophone to the bed for the B curves was four times greater than for the A curves.

Curves A and B represent the variation of SPL owing to collisions up to a radius of N = 400D, for a total width of the moving strip of bed load of 800D. Curves A^1 and B^1, diverging from A and B at N = 20D, represent calculated SPL when the moving strip of bed load is only 40D wide.

When N = D, the difference in SPL between the two curves for ranges r_A and $r_B = 4r_A$ is 12 dB. As SPL increases with N, however, the difference between the calculated SPL decreases and at N = 400D is reduced to approximately 2dB. This is because relative to the SPL produced by the pebble directly below the hydrophone, the same pebble ring contributes more sound to the hydrophone farther away from the riverbed. If the hydrophones are at r_A and at $r_B = 4r_A$ from the bed and if the ranges of the hydrophones to a ring i of radius N_iD are r_A^1 and r_B^1, respectively, the ratio r_A^1/r_A will always be greater than r_B^1/r_B. Because sound attenuation owing to divergence from the source is determined by this ratio, relatively more sound will be attenuated to the lower hydrophone location. This result is of practical significance because the placement of omnidirectional hydrophones at different distances from the riverbed for identification of near-bed noise may not be useful for large widths of moving pebbles.

For a limited strip width of moving particles, represented in Figure 17 by curves A^1 and B^1, the SPL contributions from the distant ring segments become negligible by a combined effect of distance attenuation and constant number of collisions as the ring radius increases. Hence, the sound pressure levels rapidly approach saturation values. The difference of 5 dB between the two curves A^1 and B^1, shown in Figure 17, however, represents a specific case and would vary depending on the width of the moving gravel strip.

The Effects of Aerial Concentration and Saltation of Pebbles

The influence of the aerial concentration of the moving particles, represented by values n_s and n_w, and the effects of the length of particle jump n_j are illustrated in Figure 18. Theoretical prediction of SPL was made for four different particle jumps and four aerial concentrations, ranging from 1 when the lateral and transverse distances between the pebbles is zero or $n_s = n_w = 1$ to an aerial concentration of 1/64 when $n_s = n_w = 8$. For all calculations, SPL_{eq} was assumed to be constant and 40D was chosen as the width of the moving stream of particle. The results show that for any constant n_j, doubling of the rate of transport g_s corresponds to an increase of 3 dB in SPL. Similarly, when the particles begin to saltate, any doubling of the jump length decreases the SPL by 3 dB for the same rate of transport.

Forces of Collision and Saltation Effects

The effects of the force of interparticle collision and of aerial concentration of the moving particles, for movement without saltation ($n_j = 1$), are illustrated in Figure 19. On the basis of physical arguments and experimental evidence presented in Chapter 1, it was assumed that the equivalent one collision sound pressure level is a non-linear function of the average particle velocity $\bar{V}_p$ and can be represented by equation (28):

$$SPL_{eq} = C_1 - C_2 (\log \bar{V}_p + C_3)^2 \qquad (28)$$

The function is a logarithmic parabola, which depending on the values of the constants C_1, C_2 and C_3 gives a rapid increase in SPL_{eq} at low $\bar{V}_p$ followed by a gradual decrease in SPL_{eq} as $\bar{V}_p$ increases. For the numerical simulation, the values of the constants were obtained from experimental data with ceramic spheres 40 mm in diameter ($C_1 = 50$, $C_2 = 0.85$ and $C_3 = 36$) yielding $SPL_{eq} = 0$ at $\bar{V}_p = 0.01$ m/s and a maximum $SPL_{eq} = 50$ for for $V_p = 0.141$ m/s.

The simulation results, presented in Figure 19, illustrate that a wide range of SPL values can be observed for the same rate of transport depending on the values of $\bar{V}_p$. Conversely, large errors in estimation of g_s can be incurred from SPL observations if no consideration is given to the SPL_{eq}.

DISCUSSION AND ANALYSIS

The results of the numerical simulation of the theoretical bed-load transfer function show the limitations of the general SPL measurement approach used in the present investigation. It can be seen that without consideration of the physical transport conditions, SPL observation of the bed pebble noise can represent a large range of bed-load transport rates.

The transfer function, presented in equation (27), shows that even in an idealized model, the prediction of bed-load transport rate g_s depends on seven variables. In a field situation, the number of these variables is even larger to account for the variability of bed particle characteristics and their distribution on the riverbed. At present, of the seven independent variables required to determine g_s, only four can be measured or controlled. These include the SPL and the distance of the hydrophone from the riverbed r_o, which can be set by the observer. It is also possible to obtain samples of bed material and to measure the mass m and the characteristic dimensions D of the pebbles.

There are at present no means to determine the degree of pebble saltation represented by the jump length n_j, or the aerial extent of the moving stream of bed load measured in equation (27) by the index k. Most importantly, the level of sound generated

by a collision SPL_{eq} and providing a measure of the acoustic power radiated by a pebble cannot be measured in a river.

A reduction of the number of the unknown variables may be possible in some situations. For example, it might be possible to confirm visually that the movement is by rolling only, thereby establishing that $n_j = 1$. Perhaps it may be possible to determine the average velocity of the moving pebbles $\bar{V}_p$ and by reproducing the movement of a sample of pebbles in a laboratory to establish the characteristic level of collision sound SPL_{eq}. Finally, with the use of a directional hydrophone, an attempt could be made to observe pebble collision sound originating from a finite area of riverbed, thereby determining the value of the index k.

SUMMARY AND CONCLUSIONS

A relationship between the rate of bed-load transport and the level of sound generated by interparticle collisions of moving pebbles was formulated. It represents a general case in which the acoustic information is provided by the measurement of sound pressure level at a finite distance in the flow above the bed of a river with an omnidirectional hydrophone.

The relationship shows that the rate of bed-load transport is a function of at least seven independent variables, which in addition to the measured SPL are the size and mass of the bed pebbles; the position of the hydrophone relative to the riverbed; a measure of particle saltation; the aerial extent of the moving bed; and the average acoustic power generated by a single collision between a moving and a stationary particle.

Because in practice the saltation of the pebbles, the aerial extent of the stream of the moving bed and the acoustic power generated by the pebbles cannot be readily measured, the acoustic observation approach of bed-load measurement employed throughout this investigation is not considered feasible at the present time.

Field Experiments

OBJECTIVES AND SCOPE

The specific objectives of the field study program were

1) to record underwater noise in gravel-bearing rivers during periods with and without bed-load movement,
2) to record and determine the frequency spectra of artificially generated sound in water by different sizes of gravel pebbles,
3) to identify, if possible, from spectral characteristics of the river noise the sound components owing to gravel particle collisions, and
4) to relate, if possible, the pressure spectrum levels in different frequency bands owing to gravel sound to the bed-load transport rates established by independent sampling methods.

The scope of the field program was determined by logistics associated with field operations. Because of costs, observations were carried out at only two established sediment survey sites. Available site equipment was used for support of the acoustic apparatus, and flow velocity and bed-load measurements were made in conjunction with regular hydrometric and sediment survey programs. Study rivers were selected for their relatively short and predictable spring runoff periods to minimize the duration of field operations.

OBSERVATION SITES

The field observations were carried out at two sites on the Vedder and Fraser rivers in British Columbia. The location of these sites is shown in Figure 20.

Vedder River Site

Location

The Vedder River site was approximately 11 km southwest of the city of Chilliwack, near the village of Yarrow. The river observation section, located approximately 150 m downstream from a railway bridge, was equipped with a cableway for hydrometric and sediment measurements. Flow discharge and sediment transport observations at this site had been carried out regularly for a number of years.

Geometry

The normal width of the Vedder River at the observation site, shown in Figure 21, is about 85 m. At low flows, its depth averaged about 0.6 m, over two thirds of the cross section, and was 1.2 m near the left bank. During high flood flows, the river depth was observed to increase by at least 1 m.

Access

Normally, the site was accessible by a road along its right (north) bank downstream from the observation cross section. Equipment was brought by a vehicle to the foot of the loading tower and carried up for placement in the cable car. When the river stage exceeded 9.75 m, however, the road became inundated by water, and all acoustic measurement equipment was moved on a rubber raft along the side of the submerged access road. Acoustic observations at the site were terminated when parts of the access road were washed out and other parts became clogged by river debris, making it treacherous for personnel to move the raft to and from the loading tower manually.

Debris

At high stages of flow, the Vedder River carried considerable debris. It was mainly composed of logs, up to 0.5 m in diameter and up to 20 m in length, and of uprooted trees of various sizes. Most of the debris floated on the surface, but occasionally observations were made of submerged debris including a ball of tree roots at least 2 m in diameter. The heaviest debris movements were observed immediately following sudden increases in flow when loose materials accumulated on the river banks, since previous high flows were refloated by the rising stage of water.

Bed Material

The bed material at the observation cross section was gravel, with pebbles ranging in size from 1 cm to 15 cm. They were visible from the cable car above the river when the flow was less than 150 m^3/s and the river carried little suspended material.

Fraser River Site

Location

The observation site on the Fraser River was near the village of Agassiz, about 15 km northeast of Chilliwack. The measurement cross section was approximately 400 m downstream from a major highway bridge and had been used by the Water Survey of Canada as a network station for hydrometric and sediment observations for several years.

Geometry

As shown in Figure 22, the Fraser at the sampling cross section was over 500 m wide and up to 9 m deep.

Access

The site was readily accessible from its south bank. A small wharf was located near the site, where measurement equipment could be transferred to and from a catamaran from which all observations were made.

River Traffic and Debris

Considerable commercial river traffic, mainly of log rafts, occurred during the study periods at this site but did not interfere with the acoustic or other measurements. The Fraser River also carried considerable debris. When necessary, collisions with floating logs were avoided by temporarily moving the catamaran off the observation station.

Bed Material

Basket sampler recoveries had shown that bed materials at the Agassiz site were gravel-sized particles. Visual observations of the bed have never been made because of the suspended sediments in the river water at all times of the year.

FIELD MEASUREMENT EQUIPMENT

Observation Platforms

Vedder Site Cableway

All observations at the Vedder site were made from a cableway. It spanned the river and had a cable car equipped with a power drive for the positioning of measuring equipment at any station across the river. The cable car also had a power hoist for the vertical positioning and recovery of sampling apparatus weighing up to 150 kg. Power was provided by 12-volt batteries recharged daily at local service stations. The cable car was reached from a special loading tower on the north bank of the river. Depending on the gauge height and the position of the cable car over the river, the observers in the car were located between 2 m and 4.5 m above the surface of the water.

Fraser Catamaran

All observations at the Fraser River site were made from a Water Survey of Canada catamaran specially equipped for hydrometric and sediment survey work in large

rivers. It was held stationary at a measurement station by an experienced boatman, who kept the bow pointed upstream and continuously adjusted the engines' rpm to overcome the downstream drag caused by river flow. Power for hoisting machinery was provided from the engines and was adequate for handling equipment weighing more than 200 kg.

Sound Measurement Apparatus

Field observations of underwater noise were made using two different hydrophone and data recording systems. These two systems, ITC and Ithaco, differed in the type of equipment used. Both systems, however, were employed in a similar way for recording the underwater noise on magnetic tape for spectral analysis at a later time.

Details and performance characteristics of the ITC system have been described by White. Similar information on the Ithaco system is presented in Appendix A.

The ITC system was clearly superior in performance to the Ithaco system. In the band from 10 Hz to 30 kHz, the ITC system frequency response was ±2 dB and its spatial response was omnidirectional. In contrast, the frequency response of the Ithaco system was ±5 dB in the band from 0.2 kHz to 6 kHz only, and it showed significant directional characteristics at frequencies above 5 kHz. Furthermore, the sensitivity characteristics of the Ithaco sensor, as mounted in the hollow of a lead body shown in Figure 23, differed between the two independent calibrations carried out on November 2, 1973, and February 18, 1975. Because of the variability of the system sensitivity at low frequencies, shown in Figure 24, interpretation and comparison of spectral characteristics of sound observed with the Ithaco system were viewed with caution.

The Ithaco system was not used at the Agassiz site on the Fraser River. The 70-kg lead body was too light to overcome the horizontal flow drag on the relatively long submerged part of the cable even with attached fairing, and the hydrophone assembly could not be positioned at required distances above the riverbed. In contrast, the ITC hydrophone sensor attached to the 160-kg lead body, illustrated in Figures 25 and 26, could easily be deployed at any depth at the Fraser River site.

A major disadvantage of the ITC system for field operations was its bulk and weight. Together with the Honeywell tape recorder, power supply batteries and the auxilliary electrical equipment, the system weighed about 400 kg and was difficult to handle in the field. The system belongs to the research instrument category and cannot be considered as a routine measurement instrument.

Bed-Load and Flow Velocity Measurement Apparatus

In addition to acoustic observations with the two hydrophone systems, measurements were also made of flow velocity distributions, bed-load transport rates and river stage observations. Equipment and procedures used in obtaining these measurements were those employed by the Water Survey of Canada in routine hydrometric and sediment survey practice.

Gurley Price meters were chosen to record velocity measurements. Bed-load transport observations were made using either the half-size VUV or the full-size (0.6-m wide) basket samplers.

DATA ACQUISITION AND REDUCTION PROCEDURES

Field Observation Period

All data acquisition field work was carried out during the 1973 and 1974 spring runoff periods. These periods were chosen because of the highest probability of bed-load movement due to the occurrence of sufficiently high flows.

Personnel and equipment were in the field from May 16 to May 30, 1973, and from May 22 to June 19, 1974. The actual days of field sampling operations in 1974 are indicated on the flow hydrographs shown in Figures 27 and 28 for the Vedder and Fraser rivers, respectively.

Flow Conditions

During the 1973 spring runoff, Vedder River flows were abnormally low because of low snow accumulation during the winter in the watershed. Maximum flow during the field study period reached 200 m^3/s, but no bed-load movement was ever detected with basket samplers.

During the 1974 field operations, the Vedder River exhibited flow peaks on May 26 and June 4, representing surface runoff owing to rainfall on May 24 and May 25, and June 2 and June 3. The spring runoff on account of snowmelt at high altitudes in the watershed started on June 9, and is distinguished from rainfall runoff by diurnal variations. Snowmelt runoff peaks occurred daily between 2:00 hours and 3:00 hours, and daily minima occurred between 15:00 hours and 16:00 hours.

Because rising stage conditions are generally more favourable to movement of bed load, at the Vedder site acoustic observations carried out after June 9, 1974,

were on the rising limb of the average runoff hydrograph. Since most of the daily rise took place during hours of darkness, acoustic and bed-load measurements were made immediately after daybreak - some four hours to five hours after the daily peak.

At the Fraser site, acoustic and related observations were made on only two occasions, both in conjunction with routine survey programs by the Water Survey of Canada. As indicated in Figure 28, Fraser site observations were made also on the rising stage.

Sampling Sequences

Since hoisting apparatus at both sites could handle only one instrument at a time, simultaneous observation of underwater noise, bed load and velocities was not possible. By necessity, these parameters were measured in sequences, which are summarized for 1974 in Figure 29.

Generally, at low flows and in the absence of bed-load movement, the measurement sequence was not considered to be important. At high flows, however, an effort was made to minimize the time delay between the acoustic and bed-load observations. At the Vedder site during the critical study period starting June 12, 1974, hydrophone observations using the ITC system were carried out immediately after daybreak and were followed by bed-load sampling. The minimum period of time to complete both measurements was slightly more than three hours (June 12, 1974). With increasing flows, on account of floating logs in the river, this period eventually increased to 4.5 hours (June 14, 1974).

At the Fraser site, acoustic observations were made after completion of regular hydrometric and sediment measurements. Hydrophone measurements followed immediately after bed-load sampling, which indicated location of bed-material movement in the river cross section.

Acoustic Sampling Procedures

All acoustic sampling operations from the cable car at the Vedder site were performed by a two-man crew. One man operated the electrical controls of the carriage drive and the instrument hoist. In addition, he continuously observed the river flow upstream from the cableway to detect floating debris that could damage or cause loss of the sensor in the water. The other man operated the acoustic data acquisition equipment and kept data records. Because the equipment hoist motor was insufficiently powered to handle the 160-kg ITC hydrophone assembly, he also operated a manual crank to raise the hydrophone out of the water.

In a typical sampling test, the cable car was moved to a preselected station, the hydrophone was lowered to the surface of the water to establish a reference level, and then was lowered to a predetermined observation depth. The tape recorder was activated and a 40-second long underwater noise sample was recorded. The hydrophone was then raised or lowered to another sampling depth, or raised above the water level for cable car positioning at another station. The ITC hydrophone assembly, prepared for positioning in the river, is shown in Figure 30.

In a typical test, up to 20 individual 40-second long samples could be recorded on a single magnetic tape track on the ITC system. On the Ithaco system, one tape track contained up to 35 samples.

Particle-Size Effect Tests

For tests to determine the effects of particle size on the frequency characteristics of the noise which their collisions generate, pebbles were obtained from the shallow parts of the Vedder River near the north bank downstream from the study site. They were hand-sorted into three size groups, illustrated in Figure 31.

For testing a sample of given size, pebbles weighing about 15 kg were placed in a burlap bag with ropes attached to both ends. With the hydrophone located at mid-depth of flow at station 12.00 m, the bag containing the pebbles was put into the water and positioned at a predetermined test location. One end of the bag was raised forcing the pebbles to the other. Sound was generated by slowly lifting the heavy end of the bag under the water using a rope, allowing the pebbles to tumble in the bag. The bag was lifted to produce continuous sound for a recording of five-second duration.

The procedure was repeated for the 1.9-cm, 3.8-cm and 7.5-cm pebble samples positioned at about 0.6 m from the side of the hydrophone, and for the 1.9-cm pebbles positioned 0.45 m upstream from the hydrophone. Sound recordings were made using the ITC hydrophone system only.

Acoustic Data Processing

The underwater noise recorded in the field was frequency-analyzed using the Ithaco 411 M10Z variable bandpass filter and 3161 logarithmic amplifier system.

To obtain sound pressure level information in each frequency band, the field data tape recordings were played back through the analysis system, and its output was recorded on a graphic recorder. The playback process was repeated for different frequency bands set on the bandpass filter. The chart records of all bands of a sample were aligned, and one or more common subsamples of up to five seconds in duration

were identified on each frequency band chart. The maximum and minimum chart values in each of the subsamples were recorded and entered on computer cards for processing.

Sound pressure levels were obtained by adjusting the chart values for hydrophone sensitivity. Average SPL values in a subsample were then determined from equation (29) by assuming that the fluctuating pressures were distributed about a mean value midway between the highest and the lowest values as suggested by Beranek:

$$SPL_{avg} = 10 \log \frac{10^{SPL_h/10} + 10^{SPL_\ell/10}}{2} \qquad (29)$$

where SPL_h and SPL_ℓ are the maximum and minimum SPL values in decibels re 1 μbar in a subsample.

The extent of frequency analysis of the field recordings obtained by the two different hydrophone systems in the two years of study is summarized in Table 5.

Table 5. Frequency Analysis Summary

Year	System	Passband	Number of bands	Frequency range (Hz)
1973	Ithaco	consecutive one octave	6	100-6,300
1974	Ithaco	alternate one-third octave	12	50-10,000
1974	ITC	alternate one-third octave	15	50-40,000

Frequency analysis for alternate one-third octave passbands was carried out with the 1974 data to reduce the processing time. Because of the continuous nature of the recorded sound, elimination of alternate bands did not materially alter the analysis of the results.

RESULTS

General Remarks

Summaries of 1973 and 1974 field study programs listing basic experimental information are given in Tables 6 and 7.

Table 6. Summary of 1973 Field Observations (Vedder River Site)

Date	Time of acoustic observations (PDT*)	Number of sampling points	River stage		River discharge (m^3/s)
			Elevation (m)	Time (PDT)	
May 18	17:50-18:44	19	9.54	9:40	170
May 19	14:55-17:19	37	9.46	11:25	144
May 21	11:30-15:20	14	9.27	13:20	103
May 23	10:30-11:45	24	9.23	12:00	95
May 24	13:20-15:25	28	9.53	14:30	170
May 25	9:00-10:30	21	9.45	8:45	147
May 26	10:45-13:30	20	9.31	11:40	113
May 28	9:30-10:15	17	9.19	9:30	88
July 13	12:55-13:40	20	9.08	13:00	69

*Pacific Daylight Time

The experimental results obtained in the regular sampling series tests and in the special tests are presented in four parts:

1) the effects of hydrophone distance to riverbed,
2) the frequency characteristics of the underwater noise, its variability across the river and its spectra at a river station for different flow conditions,
3) bed-load transport measurement results, and
4) results of the special tests on the influence of pebble size on the acoustic spectrum which they generate by interparticle collisions.

Because of the superior quality of data obtained with the ITC system, only selected results obtained with the Ithaco system are included in the presentation of results.

Hydrophone Position Effects

The variability of observed SPL with hydrophone distance from the bed of a river was investigated with the Ithaco system in 1973. A typical result, obtained at the Vedder site in the absence of bed material movement, is presented in Figure 32. Lines indicating different river stage elevation and hydrophone distances to the riverbed were drawn to facilitate the interpretation of the results and to indicate trends owing to considerable data scatter.

Table 7. Summary of 1974 Field Observations

Date	Site	Hydrophone test numbers		Bed load	Flow observations				Remarks
		ITC system	Ithaco system		Gauge Ht (m)	Discharge (m^3/s)	Velocity (m/s)	Temperature (^oC)	
May 25	Vedder	1	A	0.5 VUV	9.43	148.7	✓	8.2	
May 26	Vedder	2		0.5 VUV	9.61	189.72	✓	6.7	
May 28	Vedder	3		none	9.40	140.88	-	9.2	Clear water
May 30	Fraser/A*	4		basket					
June 3	Vedder	5	B	basket	9.63	208.13	✓	7.4	
June 4	Vedder	6		basket	9.69	220.87	-	9.2	
June 5	Fraser/M†	7	C	none			-		Catamaran operations trials
June 7	Vedder	8	D	0.5 VUV	9.46	158.57	✓	9.2	
June 8	Vedder	9		none		148.66	-		Special tests
June 12	Vedder	10,11, 12	E	basket	9.75	240.69	✓	9.2	
June 13	Vedder	13,14	F,G	basket	9.86	283.17	✓	8.3	
June 14	Vedder	15,16 17,18	H	basket	9.94	319.98	-	9.2	Very heavy river debris
June 15	Vedder	19		basket	10.00	342.63	✓	7.5	
June 19	Fraser/A	21,22, 23		basket			✓		

*Fraser at Agassiz
†Fraser at Mission

The results show that in the one-octave passband between 400 Hz and 800 Hz, the SPL increases with river stage. For a constant river stage, however, the SPL decreases with distance from the bed.

To determine the influence of hydrophone position on the pressure spectrum level in greater detail, data obtained with the ITC system were analyzed statistically. The PSL in three frequency bands centred on 354 Hz, 2236 Hz and 8944 Hz was tested for independence of position at different river stations, assuming a linear regression in the form given by equation (30):

$$PSL = b\,(y) + B \tag{30}$$

where y is the hydrophone distance to the riverbed, b is the regression coefficient, and B is the intercept on the PSL axis. The statistical tests used the null hypothesis H_0: $b = 0$ against H_1: $b \neq 0$, under 0.05 level of significance.

The results of the statistical analysis of the effect of hydrophone position on the observed PSL, summarized in Table 8, are:

1) PSL was independent of the hydrophone distance to the riverbed in the one-third octave frequency bands centred on 2236 Hz and 8944 Hz at both the Vedder and the Fraser river sites, and in the 354-Hz band at the Fraser site.
2) PSL was dependent on the measurement distance to the riverbed in eight of the twelve test conditions at the Vedder River site in the 354-Hz band.
3) All observed PSL in the 354-Hz band at the Vedder site decreased with distance from the riverbed.

Frequency Spectra

At the Vedder site the frequency characteristics of the sound samples with the ITC equipment for identical flow conditions are presented in Figures 33 to 39. Each Figure contains spectra obtained at nine sampling stations during a test period of 45 minutes or less. Sampling station locations are shown in Figure 21. The seven graphs demonstrate variability of spectra across the river. Only spectra obtained in tests 3, 5, 6, 10, 13, 15, 16 and 19 were selected for presentation and analysis because of the proximity of the acoustic and bed-load sampling times. Preliminary analysis also showed that inclusion of the results of tests 1, 2, 8, 11, 12, 14, 17 and 18 would give no additional information, as all the results were similar.

Individual spectrographs represent pressure spectrum levels in different one-third octave bands centred on the frequency values shown on the abscissa. For plotting

Table 8. Summary of Effects of Observation Distance to Riverbed

T	STA (m)	N	N_y	Y_{min}-Y_{max}	f = 354 Hz			f = 2236 Hz			f = 8944 Hz		
					S	b	$S_{0.05}$	S	b	$S_{0.05}$	S	b	$S_{0.05}$
10	38.10	5	2	0.46-0.76	2.21	-13.28	s	0.71	3.16	ns	0.43	0.33	ns
	45.72	4	2	0.46-0.76	3.00	- 9.33	s	1.13	4.89	s	0.99	-0.01	ns
V	53.34	5	2	0.46-0.76	1.31	- 9.67	s	0.35	2.42	ns	0.21	0.83	ns
13	38.10	5	3	0.34-0.85	2.38	- 8.67	s	0.61	1.32	ns	1.36	1.10	ns
	45.72	9	3	0.32-0.82	2.62	- 0.24	ns	0.86	-0.07	ns	0.76	-0.03	ns
V	53.34	9	4	0.24-0.98	2.02	- 1.66	ns	0.69	0.34	ns	1.48	-1.33	ns
15/16	38.10	6	3	0.30-0.76	1.85	- 9.66	s	0.25	0.24	ns	0.87	-3.00	ns
	45.72	11	3	0.30-0.76	1.47	- 4.53	ns	0.83	-0.36	ns	1.39	0.03	ns
V	53.34	11	3	0.30-0.76	1.35	- 6.29	s	0.60	-0.57	ns	1.00	0.70	ns
19	38.10	3	2	0.46-0.76	0.72	- 2.33	ns	0.61	2.66	ns	0.40	2.16	ns
	45.72	4	2	0.46-0.76	1.58	- 7.55	s	0.47	0.44	ns	0.70	0.66	ns
V	53.34	6	2	0.46-0.76	2.05	-13.80	s	0.75	-0.33	ns	1.36	-2.40	ns
21	182.88	6	6	0.67-6.16	2.37	0.19	ns	0.32	0.00	ns	0.74	0.06	ns
F	228.60	5	5	0.67-4.92	2.09	0.43	ns	0.90	-0.28	ns	0.54	-0.27	ns

Legend:

T - test number
STA - measurement station
N - number of observations
N_y - number of observation depths
Y_{min}-Y_{max} - minimum and maximum observation distances to riverbed
S - standard deviation of all PSL values
b - regression coefficient
$S_{0.05}$ - significance at 0.05 level under H_0: b = 0 (s - significant; ns - not significant)
V - Vedder site
F - Fraser site

of the spectrographs, average PSL values obtained at observation points closest to riverbed were used.

The spectral characteristics of the underwater noise at the Vedder site obtained with a stationary hydrophone are similar to all positions across the river. At low frequencies the spectra have a slope that averages -12 dB per octave. A minimum occurs between the frequencies of 150 Hz and 350 Hz; the spectrum then increases to a maximum located in the range of frequencies between 1.8 kHz and 5 kHz and decreases above these frequencies.

The shape of all spectrographs at the Vedder site is similar under all conditions, but the levels of individual spectra vary with the sampling position across the river. The maximum PSL were found to occur in the middle of the river at stations 38.10 m, 45.72 m and 53.34 m. The minimum PSL values were observed at stations 15.24 m and 76.20 m which are nearest the banks of the river.

The differences between the maximum and minimum PSL observed at different stations in a test ranged between 8 dB and 12 dB at frequencies above 350 Hz and reached up to 20 dB below 350 Hz.

Spectrographs obtained by the two data acquisition systems are compared in Figures 40, 41 and 42. The spectra chosen for comparison correspond to identical river stations and hydrophone depth locations with minimum time lag between observations with the ITC and Ithaco systems.

Within the sensitivity variations, the spectra obtained by the two systems are similar between frequencies from 400 Hz to 4000 Hz. Below and above this range the spectra exhibit significant differences.

The spectrographs obtained from Fraser River site tests 4 and 21 are shown in Figures 43 and 44. Their shape is similar to the Vedder site spectrographs except that the difference between the minimum PSL at frequencies near 350 Hz and maximum at 5 kHz is substantially smaller at the Fraser site. The peaks on test 4 spectra at 561 Hz and 2236 Hz are not considered to be due to natural river sources, but to a malfunctioning catamaran engine noise.

The spectrographs of Fraser site test 22, obtained when the catamaran engines were shut off and the catamaran drifted with the river current, are shown in Figure 45. They differ distinctly from the spectrographs obtained with a stationary hydrophone, since the negative sloped portion of the spectrum at low frequencies has been eliminated.

The variability of noise spectra between different tests at identical observation stations at the Vedder site is indicated in Figures 46 to 54 and for the Fraser, in Figure 55. The spectrographs show that the spectral levels increase with flow stage in the river. Between tests 3 and 18, maximum increase in PSL occurred in the band between 0.5 kHz and 2 kHz and, depending on the observation station, ranged from 25 dB to 33 dB. The frequency of the maximum PSL was also influenced by the flow. At low flows maximum PSL occurred at higher frequencies of about 5 kHz. As the flows increased, the frequency of maximum PSL occurred at 1.8 kHz in test 19.

Bed-Load Measurement Results

The complete bed-load measurement results, showing transport rates determined from all individual basket sampler catches, are presented in Figures 56 to 61.

The rate of bed-load transport g_s was computed from equation (31):

$$g_s = \frac{W}{T\,L}\,\varepsilon \tag{31}$$

where W = mass of sample

T = sampling duration

L = width of sampler, and

ε = sampler efficiency, assumed to be equal to one.

The results demonstrate the variability of bed-load movement across the river and the variability of transport rates at a station as determined by repeated samplings. At the Vedder River site, movement of bed load was confirmed between stations 30 m and 70 m. Maximum transport rates were measured at station 53.34 m, but even there the variation in the transport rate ranged between 0 and 40 kg/m min during a single observation period. At the Fraser River site, the maximum transport rates were measured between stations 200 m and 230 m. The results of repeated measurements of some stations also indicate a range of transport rates from 0 to 60 kg/m min or 90 kg/m min.

Figures 56 to 61 also show the variation of PSL at 1-kHz frequency across the rivers at the study sites. Although maximum PSL and g_s values occurred at a sampling station in a number of tests, the results were not consistent in all tests.

Effects of Particle Size on Sound Spectra

The spectra of the noise generated by different sizes of river gravel particles contained in burlap bags are presented in Figure 62. The results are qualitative, since the sound generating movement of the gravel was produced manually and could not be controlled.

The spectra show that when the source was located 0.6 m to the side of the hydrophone, the size of the particles influenced the frequency of the maximum PSL. For the 7.5-cm particles, the maximum PSL occurred at about 1 kHz; for the 3.8-cm pebbles, at 2.2 kHz; and for the smallest particles (1.9 cm), at about 4 kHz. The results obtained with the 1.9-cm particle must be considered inconclusive because the difference from the background noise PSL is very small.

The spectra obtained with the pebble bag located in front of the hydrophone appear to have been affected by flow disturbances owing to the obstruction of flow by personnel and the sample bag.

ANALYSIS

Spectral Characteristics

The underwater sound spectra obtained during periods with and without bed-load movement in this field investigation exhibit similar characteristics and reveal no distinct features that can be attributed to pebble-generated noise. This suggests that the observed spectral features originate with sound sources other than gravel particle impact. The spectral levels, however, vary with flow and observation position in the river, indicating that the observed spectral components are due to sound sources of hydrodynamic origin. Indeed, experimental evidence and other research information support this indication.

The source of the low frequency noise component, characterized by the -12 dB/octave spectrum slope, is turbulence created by the relative motion between water and the hydrophone. It formed part of the noise spectrum at the Vedder and Fraser sites when the listening hydrophone was stationary with respect to a fixed point outside the flow. When the hydrophone was permitted to move with the flow, as in the drifting catamaran tests on the Fraser, this noise component disappeared.

The turbulence origin of the low frequency noise is confirmed also by theoretical and experimental turbulent pressure level spectra of approximately -10 dB/octave derived and observed by Wentz. This slope corresponds closely with the average -12 dB/octave slope observed in the present investigation.

Noise observed at frequencies above 300 Hz appears to have been caused by air bubbles in the water and water droplets hitting the surface of water. This cause was initially suggested by the general similarity of the observed spectra in the case of waterfall spectra presented by Arabadzi (1967). The presence of the air bubble and

water droplet components was also confirmed by the description of their spectra by Franz (1959). A comparison of the spectral features identifying air bubble and water droplet noise components is presented in Tables 9 and 10.

Table 9. Spectral Features of High Flows at the Vedder Site

Slope of spectrum	Observed dB/octave	Air bubble noise Franz (1959) (dB/octave)
Below maximum frequency	6 to 13	8 to 12
Above maximum frequency	-6 to -8*	-6 to -8

*Most individual spectra exhibit slopes in this range. Few exceptions range to -13 dB/octave.

Table 10. Spectral Features of Low Flows at the Vedder Site

Slope of spectrum	Observed dB/octave	Water droplet noise Franz (1959) (dB/octave)
Below maximum frequency	3 to 6	1 to 2
Above maximum frequency	-6 to -7	-5 to -6

At low flows, the air bubble content in the flowing water is minimum, and water droplet noise originating anywhere in the river and transmitted through the water to the hydrophone predominates. As the flow increases, the air bubble content and the average size of the air bubbles increase, lowering the frequency at maximum spectral level.

Sediment Noise Identification

From the frequency characteristics of the noise recorded at the two observation sites and the identity of the background sources there is no evidence of gravel impact noise in the one-third octave band spectrum analysis. The apparent absence of an identifiable gravel noise component from the observed spectrum could have been caused by a number of factors.

Positive confirmation of gravel movement during periods of acoustic sampling by visual means or with basket samplers was not possible because of suspended materials in the water and time delays between acoustic and basket observations. Due to the intermittent nature of bed movement it is therefore possible that no bed materials moved

during the acoustic observations, but this possibility is considered to be improbable for a number of reasons. Hydrophone observations, especially at the Vedder site, were deliberately made during flow periods that were more favourable to bed-load transport than the subsequent periods of basket sampling. Multiple noise samples were obtained and analyzed at different times and various sampling stations. During days of high flow in the Vedder River, a rumbling noise, resembling sound generated by rolling pebbles, was often audible to personnel operating the acoustic recording equipment in the cable car. Also, on one occasion (test 19, station 53.34 m) gravel movement was confirmed by a 3-cm pebble lodged in the cage ring protecting the ITC hydrophone.

The most probable cause of the absence of the pebble noise component in the underwater noise spectra is its masking by the background noise. Evidence supporting this possibility is available from the results of the special tests on the effects of particle size on sound frequency distribution characteristics. Although distinctly audible to observers stationed on the river bank some 15 m away from the source location, the maximum pressure spectrum level obtained in the special tests at the frequency of 1 kHz did not exceed 3 dB. Assuming that the sound was generated by only one half of the 15 kg of the pebbles cascading in the 0.3 m wide container bag in a five-second interval, the equivalent rate of bed-load transport was estimated at 300 kg/m min. On the other hand, when only a trace of bed-load movement was detected in test 5, the minimum PSL observed at 1 kHz was 6 dB near the river bank and 15 dB at station 53.34 m where the maximum bed-load sample indicating a rate of transport of 3.27 kg/m min was obtained. Clearly, even when allowance is made for error in estimating the transport rates, the difference in PSL shows the pebble-generated sound to have a relatively low level, which can be masked by the background noise.

The absence of distinct pebble noise component in the observed spectra can also be caused by the failure of the bed-load movement to generate sound and the similarity of pebble and background noise frequency characteristics. As indicated in Chapter 1, the acoustic power generated by individual pebbles depends on the rate of change of momentum owing to collisions with other particles. Because the mass of individual pebbles remains constant, the rate of change of its momentum depends on the change of velocity and is determined by the pebble velocities before and after the impact and the angle of collision between them. An increase in the rate of bed-load transport can occur when the velocity of particles increases. But an increase in the pebble velocity generally decreases the angle of collisions, reduces the rate of change of momentum and decreases the generated acoustic power. Eventually, as the angle of collision approaches 0°, the particles begin to saltate, further reducing the number of sound-producing collisions. It is therefore conceivable that this process was also responsible for the reduction in the sound levels owing to particle collisions below the levels produced by background noise.

The frequency characteristics of the noise produced by the different sizes of pebbles in the special tests show continuous spectra with the frequency at maximum PSL decreasing with pebble size. A natural mixture of riverbed particles of different sizes would therefore create a wide spectrum that could resemble air bubble or water droplet noise spectra.

In some tests, the maximum values of bed-load transport rates g_s and PSL were found to occur at the observation stations. At the Vedder site these occurred at station 53.34 m in three of the four days with confirmed bed-load movement, and at the Fraser site, the location of maximum PSL and g_s values coincided in one of the two tests.

Although a cause-effect relationship between g_s and PSL is suggested by the result above, other evidence indicates these parameters to be unrelated. First, from station and test spectrographs and also from typical PSL distributions across the river at the Vedder site at 0.5 kHz and 1.0 kHz, presented in Figures 63 and 64, it can be seen that maximum PSL in all tests, regardless of the bed material movement, occurred near station 53.34 m. Secondly, the total difference in PSL between stations such as 15.48 m where bed material never moved and the station 53.34 m appears to be relatively constant. For example, at 1 kHz, it ranged between 8 dB and 10 dB in all except one test. In test 10, with confirmed bed-load movement, this difference was 7 dB. Also, relatively high g_s measured at stations other than 53.34 m were not reflected by comparable changes in the PSL, although this may have been due to the time lag between acoustic and bed-load observations. From these observations and previously established spectral identities of background noise sources it must be concluded that PSL variability across the river was not dependent on bed-load movement. It may indicate, however, that the highest noise levels owing to background sources occurred at river stations most favourable to bed-load transport.

The analysis of the PSL variation with observation distance from the riverbed shows PSL independence of the distance in the bands centred on 2236 Hz and 8944 Hz. The PSL, however, was found to be distance-dependent at 0.05 level of significance in the band centred on 354 Hz in eight of the 14 cases analyzed with PSL decreasing with the distance from the bed. This result is confirmed also by 1973 results showing a general decrease of SPL with distance even in the absence of bed-load movement.

Decreasing PSL with distance from the bed at the low frequency indicates source location to be near or at the riverbed. Its most probable cause are the turbulent pressure fluctuations generated by the flow at the very rough riverbed boundary. The possibility of this noise being due to gravel pebble collisions must be discounted because PSL decreased with distance also in the absence of bed-load movement.

At the high frequencies examined, the independence of PSL from the observation distance to riverbed indicates either an absence of noise frequency components or the masking of the near-bed noise sources by the background sources contained in the flow.

SUMMARY, CONCLUSIONS AND RECOMMENDATIONS

A field program was undertaken to obtain data on underwater noise and sediment transport in natural gravel-bearing rivers, for use in the study of the feasibility of acoustic technique for bed-load measurement. Observations were carried out in 1973 and 1974 at two study sites in British Columbia. Two different hydrophone systems were used to record underwater noise during the periods with and without bed-load movement. Noise samples were recorded with hydrophones at various stations across the rivers and at different distances to the riverbeds. Experiments were conducted to determine the effect of riverbed pebble sizes on the sound spectrum generated by pebble collisions. Observations were also made of bed-load transport and flow velocities.

Acoustic data processing consisted of one-octave or alternate one-third octave band frequency analysis. Individual spectrographs were analyzed for gravel pebble collision noise components and background noise source identities. An attempt was made to relate measured bed-load transport rates with observed sound pressure levels.

From the experimental results, the following conclusions were reached:

1) Gravel pebble collision sound components cannot be identified from the underwater river sound spectra between frequencies 50 Hz to 30 kHz because of masking by background noise sources.
2) Background noise sources, identified by spectral analysis and by comparison with information contained in scientific literature include, at low frequencies, the turbulence owing to the relative velocity between the flow and hydrophone, and surface water droplets and air bubbles in the water which dominate the spectra above 500 Hz.
3) The background noise spectral levels at identical river stations increase with river stage and flow.
4) The background noise levels vary with position across the river. In the Vedder River the location of maximum levels coincides with location of maximum observed bed-load movement.
5) At low frequencies, up to about 400 Hz, the background noise spectra may contain components of turbulent pressure fluctuations generated in the boundary layer near the riverbed.

6) Pebble collision generated sound spectrum depends on the size of the pebbles. The spectrum is continuous and exhibits a maximum at frequencies that decrease with increasing pebble size.

7) The Ithaco hydrophone system can be used for relative sound level measurements in the frequency range from 400 Hz to 4000 Hz, but should not be employed in comparative sound spectrum analysis.

In view of the results of this investigation and especially the failure to identify pebble-generated noise from the total underwater noise in a river in the 50-Hz to 30-kHz frequency range by frequency analysis, the following recommendations are suggested:

1) An attempt should be made to develop a signal analysis technique based on the rate of individual collisions (impacts) between particles, and the statistical distribution of hydrophone output voltage peaks.

2) Directional hydrophones should be used to minimize background noise interference in field measurements.

3) Spectral characteristics of gravel-generated noise at frequencies above 30 kHz should be investigated.

References

Arabadzi, V.I. 1967. On the Noise of Waterfalls. Sov. Phys. - Acoust. 13(1).

Bedeus, K. and L. Ivicsics. 1963. Observation of the Noise of Bed-Load. Proceedings of International Association of Scientific Hydrology, Publication No. 65.

Beranek, L.L. 1971. Noise and Vibration Control. McGraw-Hill Book Co.

Bradeau, G. 1951. Quelques techniques pour l'étude et la mesure du débit solide. La Houille Blanche, Spéc. n° A.

Broch, J.T. 1971. Acoustic Noise Measurements. 2nd ed. Bruel and Kjaer Co.

Franz, G.J. 1959. Splashes as Sources of Sound in Liquids. J. Acoust. Soc. Am. 31 (8):1080-1096.

Hollingshead, A.B. 1969. Sediment Transport Measurements in Elbow River at Bragg Creek 1968. Report to cooperating agencies, Research Council of Alberta.

Hollingshead, A.B. 1971 Sediment Transport Measurement in Gravel River. J. Hydraul. Div., PASCE, 97(HY11).

Johnson, P. and T.C. Muir. 1969. Acoustic Detection of Sediment Movement. J. Hydraul. Res. 7(4).

Juniet, M. 1952. L'Arénaphone, un appareil détecteur des mouvements des sédiments fins. Transport hydraulique et décantation des matériaux solides, Société hydrotechnique de France.

Mühlhoffer, L. 1933. Untersuchungen über die Schwebstoff and Geschiebeführung des Inn bei Kirchbichl Die Wasserwirtschaft, No. 2.

Samide, G.W. 1971. "Sediment Transport Measurements." M.Sc. thesis, University of Alberta.

Smoltczyk, H.V. 1955. Beitrag zur Ermittlung der Feingeschiebe Menganglinie. Technische Universität (Berlin-Charlottenburg) Institut der Wasserbau Mitt. 43.

Tywoniuk, N. 1971. "Background Interference Tests for WSC Hydrophone System." Unpublished report, Water Survey of Canada, Inland Waters Branch, Department of the Environment, Ottawa.

Tywoniuk, N. and R.G. Warnock. 1973. Acoustic Detection of Bed-Load Transport, Fluvial Processes and Sedimentation. Proceedings of the 9th Canadian Hydrology Symposium. Ottawa: Information Canada.

Urick, R.J. 1967. Principles of Underwater Sound for Engineers. McGraw-Hill Book Co.

Wentz, G.M. 1962. Acoustic Ambient Noise in the Ocean: Spectra and Sources. J. Acoust. Soc. Am. 34(12).

White, B.F. 1975. "A Bed-Load Transport Acoustic Monitor for Use in River System Studies." Unpublished report, Electronic Engineering Unit, Canada Centre for Inland Waters, Burlington, Ontario.

Figures 1 to 64

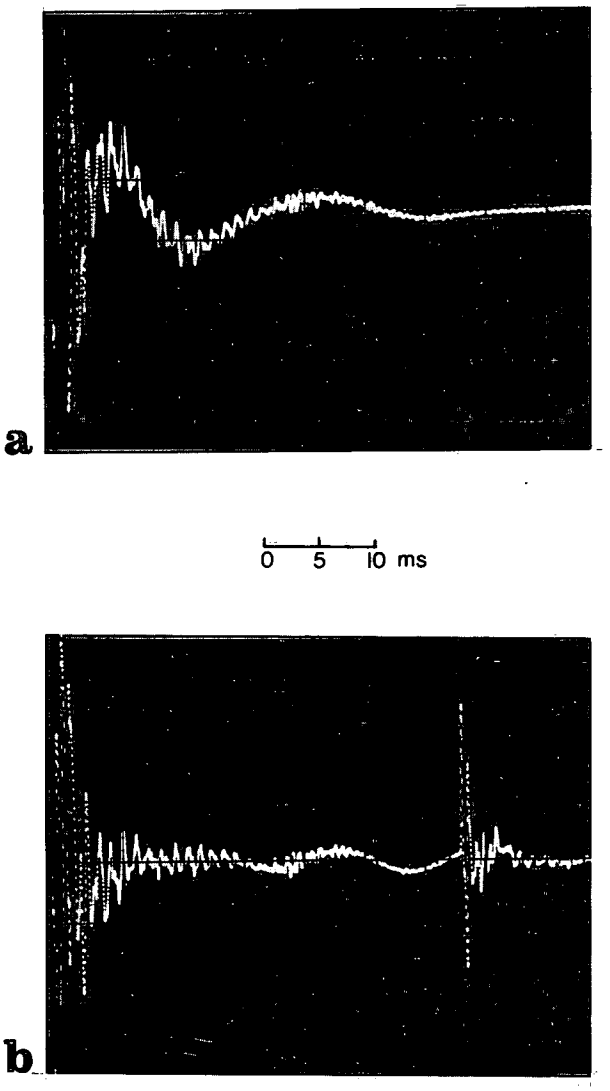

Figure 1. Collision sound transients
a) single collision and
b) two collisions.

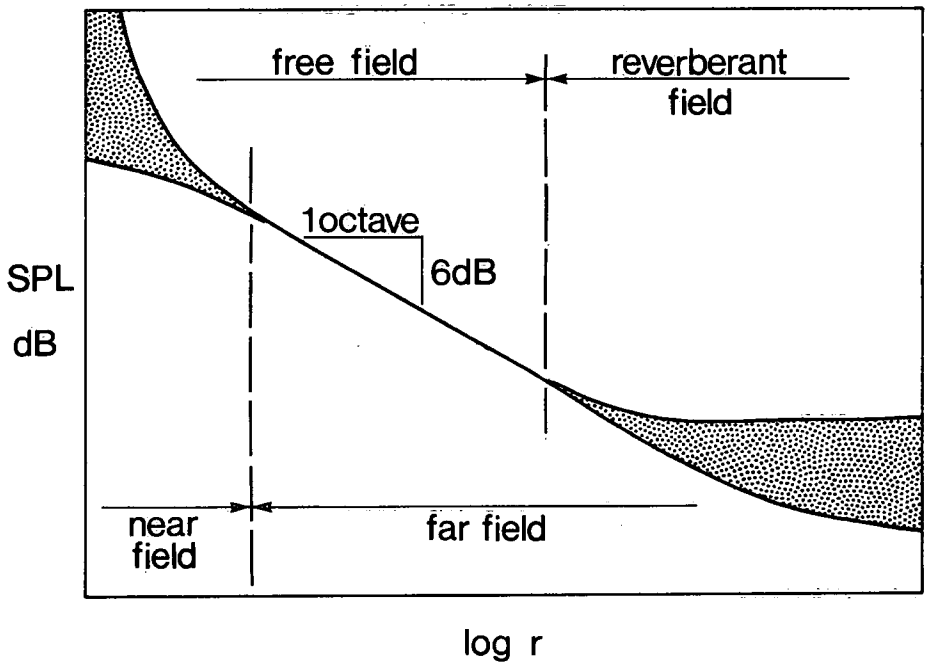

Figure 2. Acoustic fields in an enclosure (from Broch, 1971).

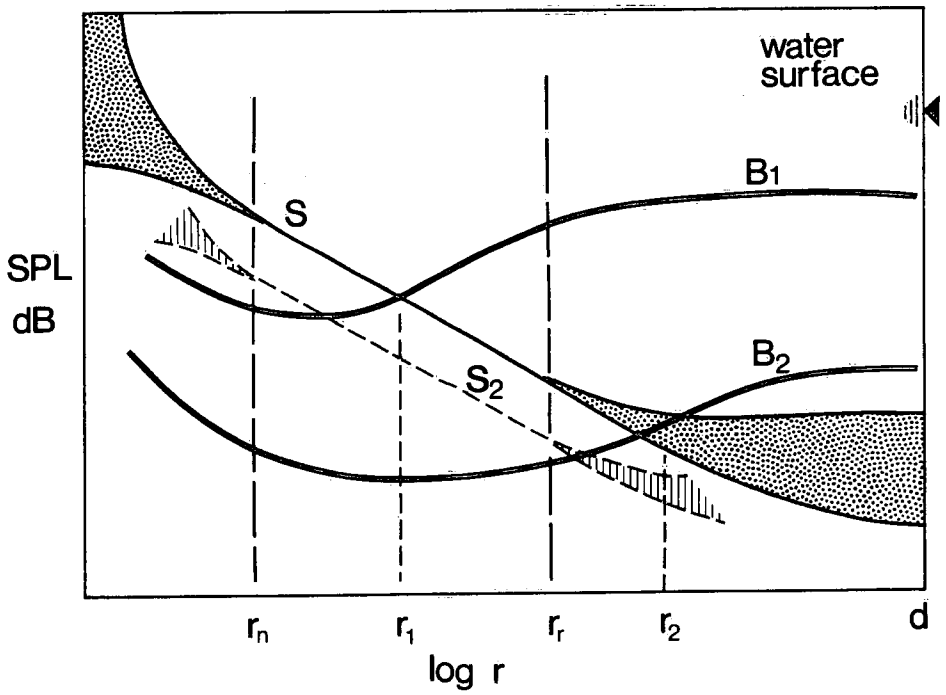

Figure 3. Effects of background noise.

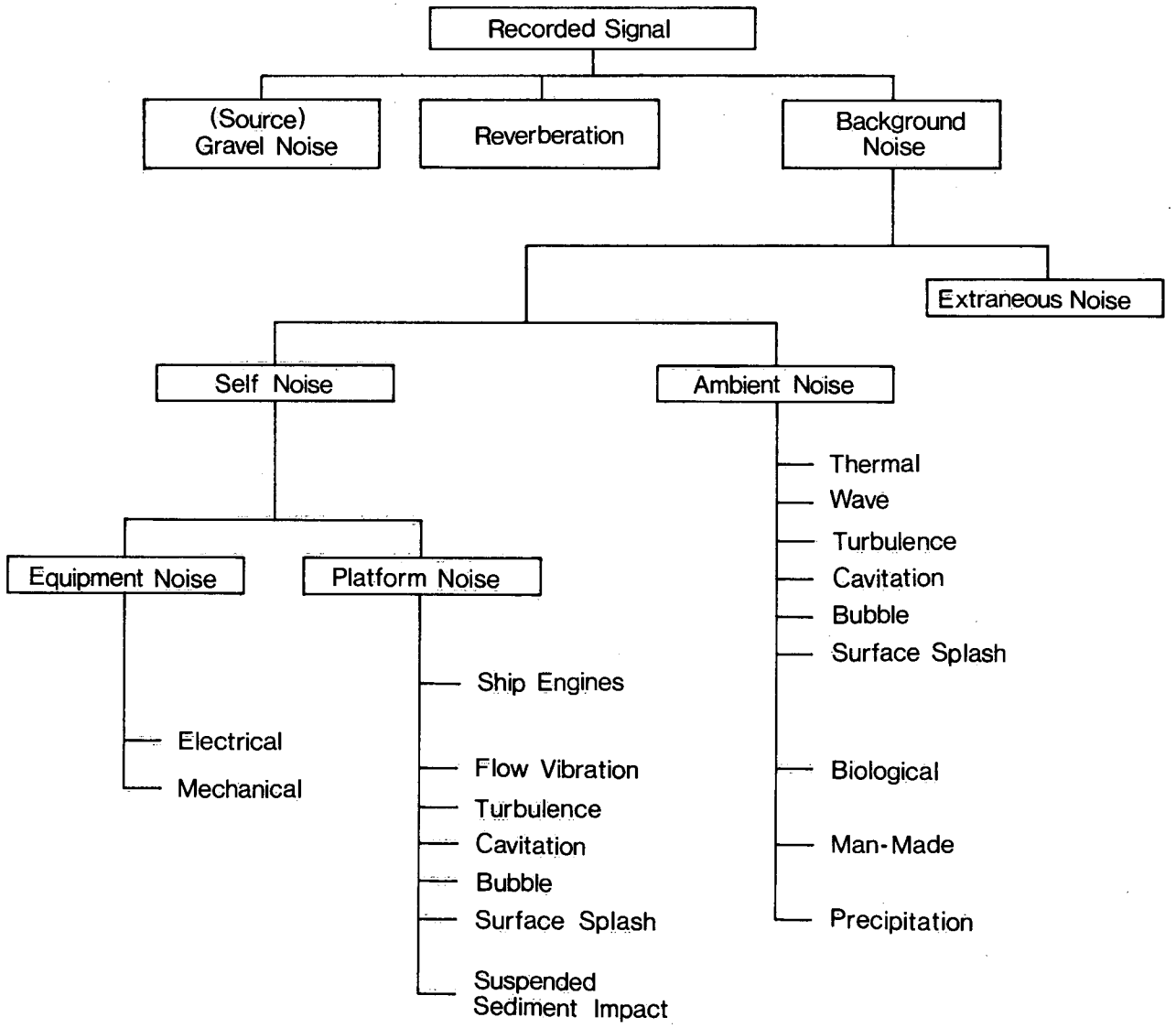

Figure 4. Sources of noise in river environments.

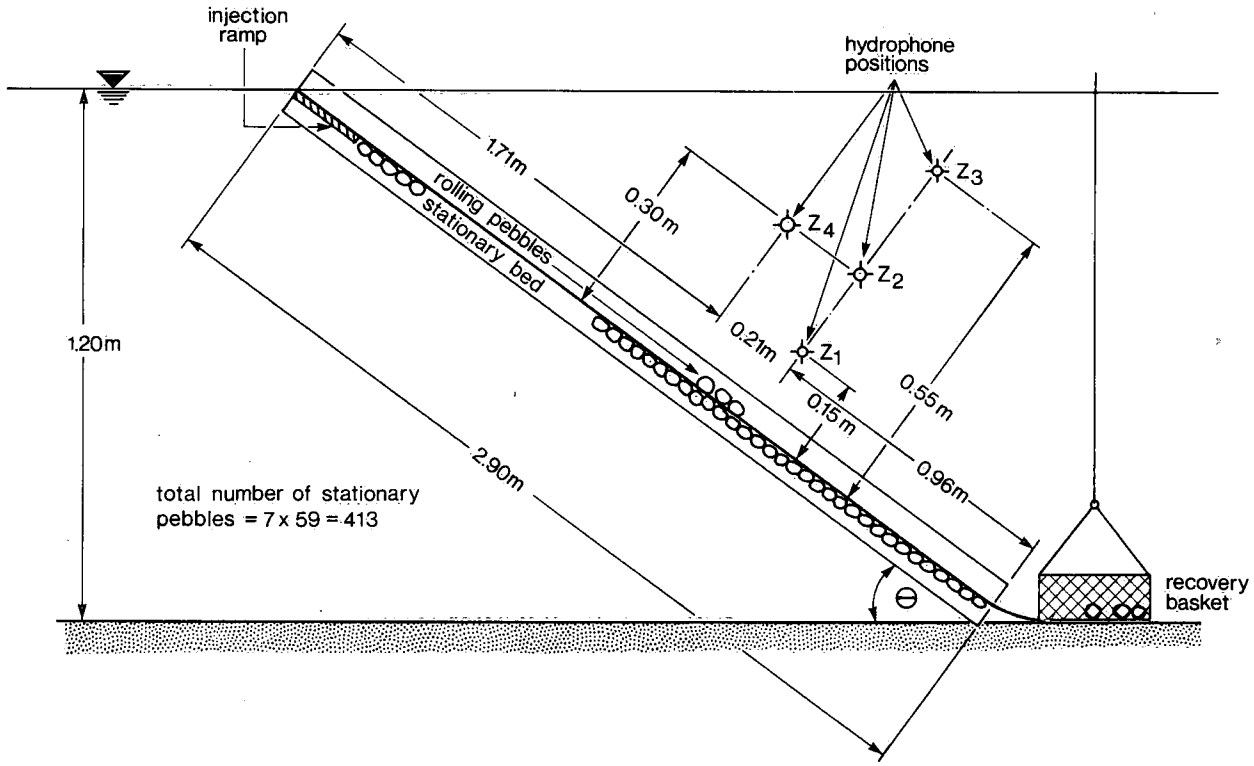

Figure 5. Pebble ramp dimensions and hydrophone positions.

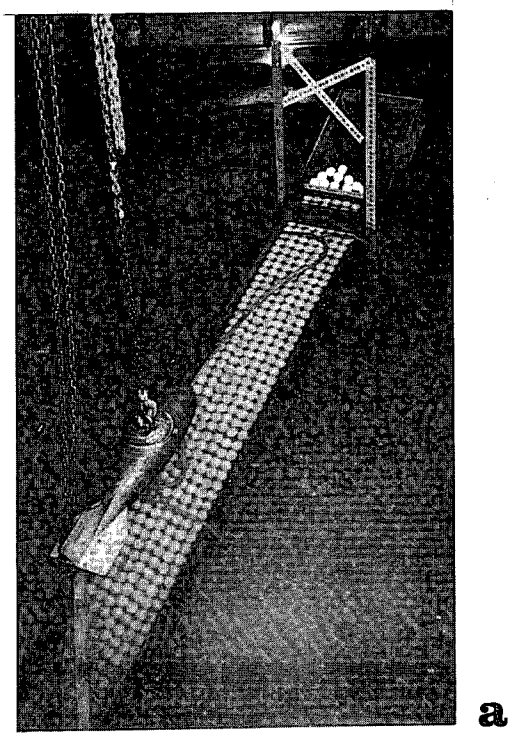

a

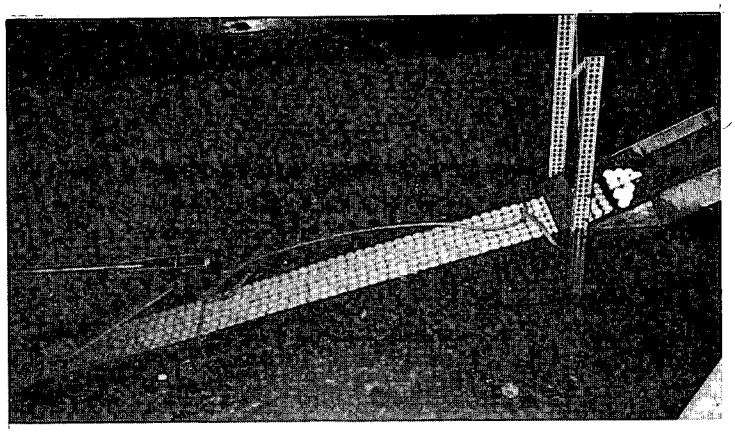

b

Figure 6. Pebble ramp with a) Ithaco hydrophone and b) ITC hydrophone.

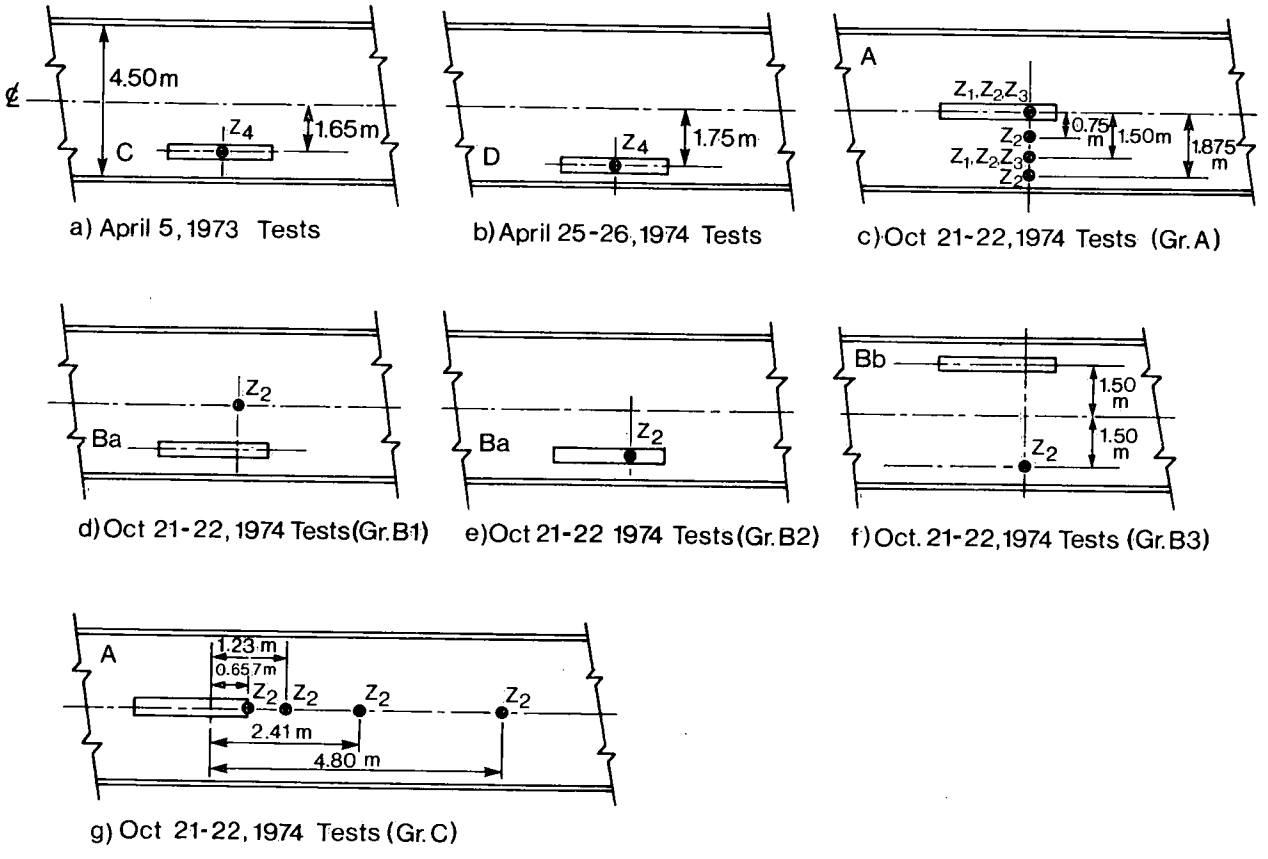

Figure 7. Hydrophone and ramp positions in the wind-wave flume.

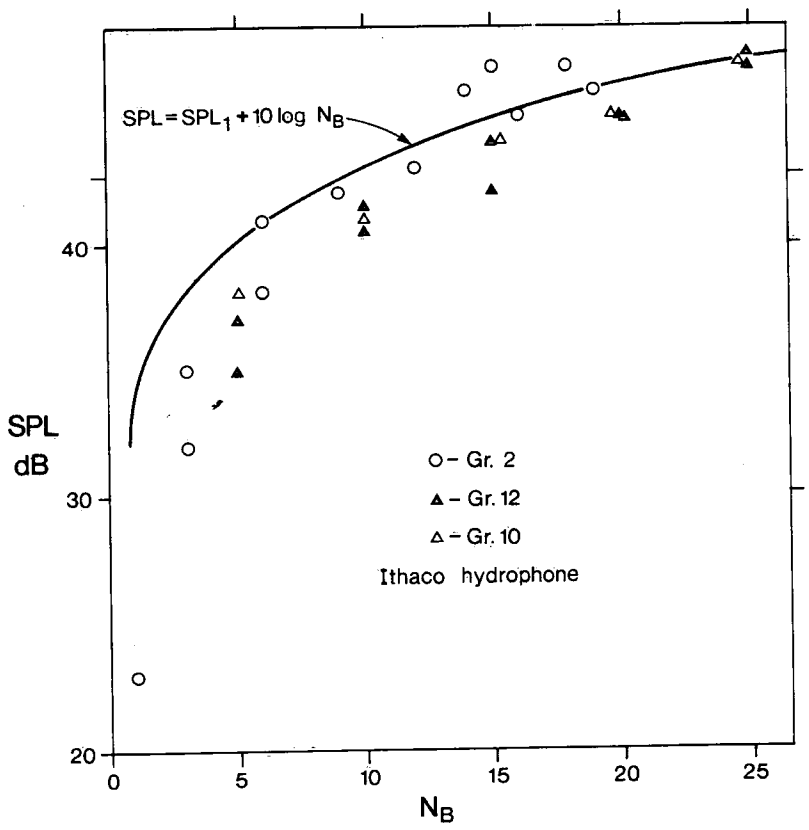

Figure 8a. SPL variation with number of rolling pebbles N_B.

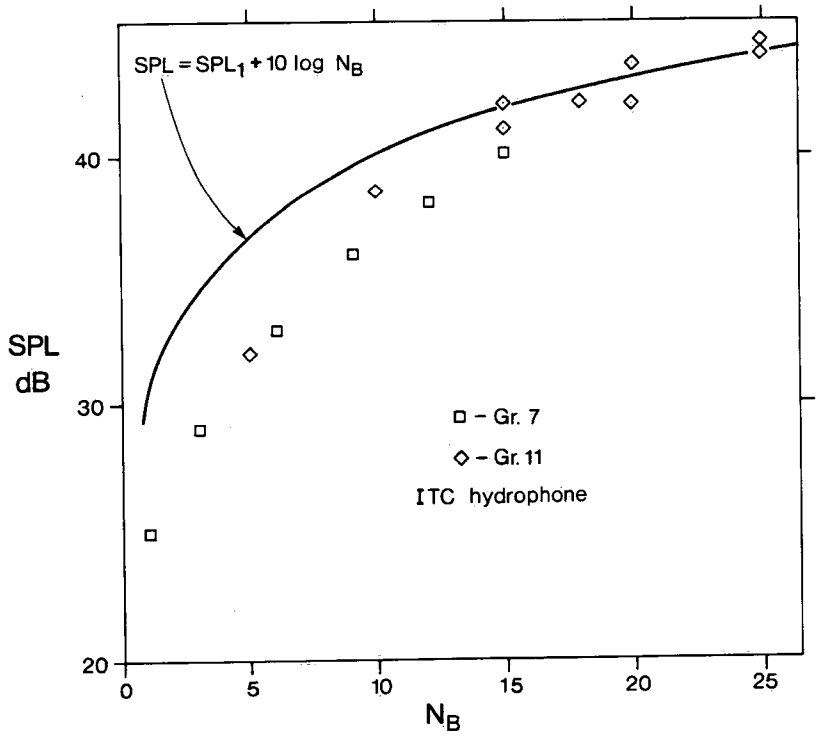

Figure 8b. SPL variation with number of rolling pebbles N_B.

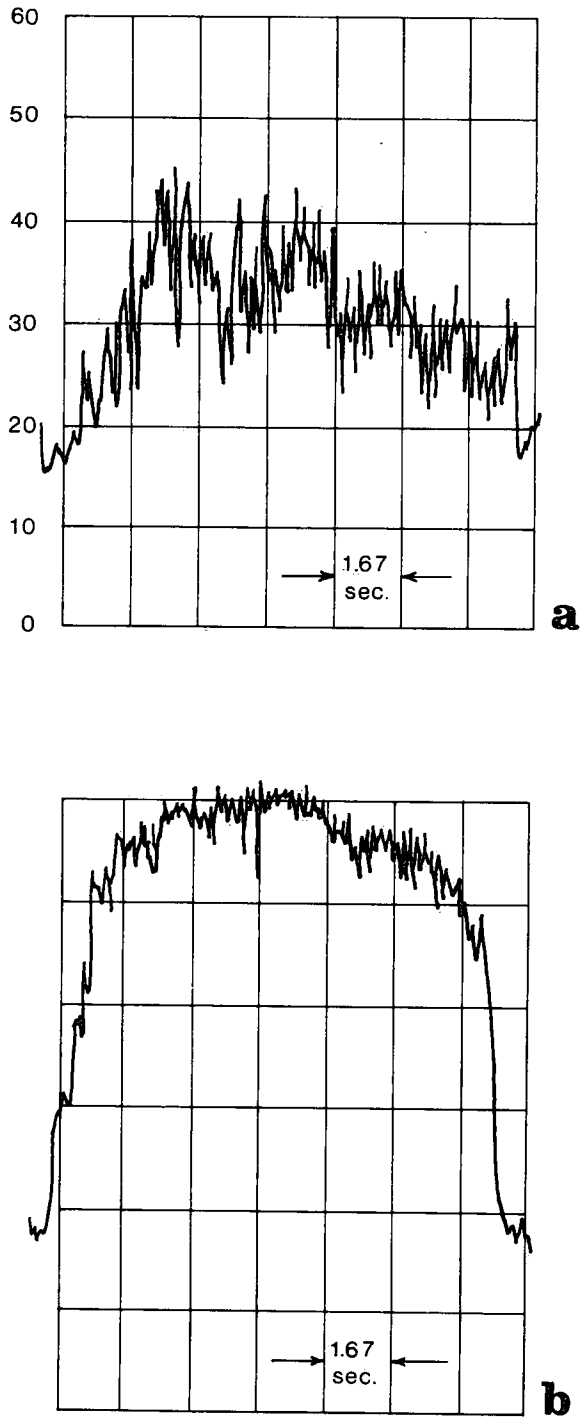

Figure 9. Recorder output a) 1 ball and b) 9 balls.

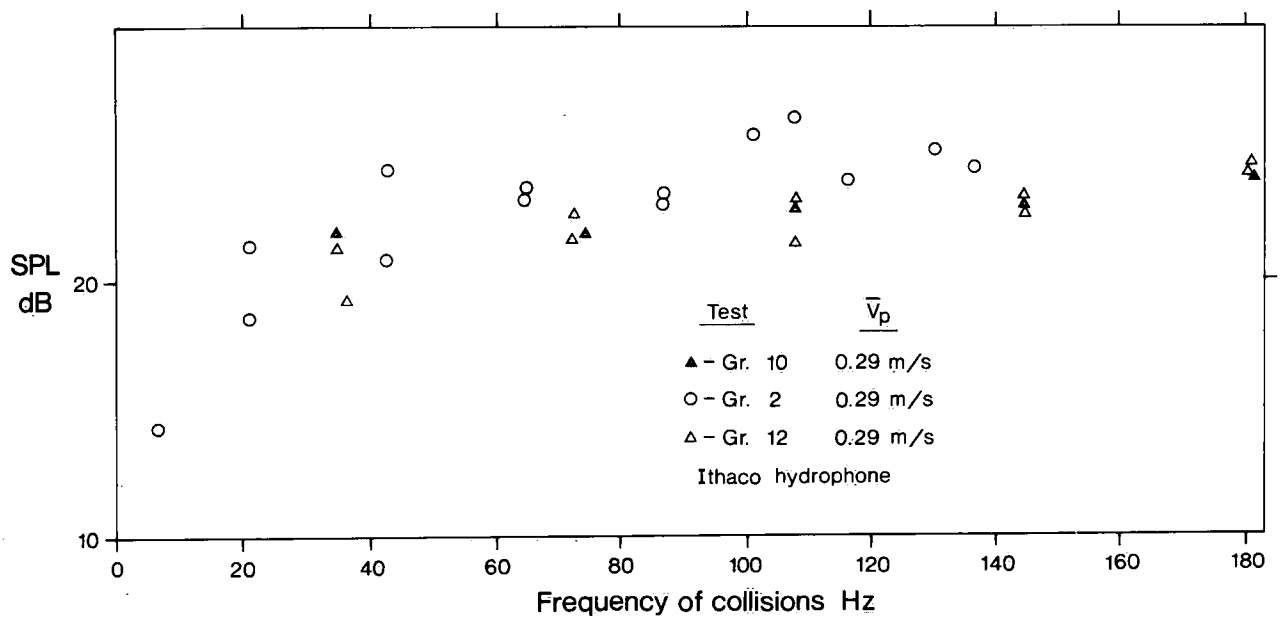

Figure 10a. One collision equivalent SPL variation with frequency of pebble collisions.

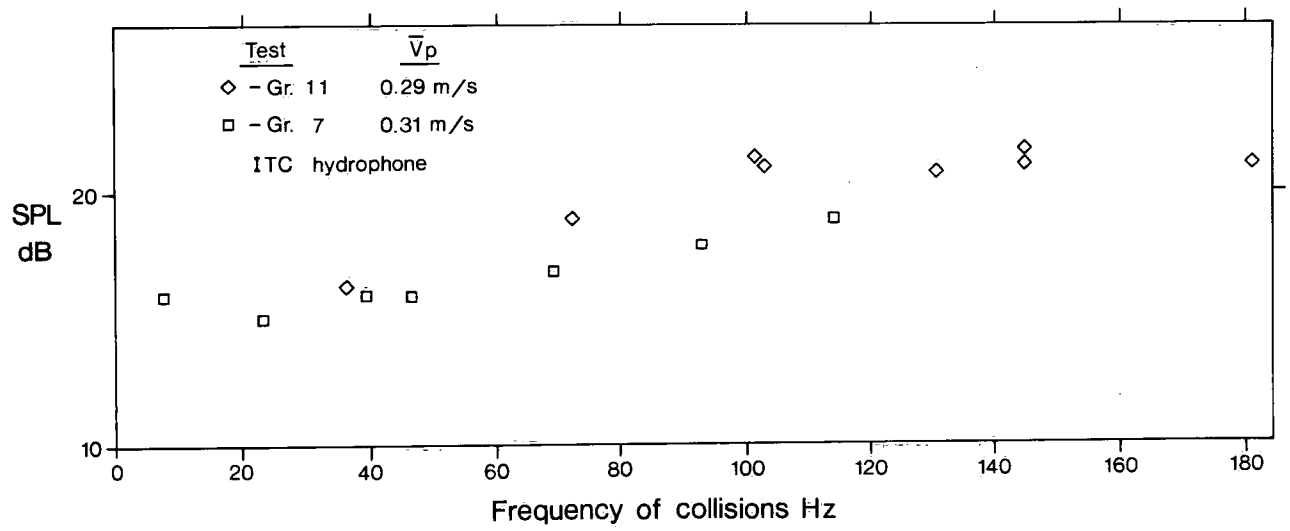

Figure 10b. One collision equivalent SPL variation with frequency of pebble collisions.

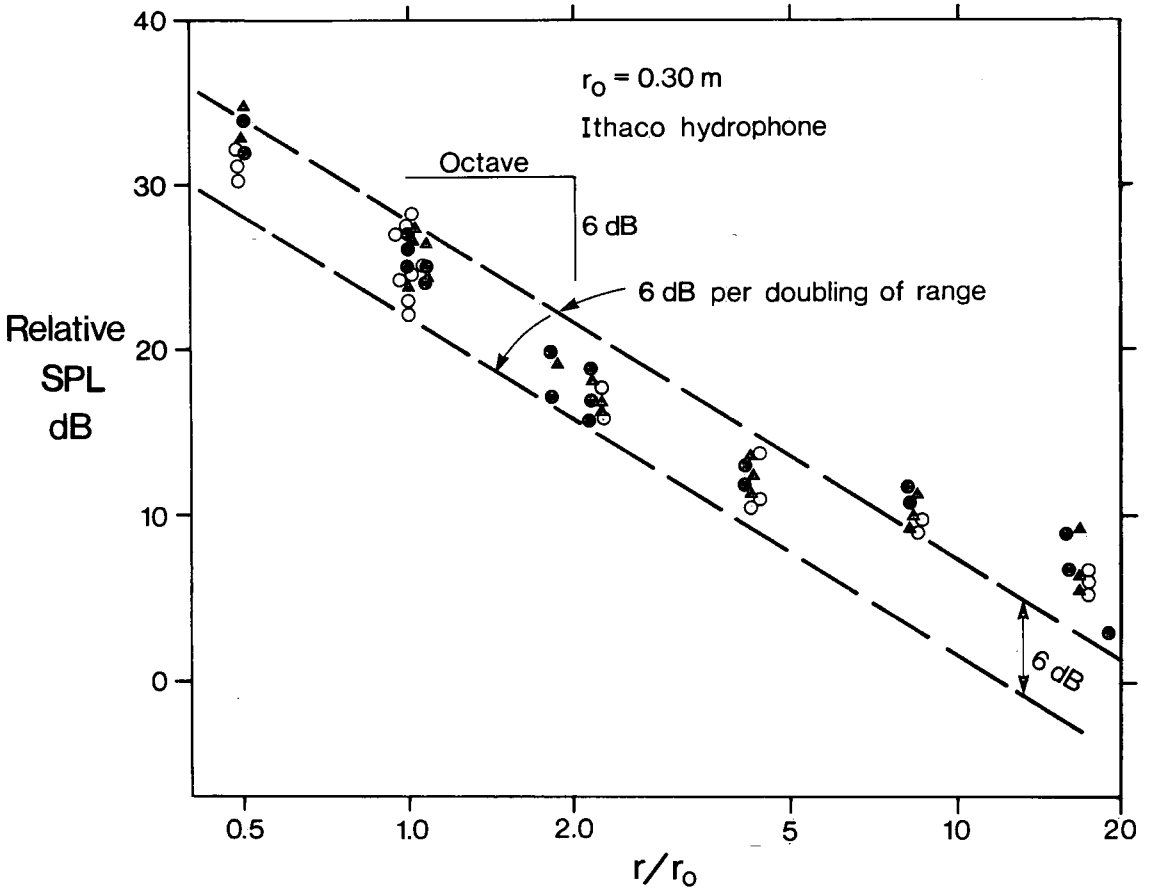

Figure 11. SPL attenuation with distance from source.

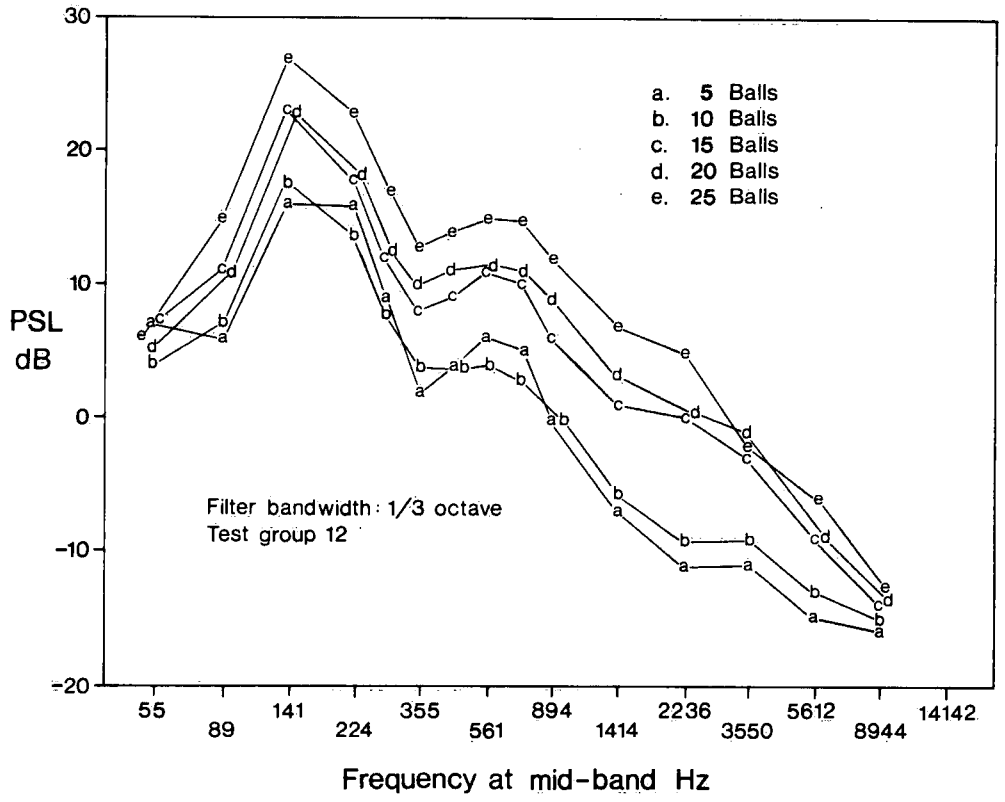

Figure 12a. Pebble noise spectra using Ithaco hydrophone.

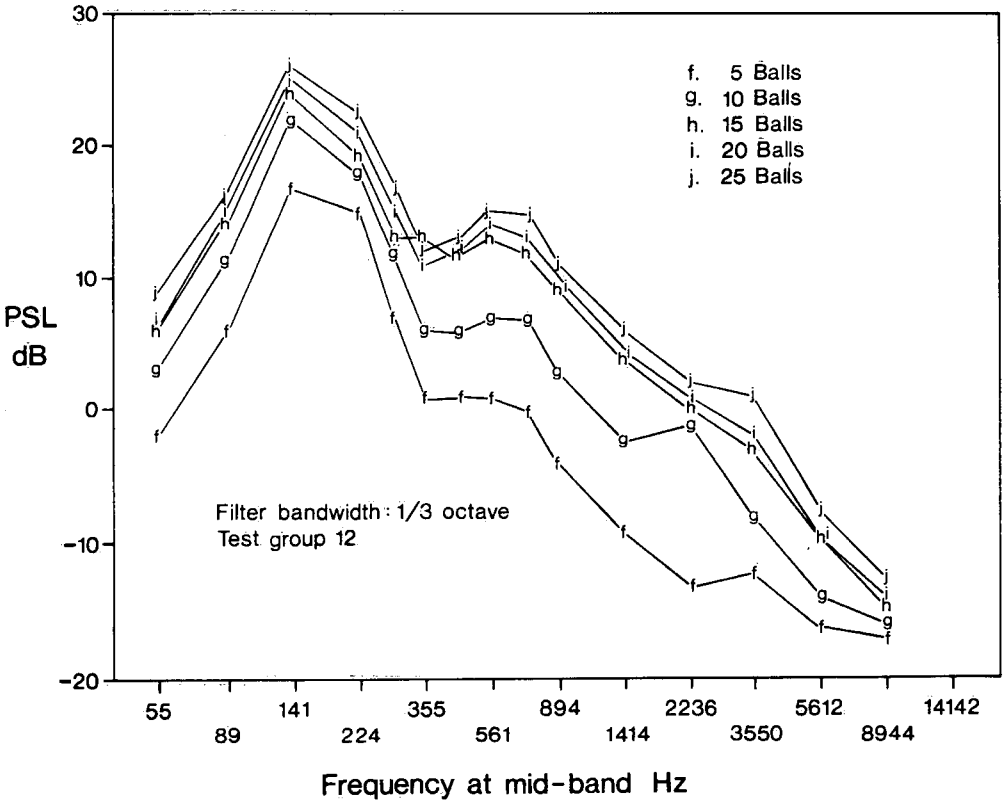

Figure 12b. Pebble noise spectra using Ithaco hydrophone.

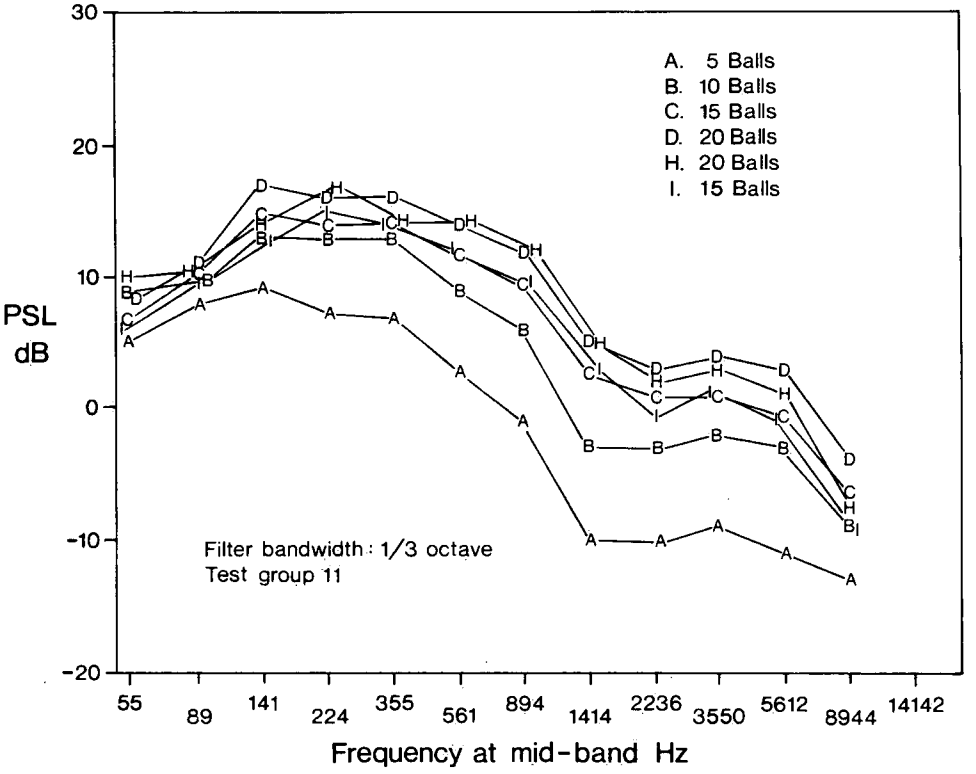

Figure 12c. Pebble noise spectra using ITC hydrophone.

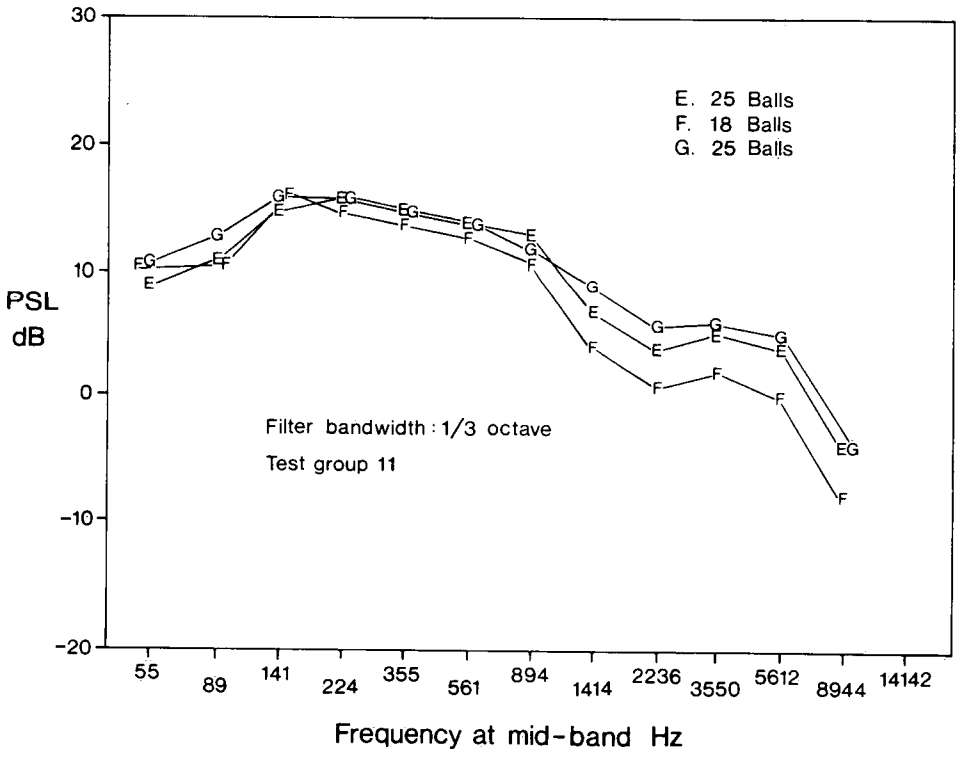

Figure 12d. Pebble noise spectra using ITC hydrophone.

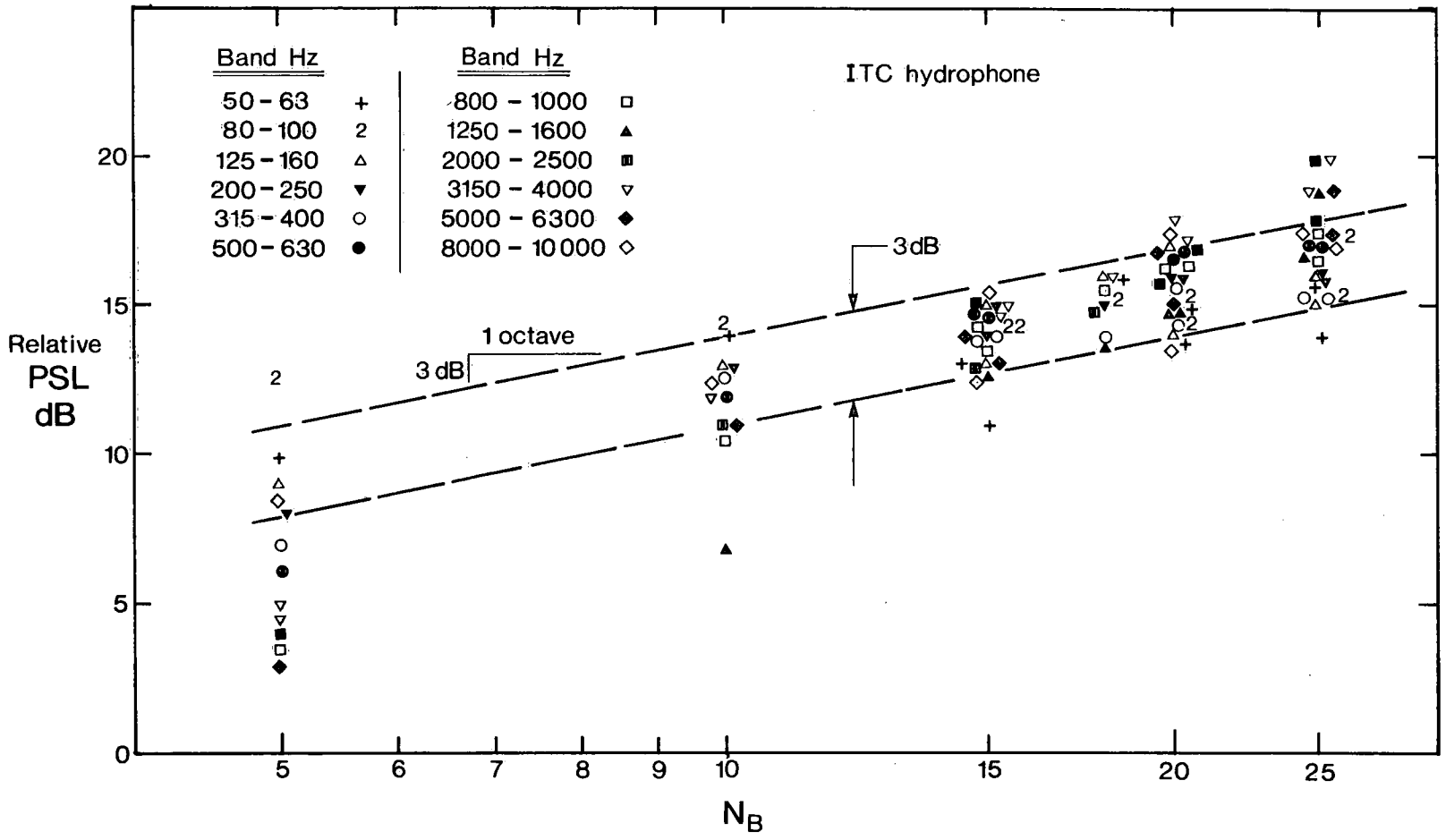

Figure 13. Relative increase in PSL with number of rolling pebbles.

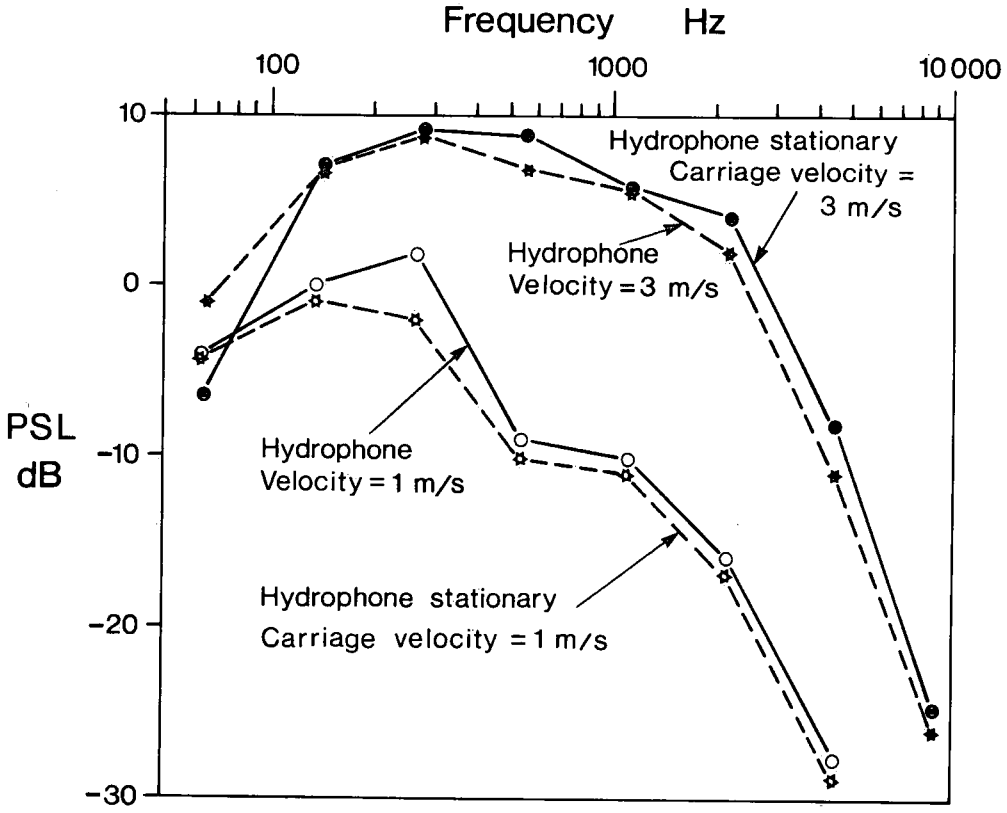

Figure 14. CCIW towing tank noise spectra using ITC hydrophone.

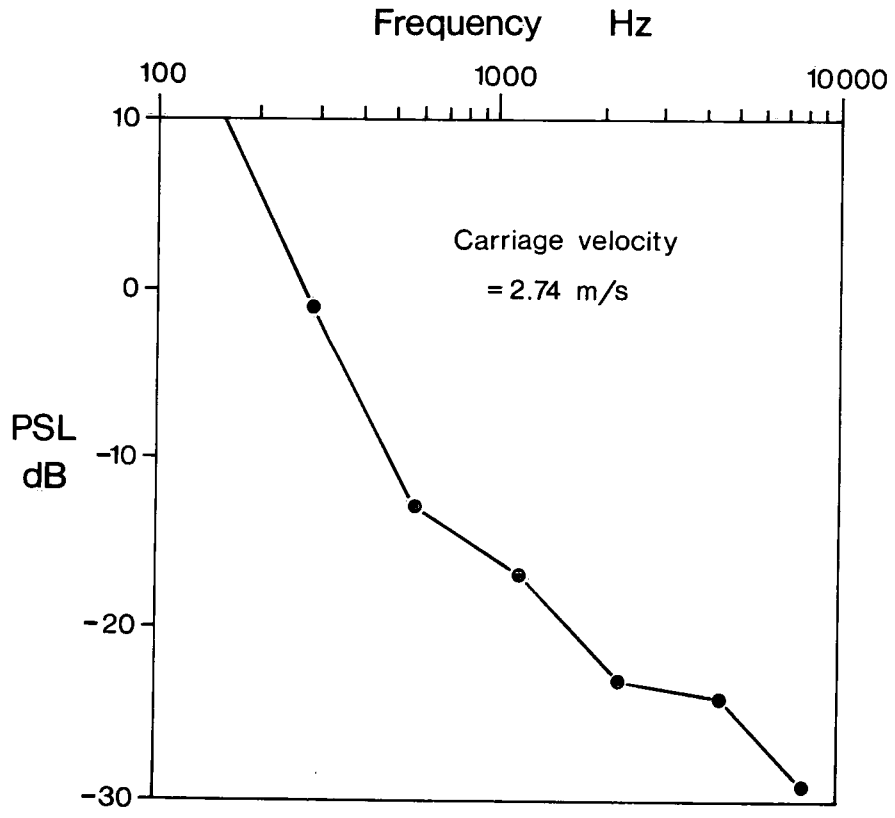

Figure 15. Calgary towing tank noise spectra using Ithaco hydrophone (from Tywoniuk, 1971).

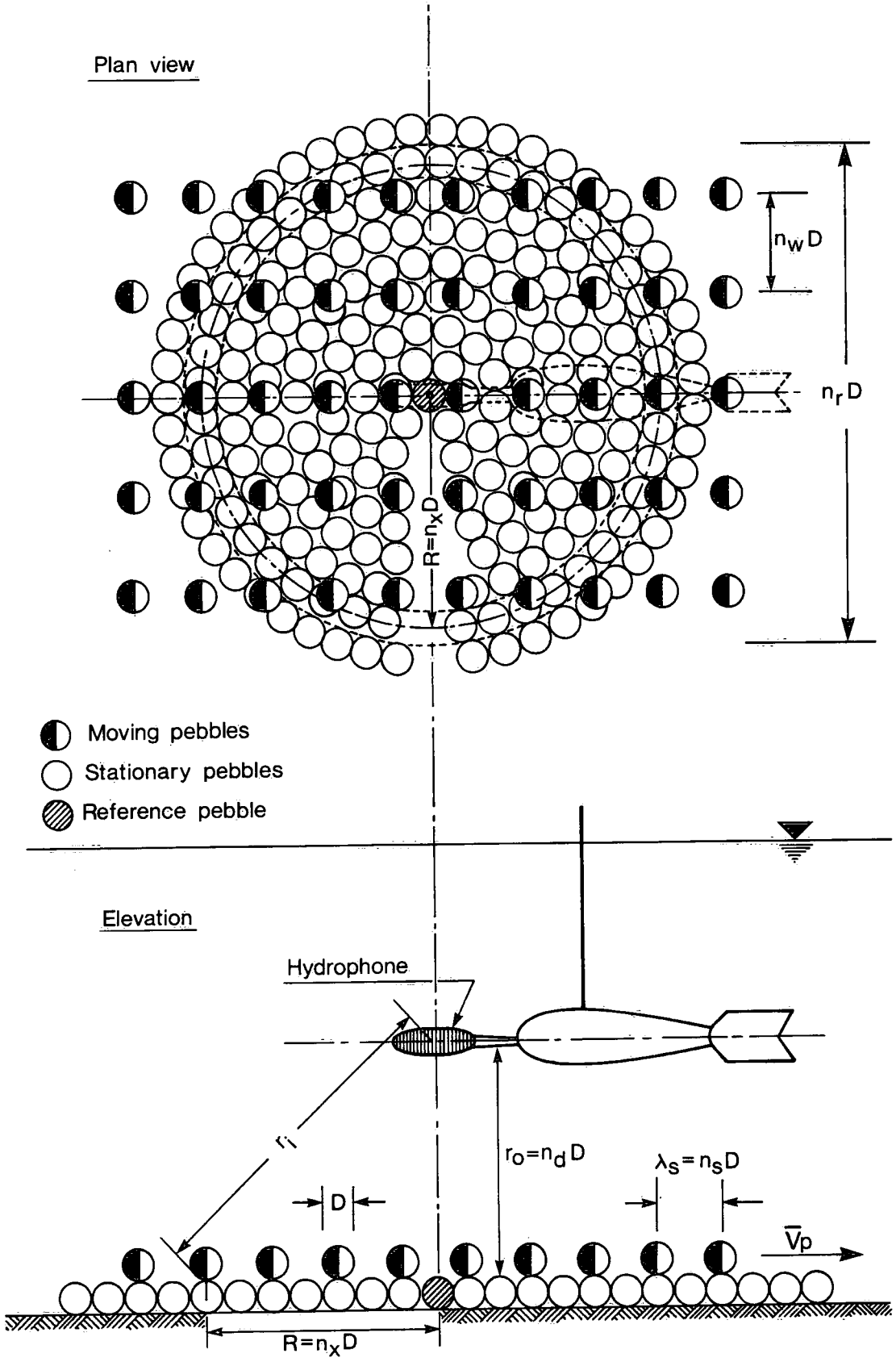

Figure 16. Pebble movement model.

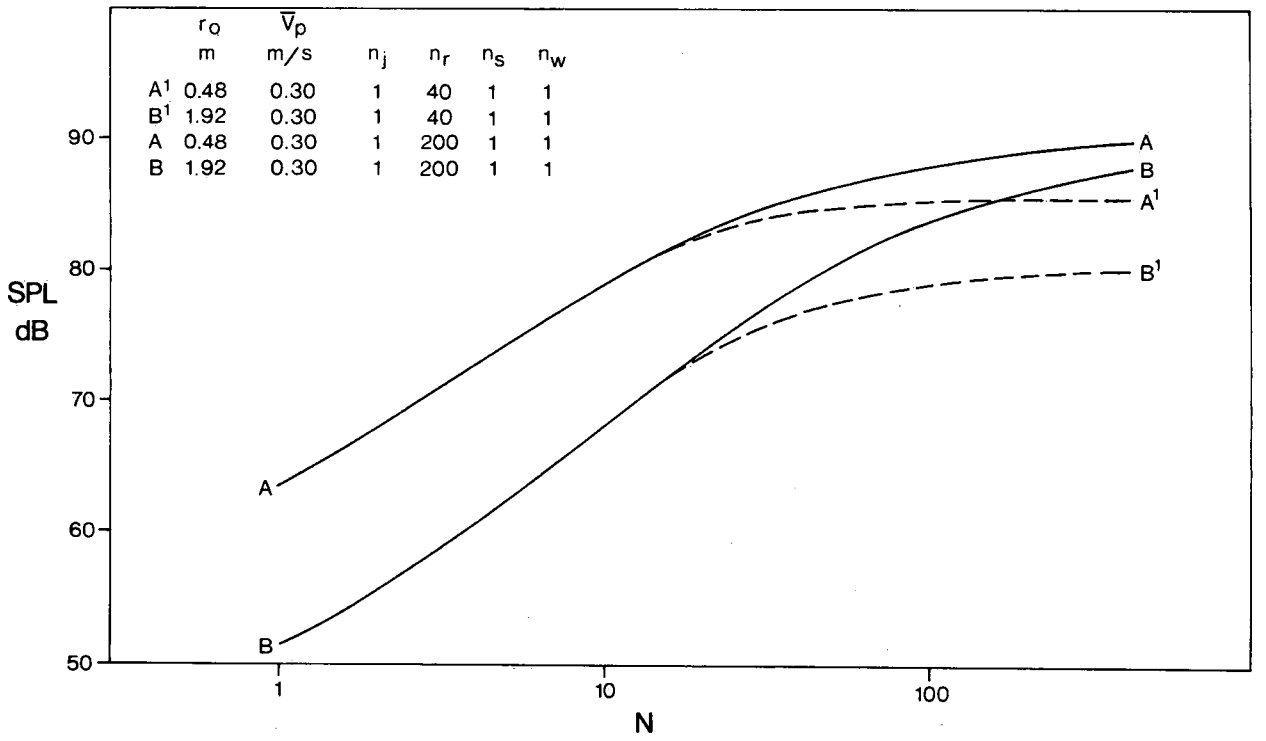

Figure 17. SPL variation with distance of hydrophone from the bed and width of moving bed.

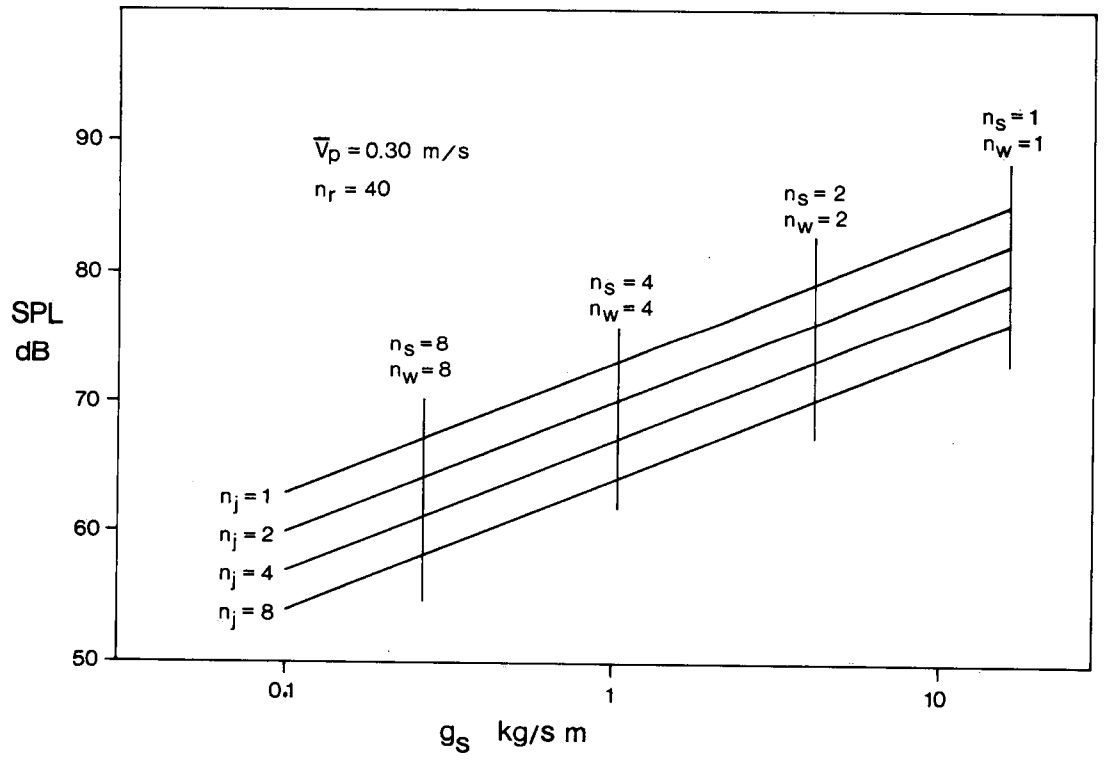

Figure 18. SPL - g_s variation for different pebble jump lengths and different aerial concentrations.

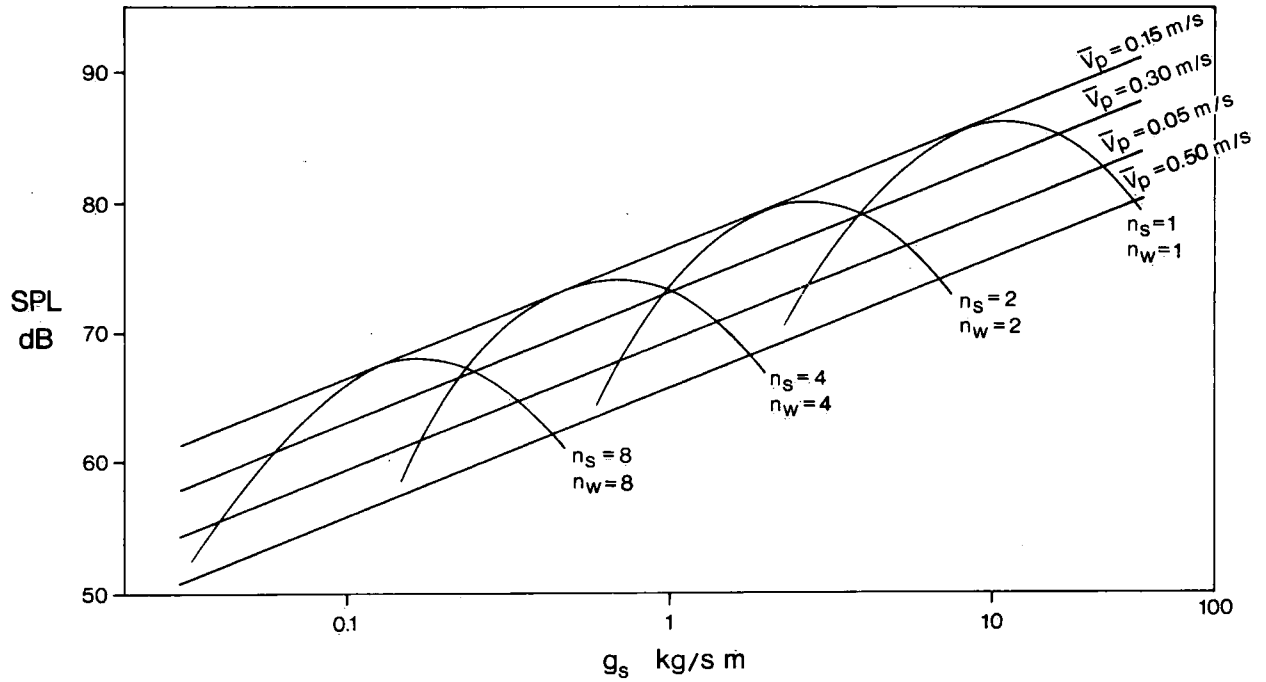

Figure 19. SPL - g_s variation for different pebble velocities and aerial concentrations.

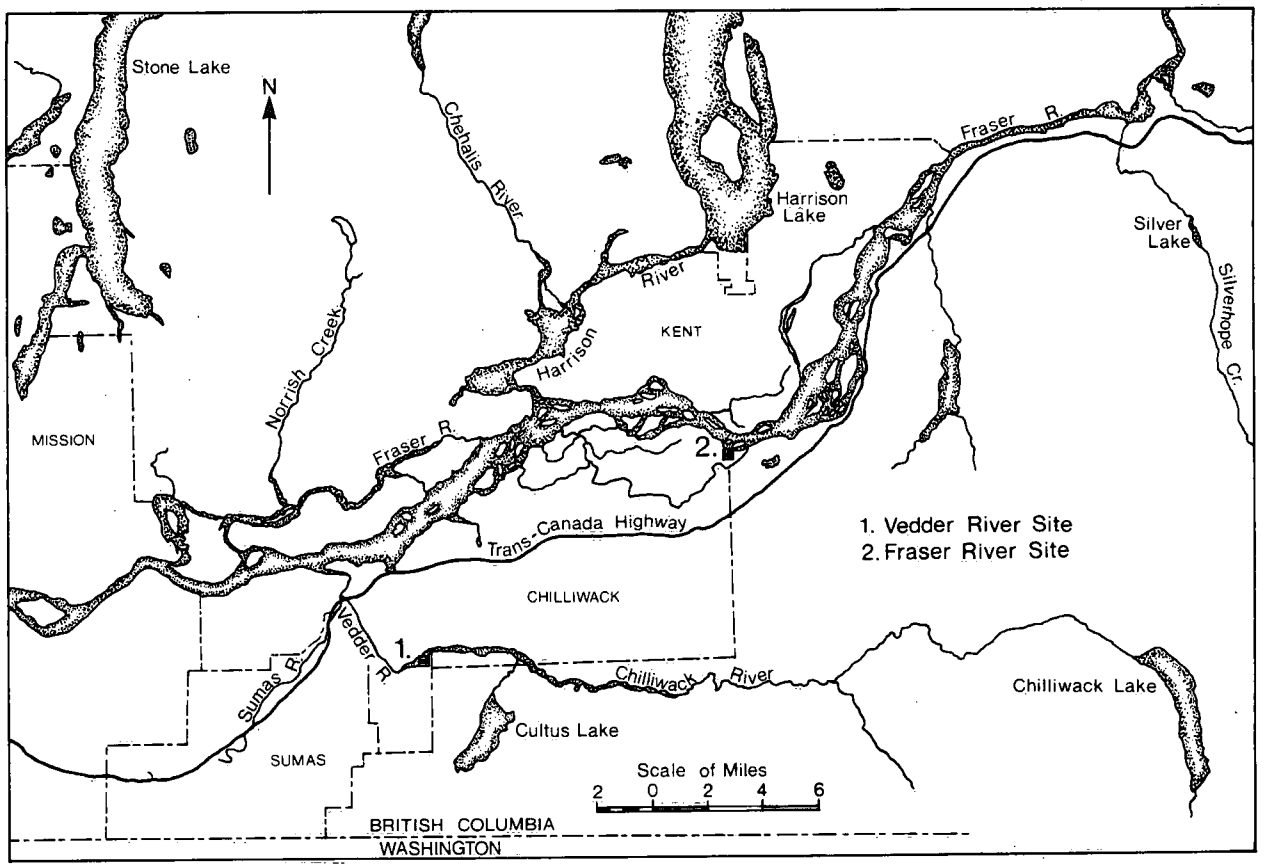

Figure 20. Site locations.

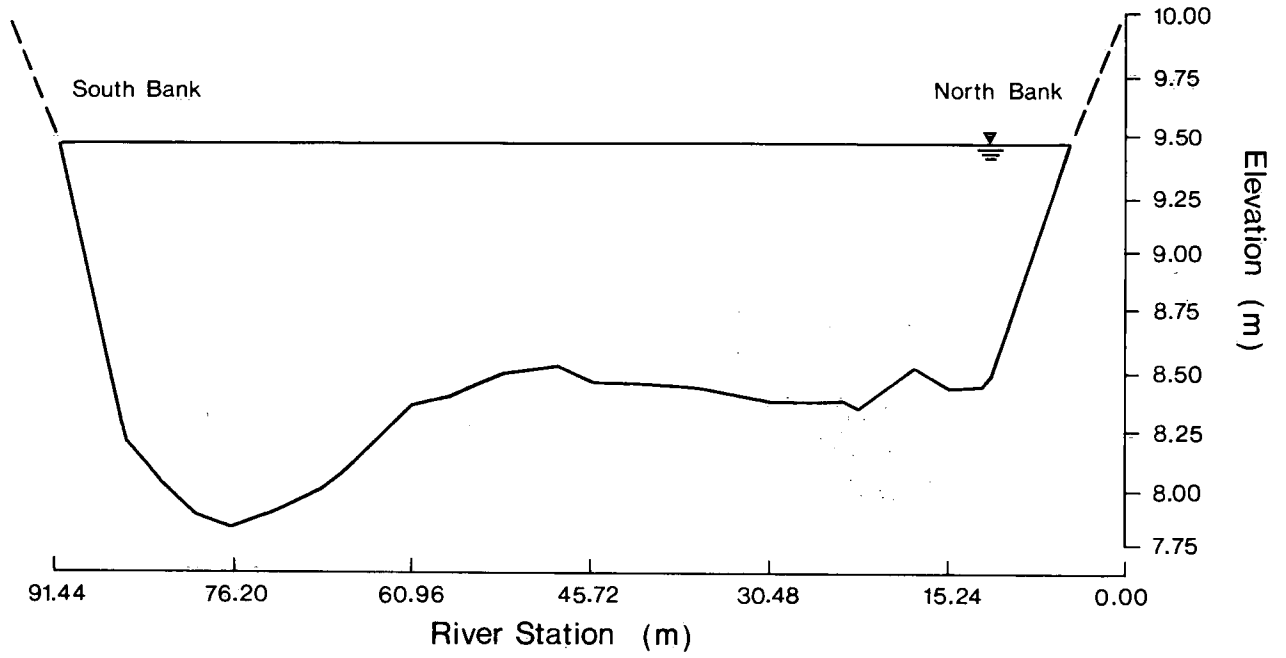

Figure 21. Vedder River site cross section.

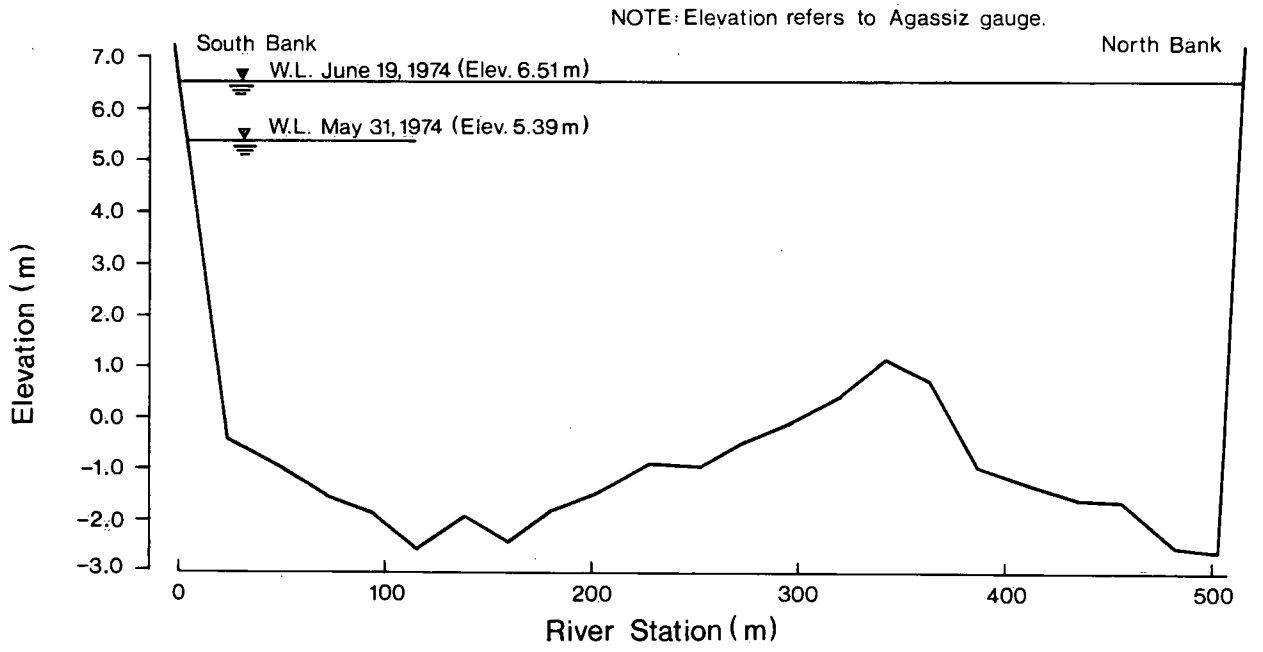

Figure 22. Fraser River site cross section.

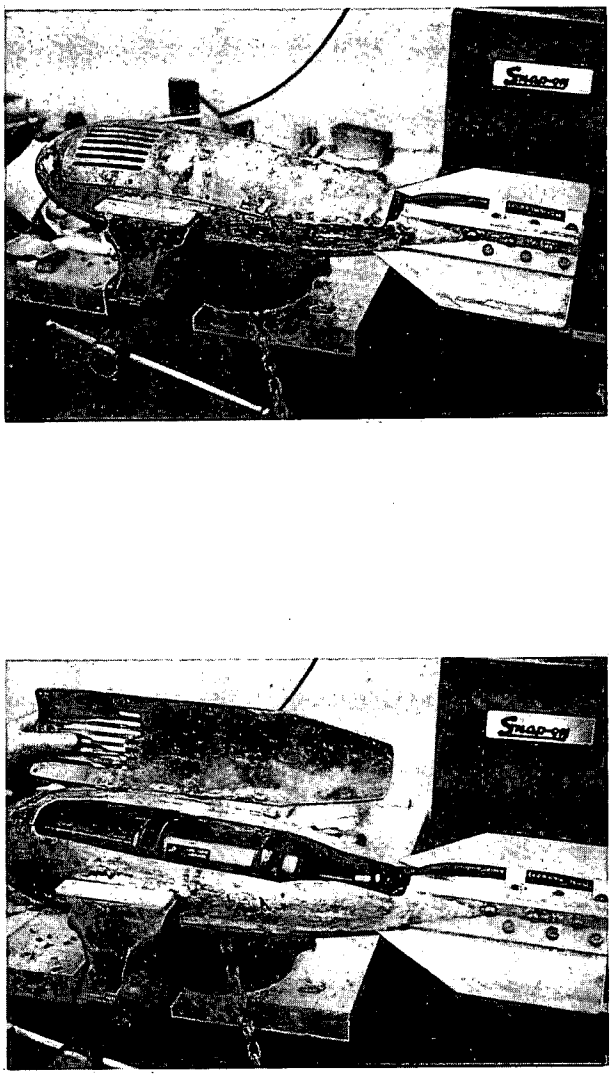

Figure 23. Ithaco hydrophone placement details.

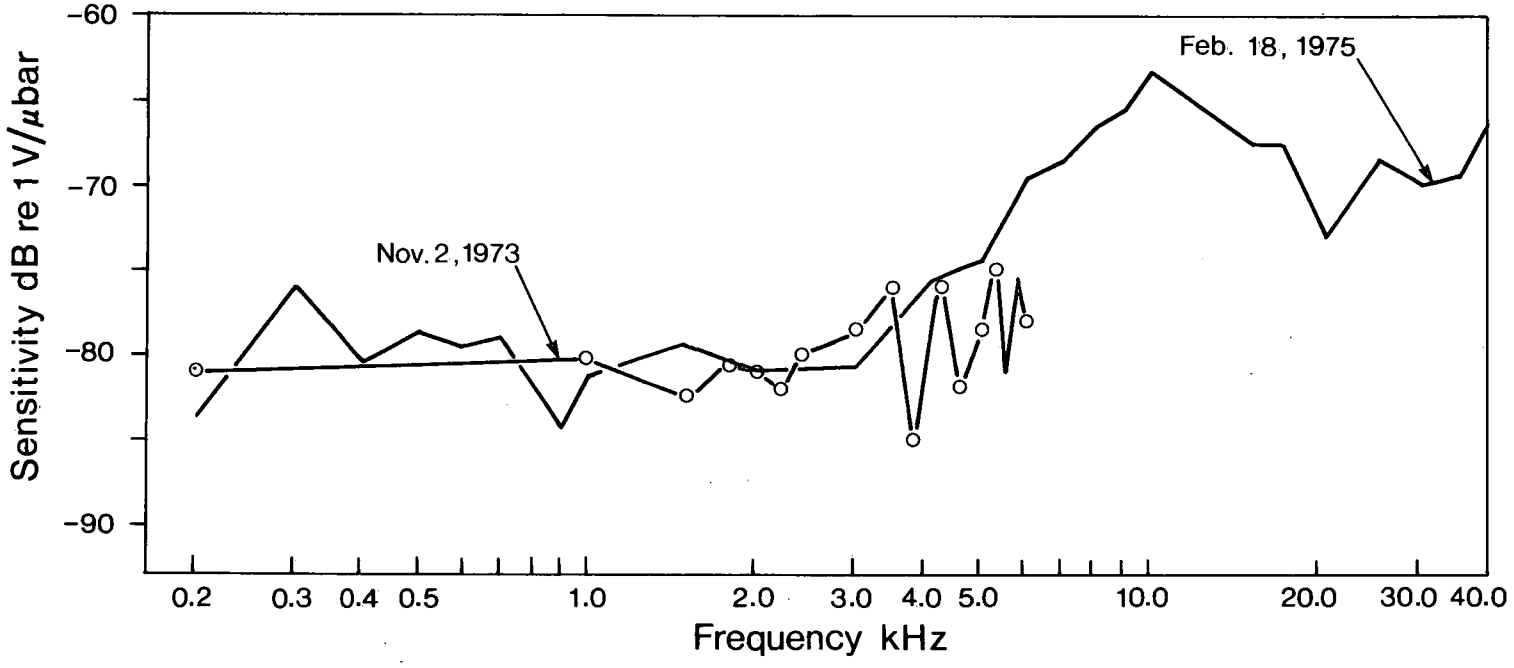

Figure 24. Ithaco hydrophone sensitivity characteristics.

Figure 25. ITC hydrophone weight assembly.

Figure 26. ITC hydrophone protective cage.

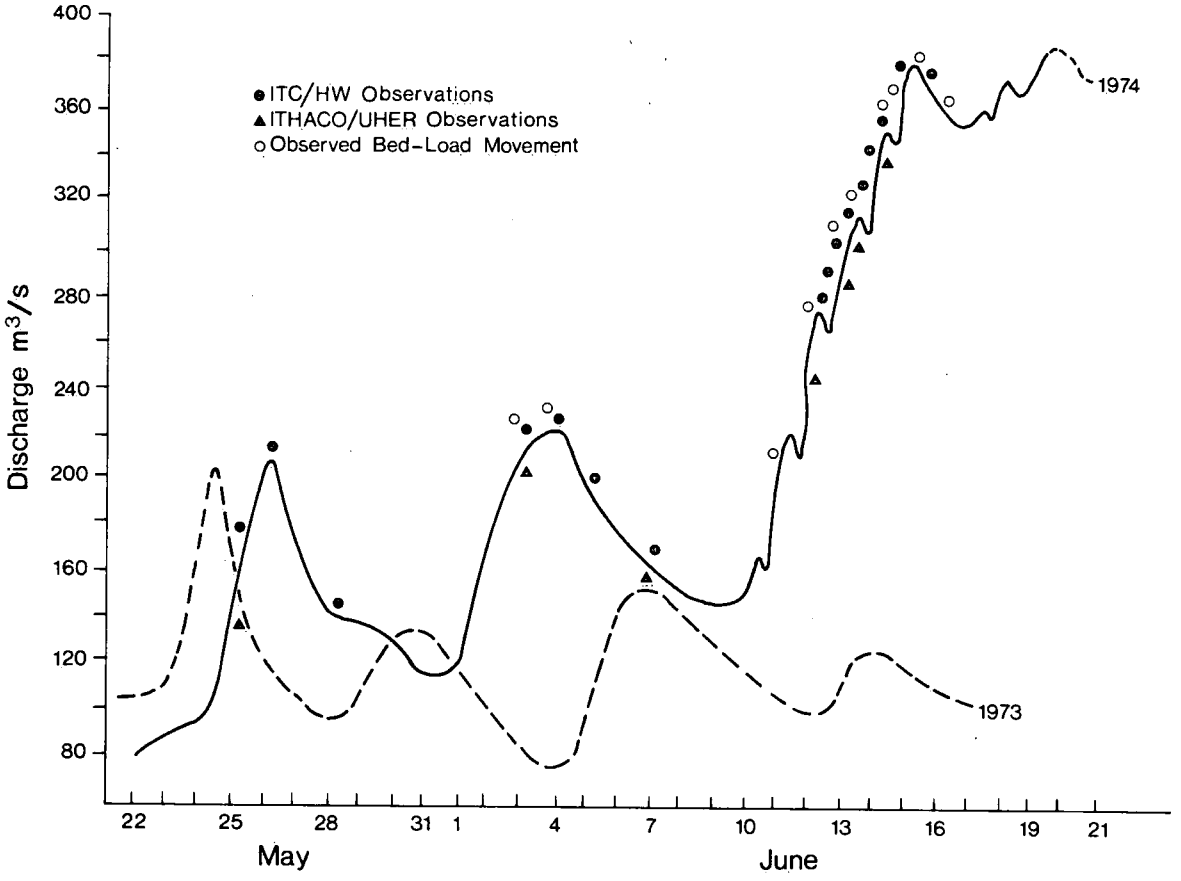

Figure 27. Vedder River flow hydrograph at Vedder Crossing.

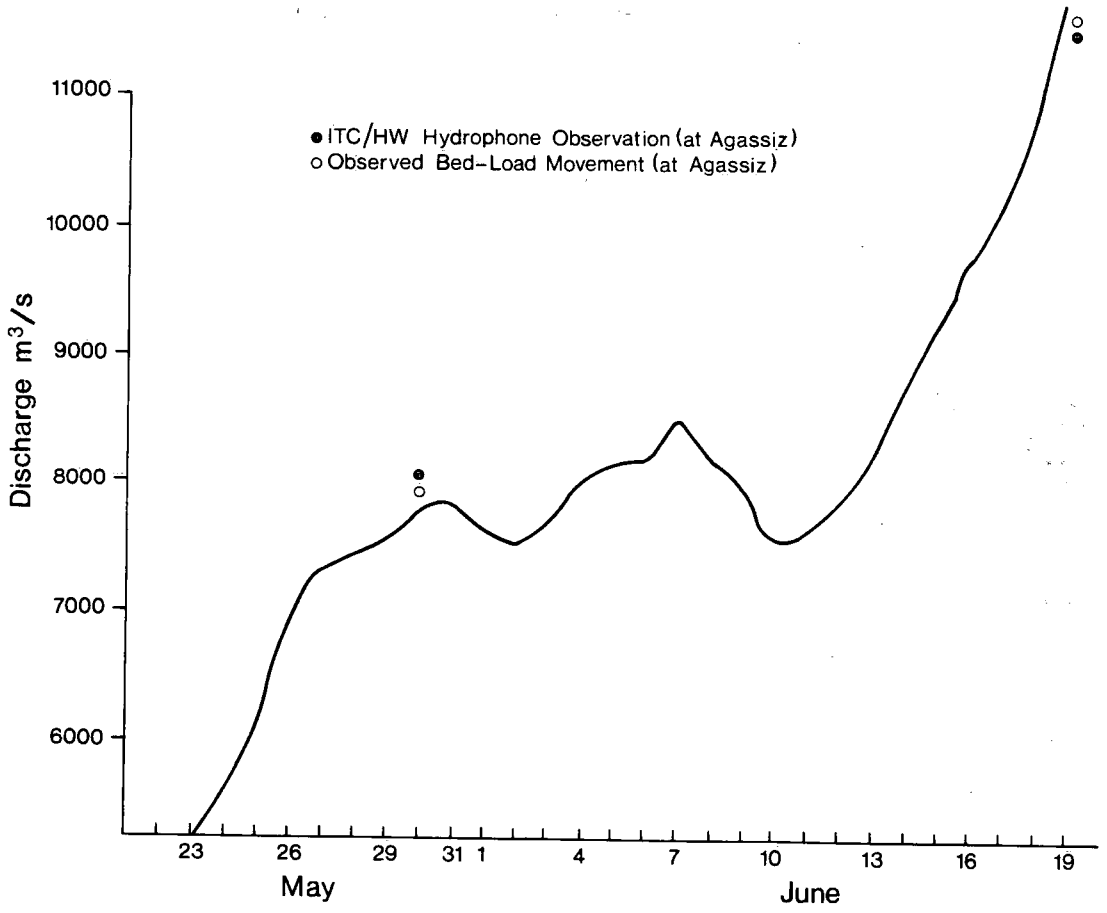

Figure 28. Fraser River flow hydrograph at Mission.

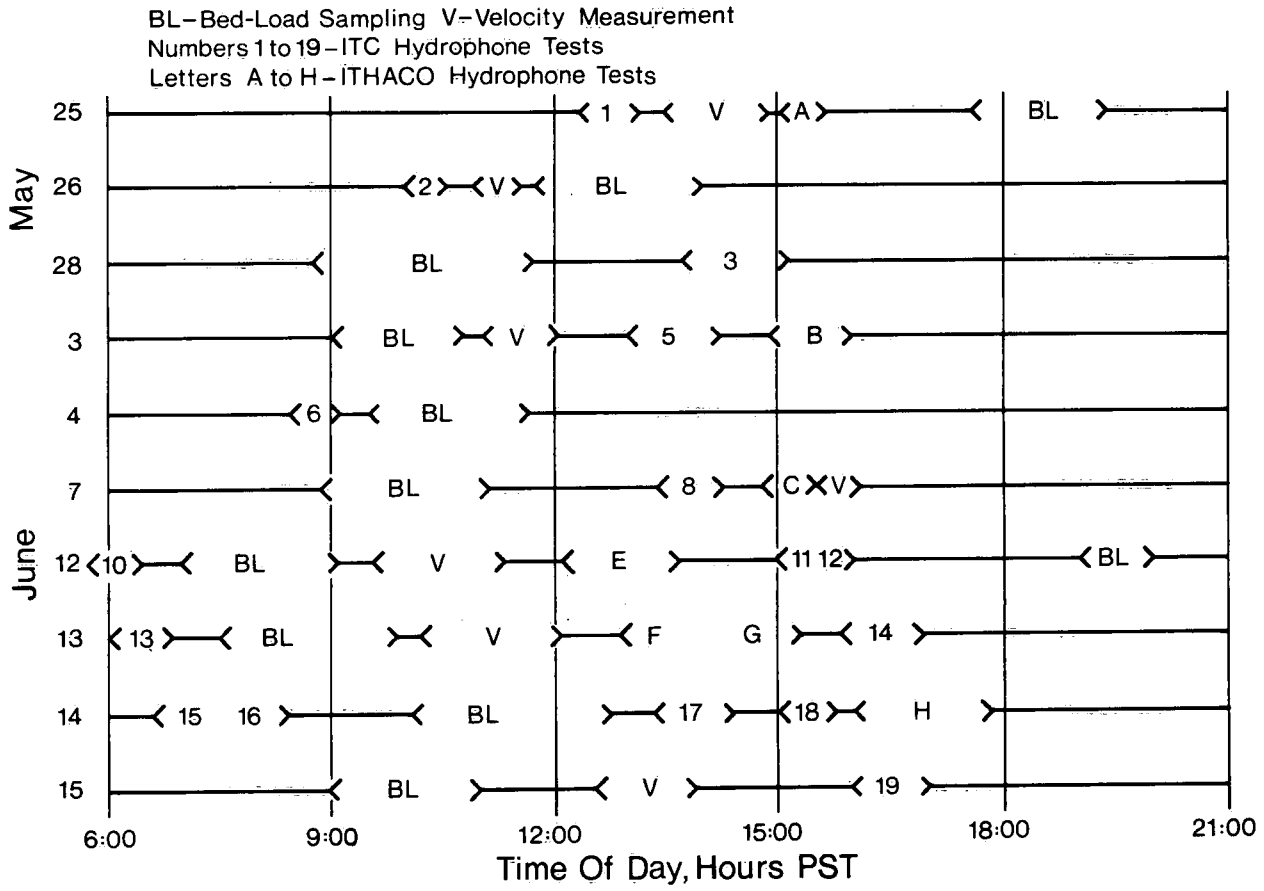

Figure 29. Sampling sequences at Vedder site.

Figure 30. ITC hydrophone under cable car at Vedder site.

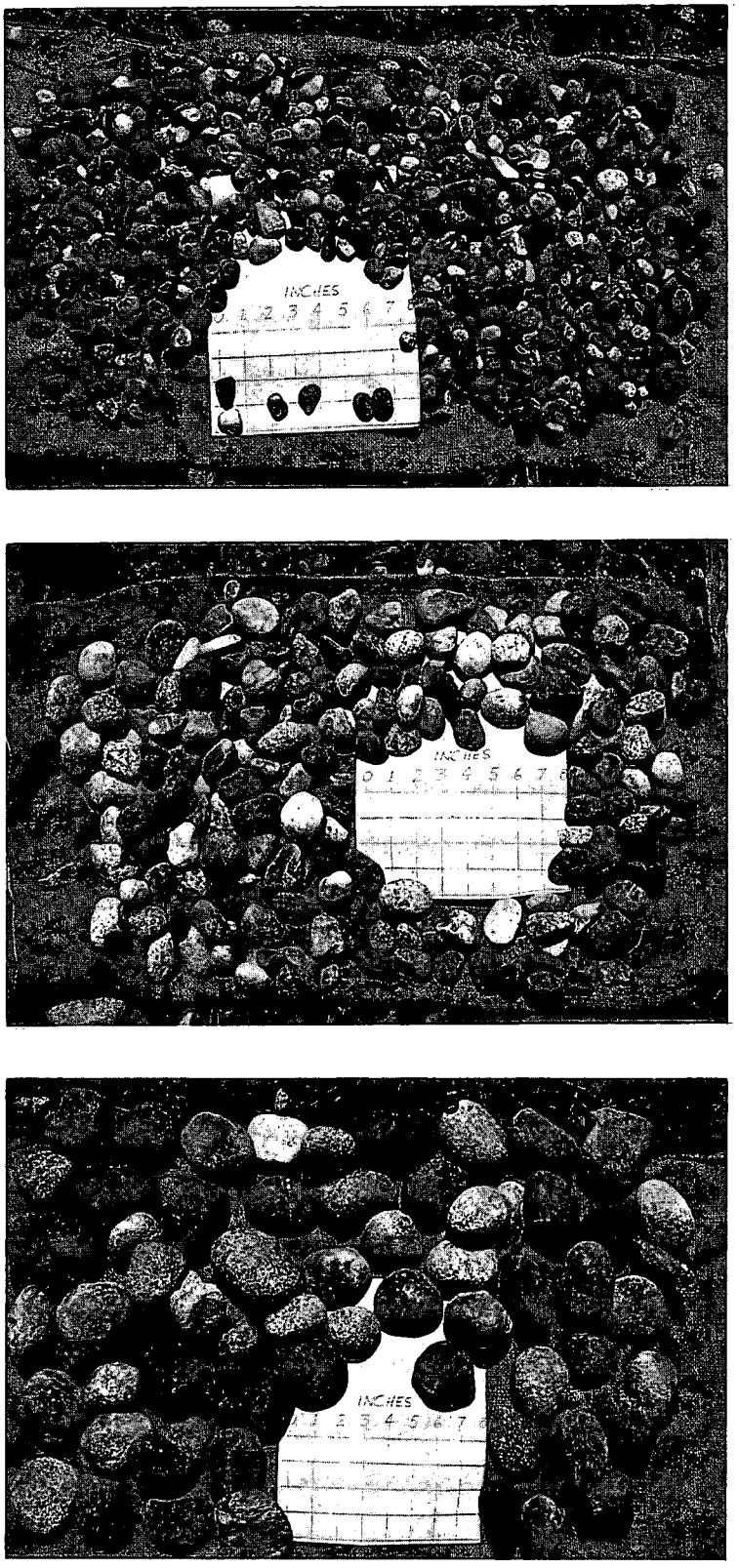

Figure 31. Special test pebble sizes.

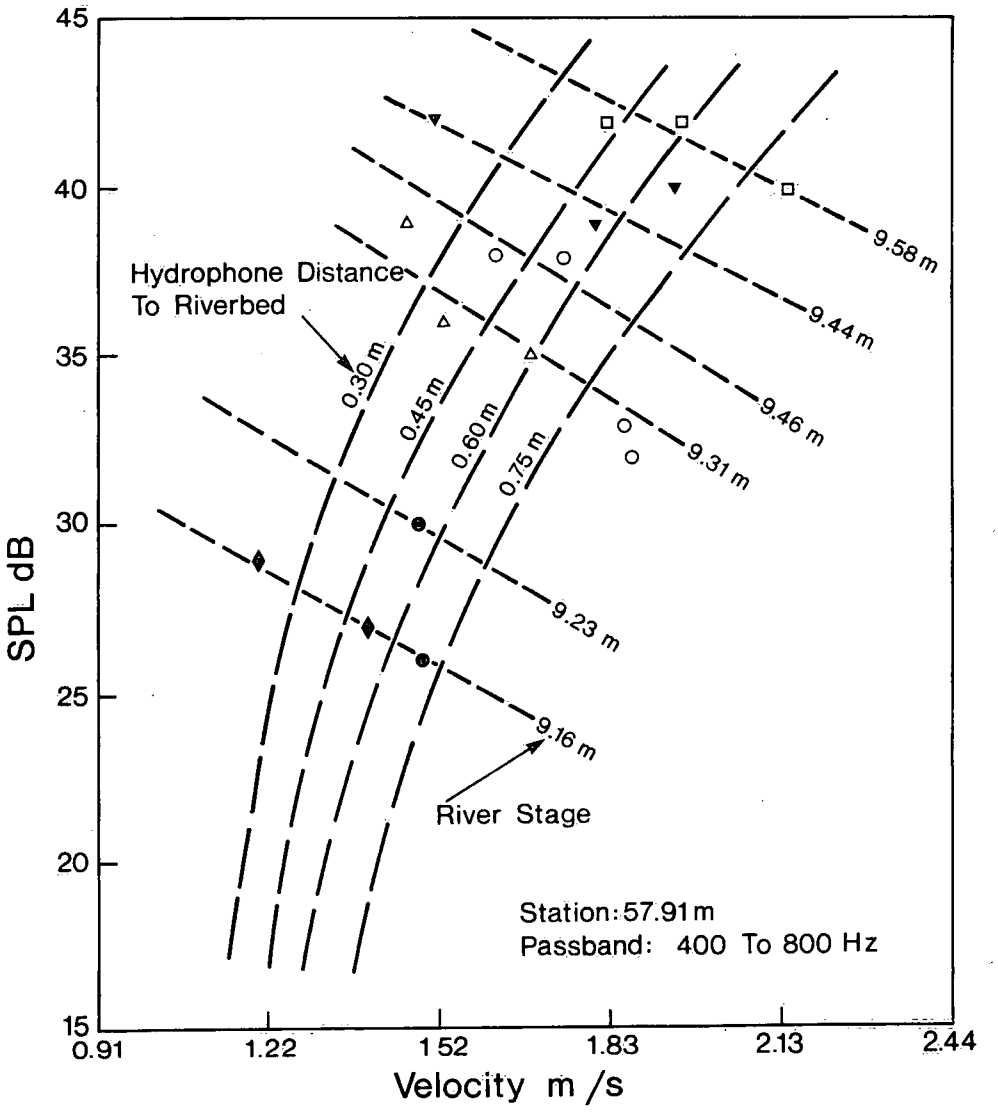

Figure 32. Velocity and position effect on observed SPL (Ithaco system, 1973).

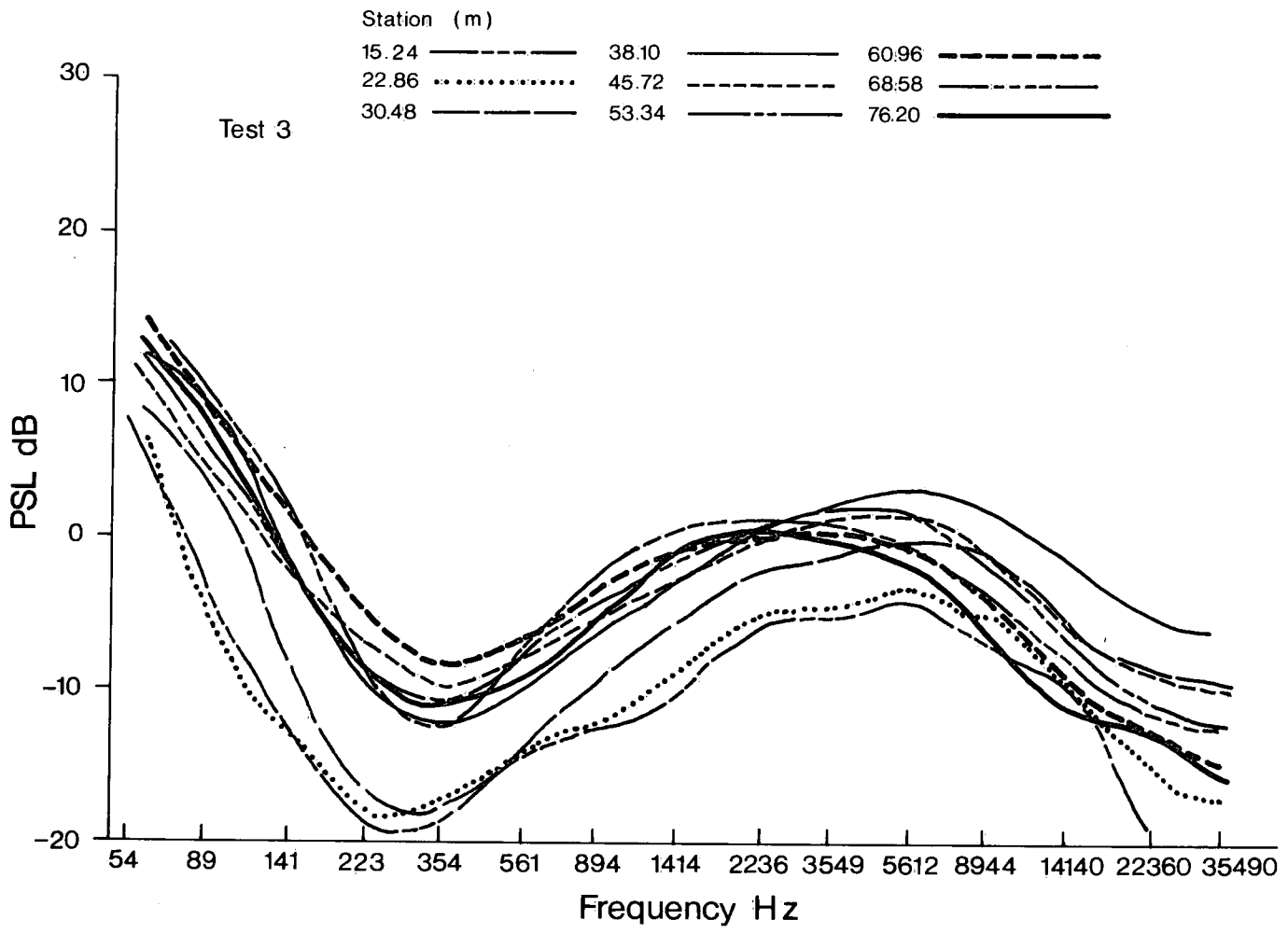

Figure 33. Frequency spectrograph, test 3, Vedder site.

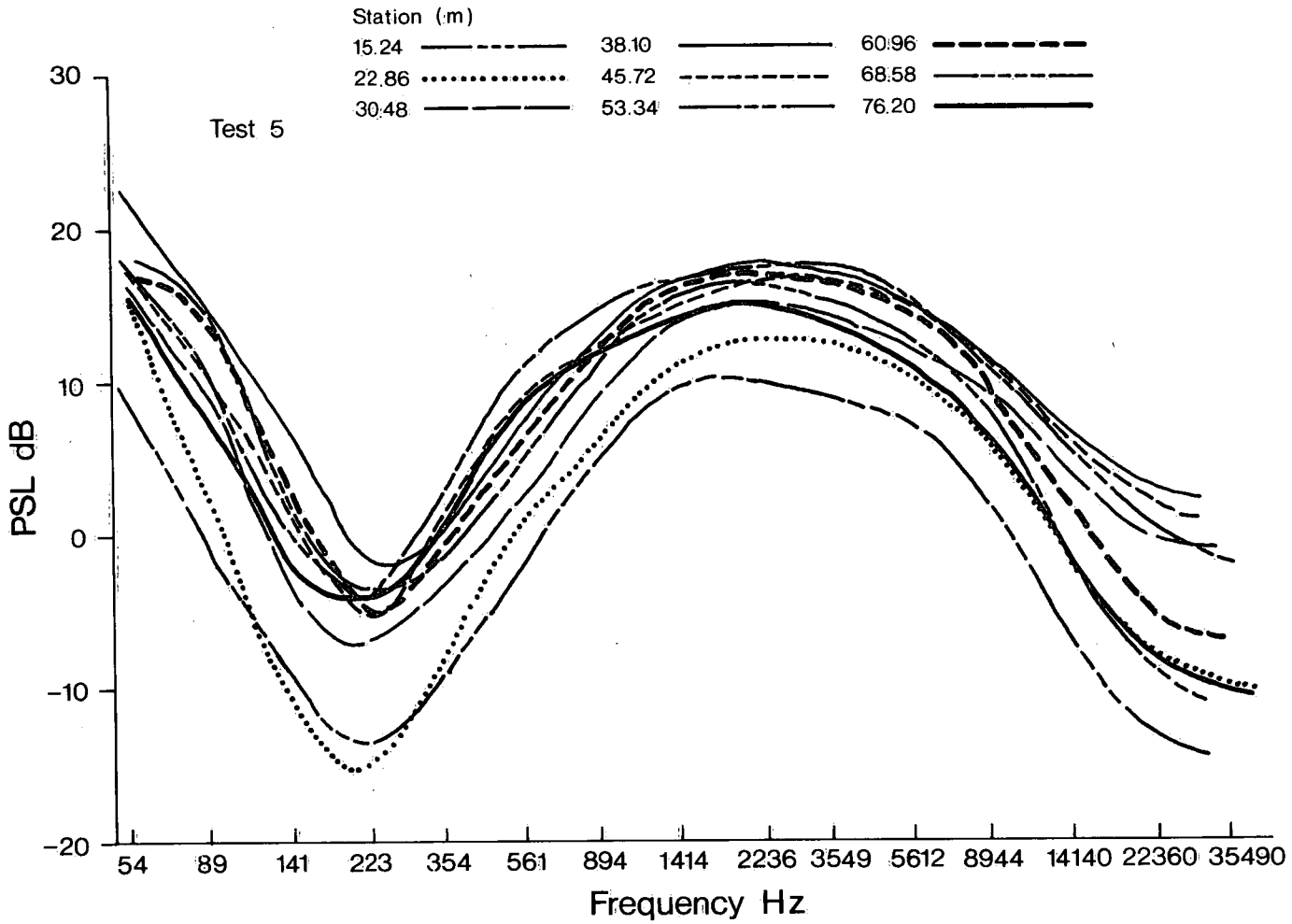

Figure 34. Frequency spectrograph, test 5, Vedder site.

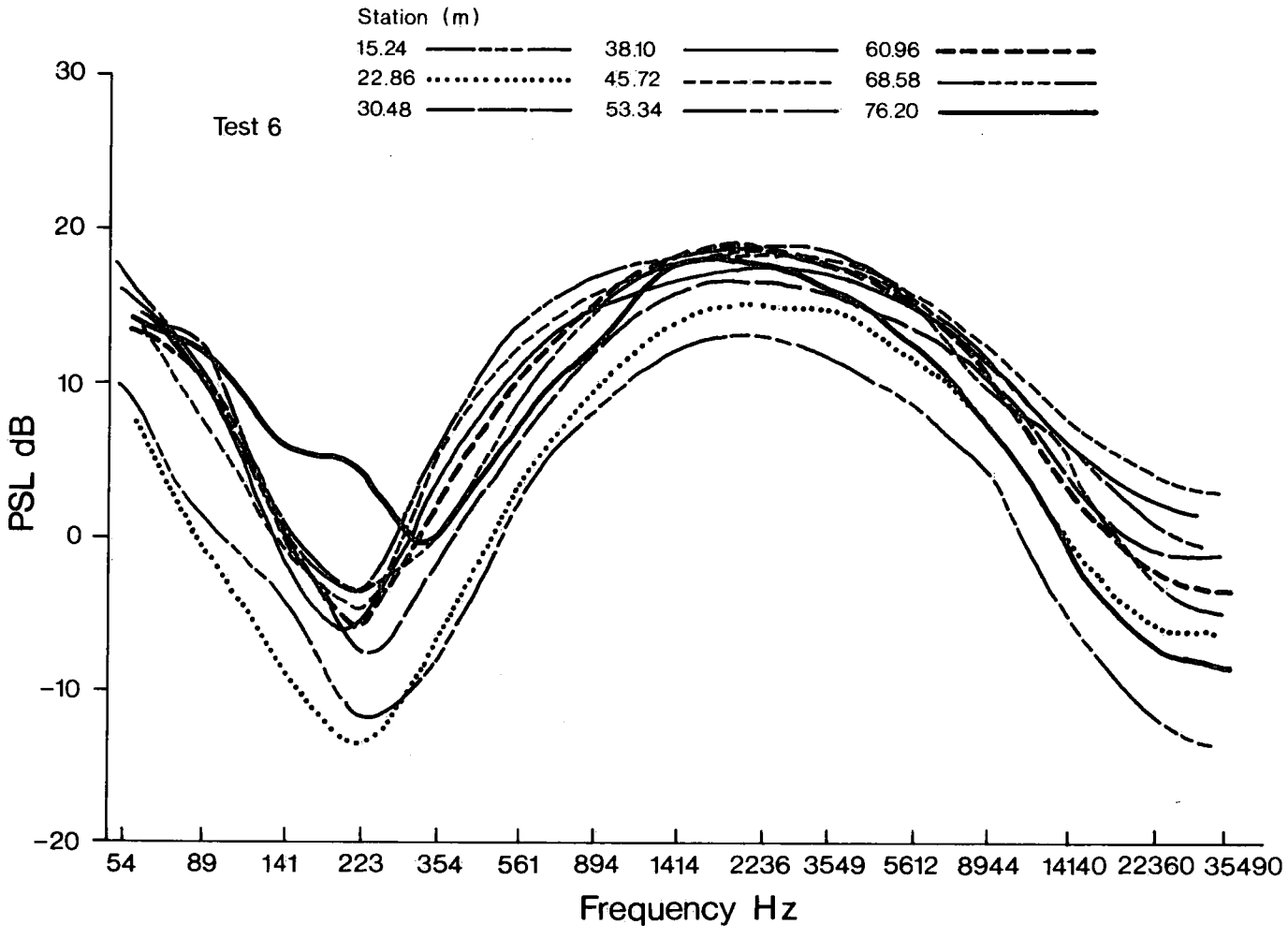

Figure 35. Frequency spectrograph, test 6, Vedder site.

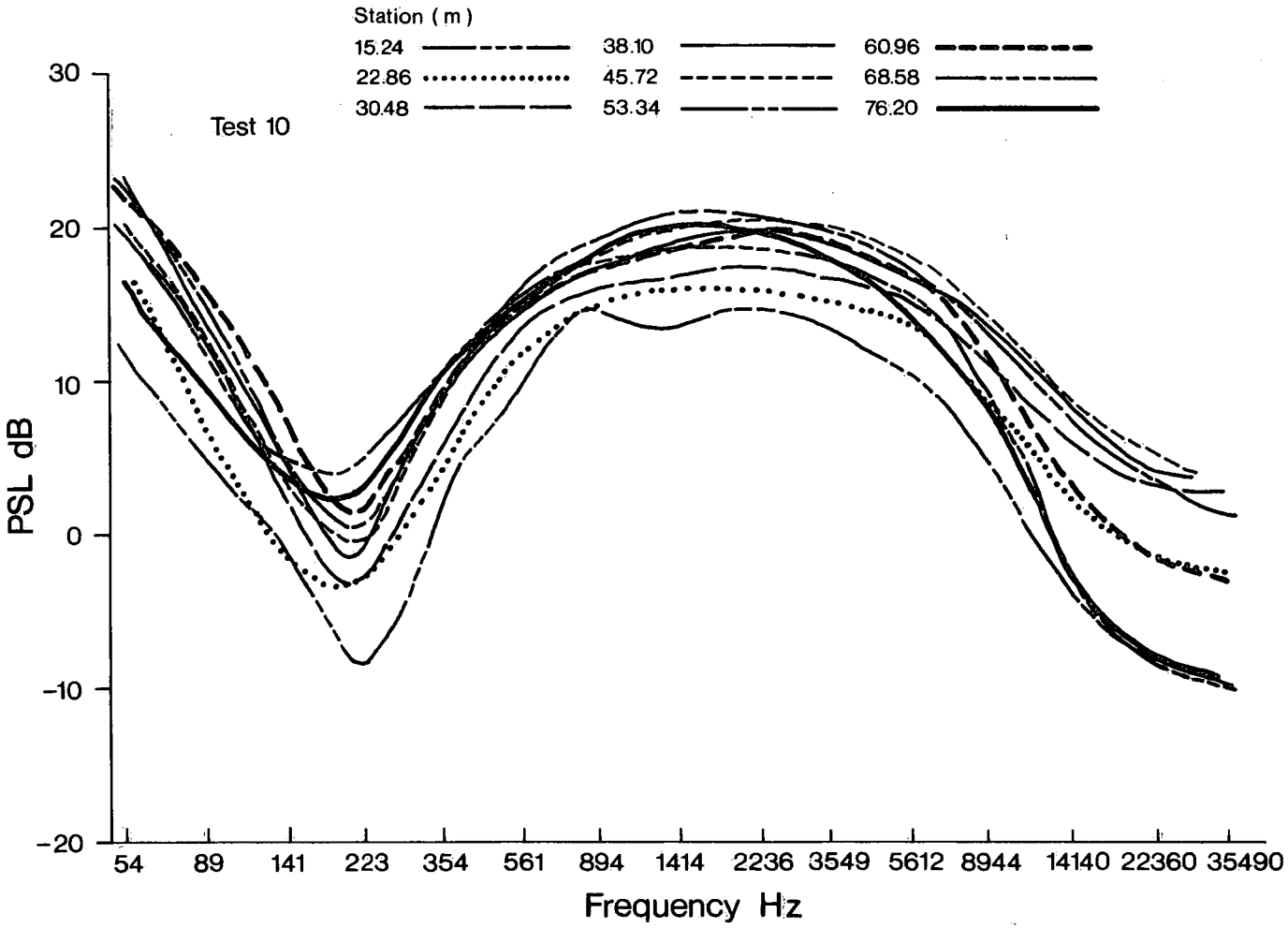

Figure 36. Frequency spectrograph, test 10, Vedder site.

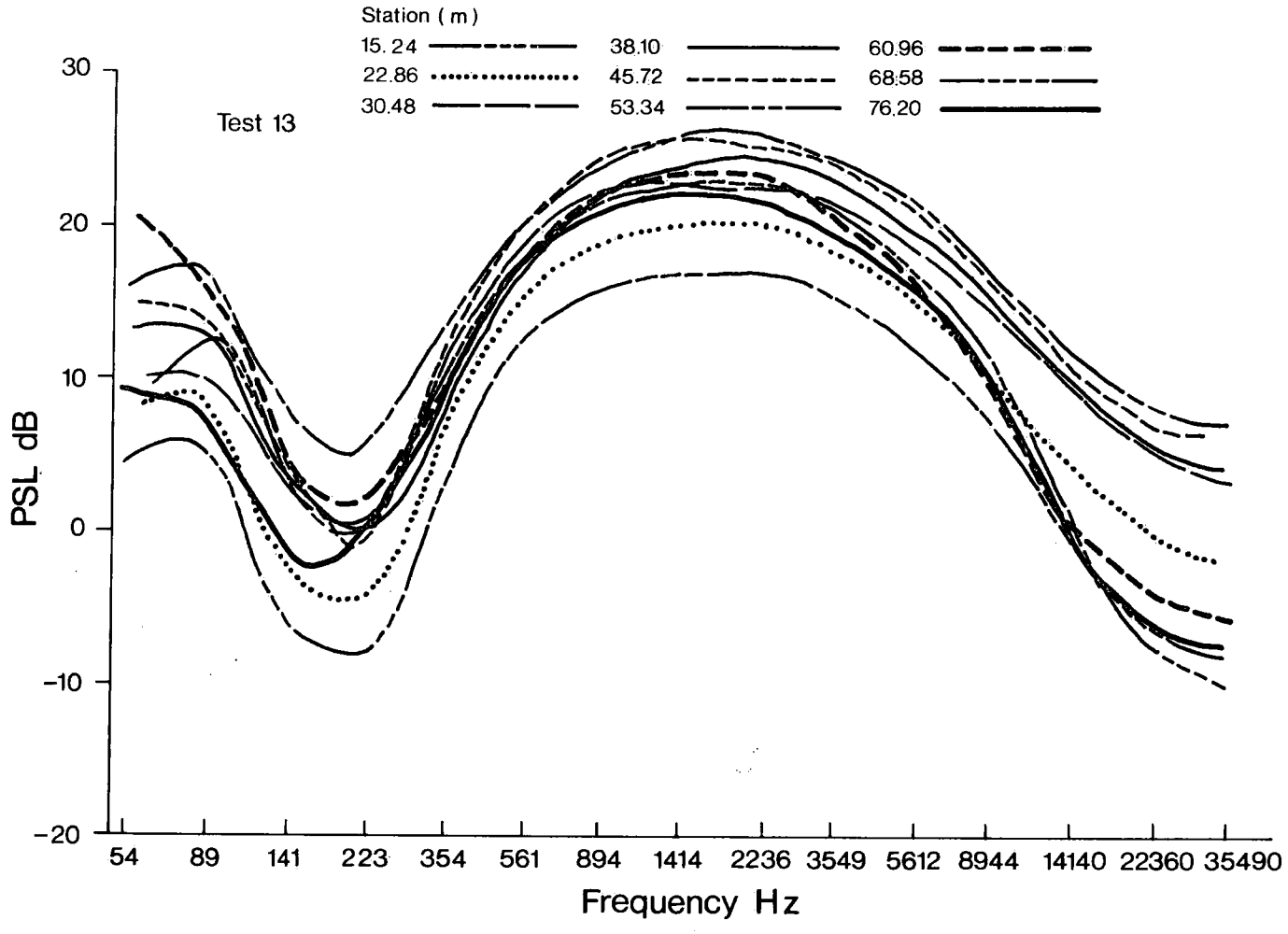

Figure 37. Frequency spectrograph, test 13, Vedder site.

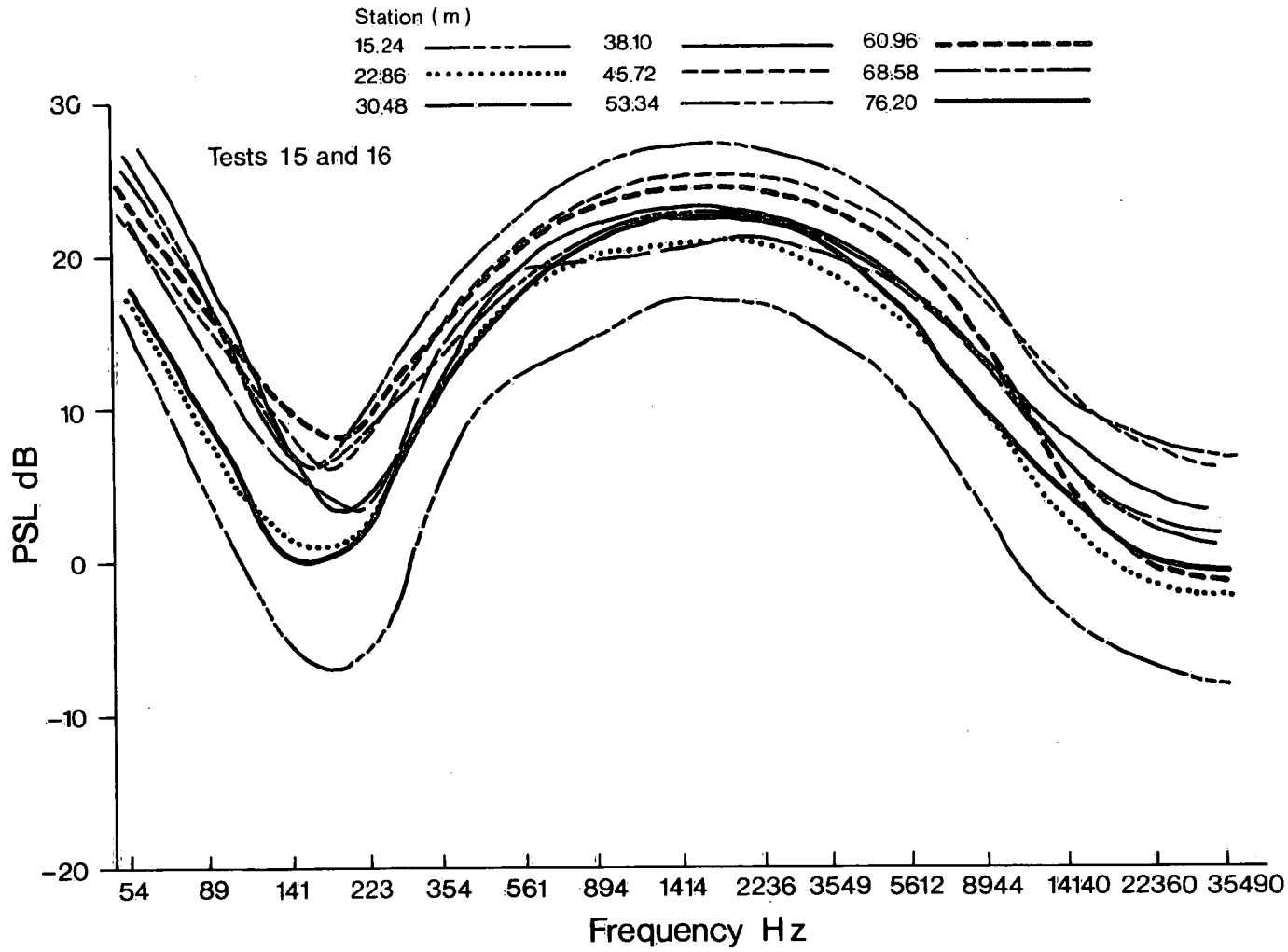

Figure 38. Frequency spectrograph, tests 15 and 16, Vedder site.

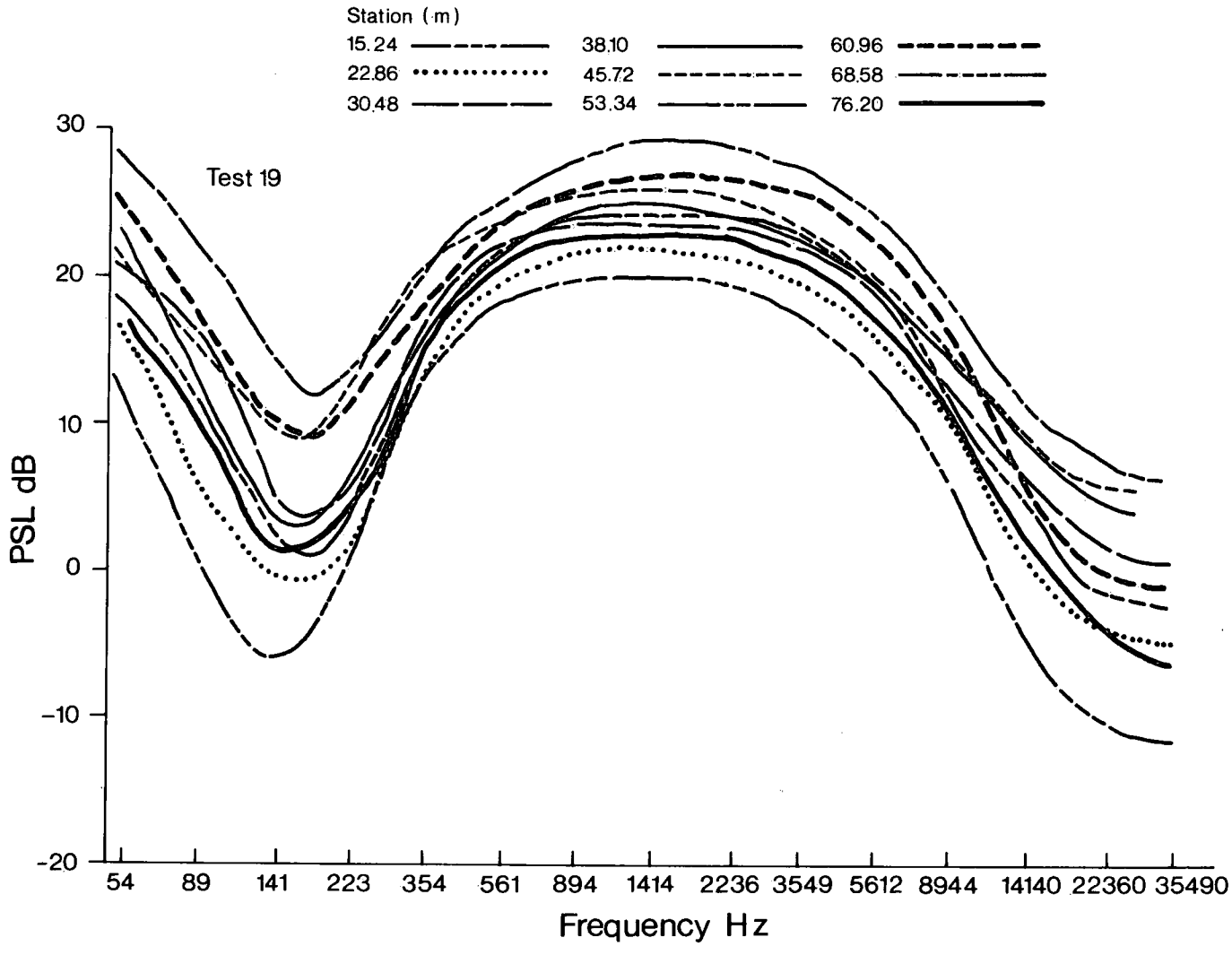

Figure 39. Frequency spectrograph, test 19, Vedder site.

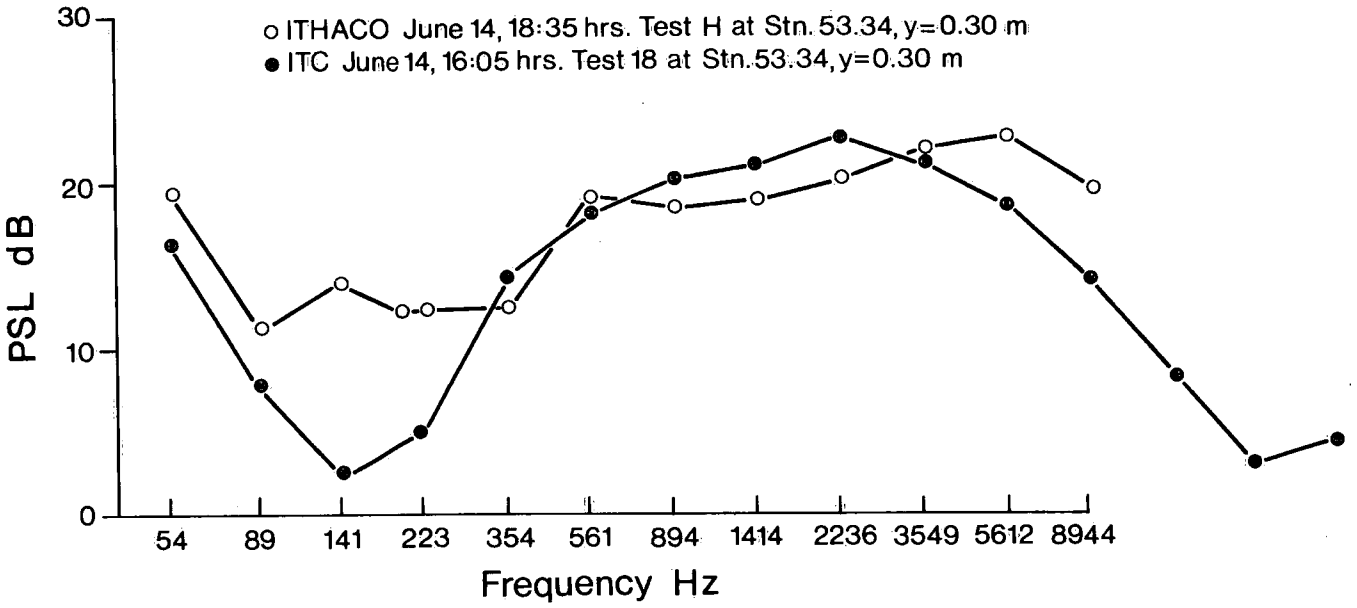

Figure 40. Frequency spectrograph comparison of tests 18 and H at station 53.34 m.

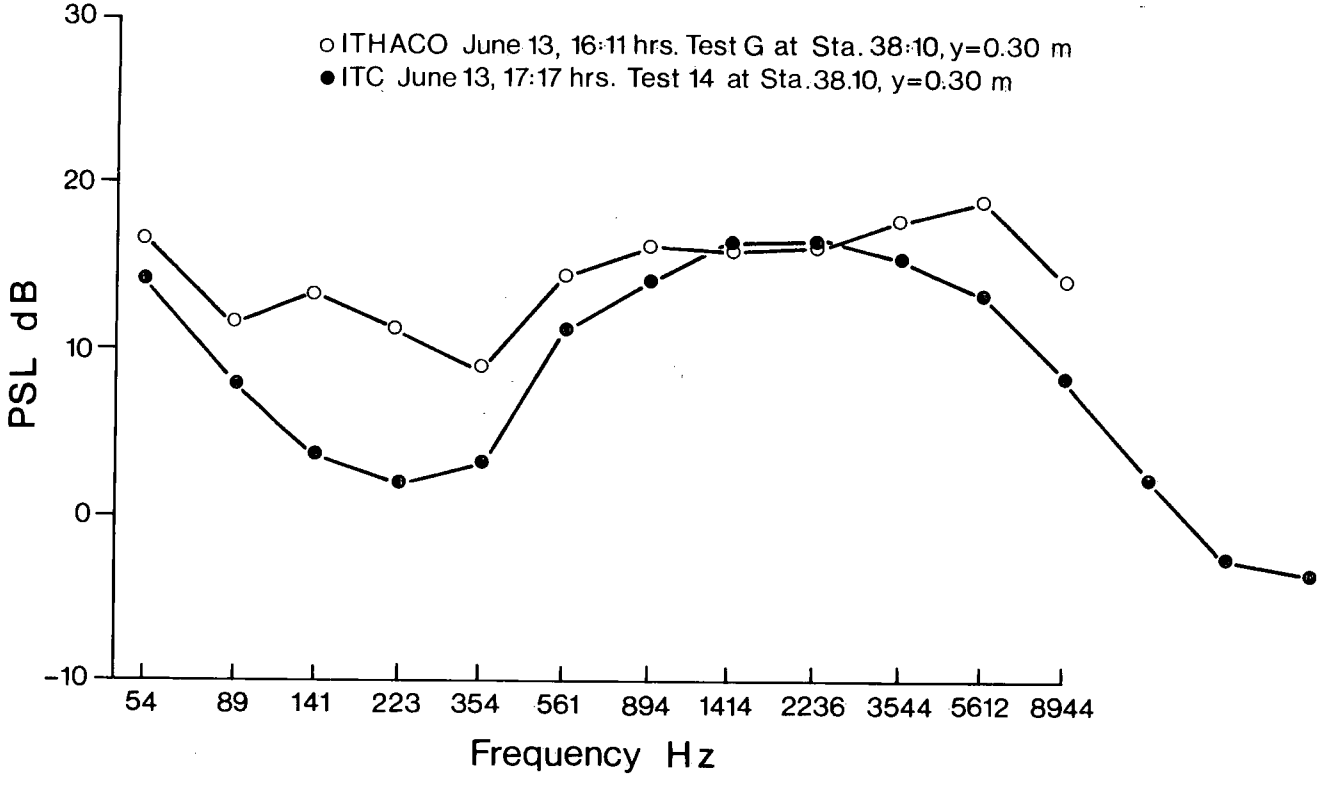

Figure 41. Frequency spectrograph comparison of tests 14 and G at station 38.10 m.

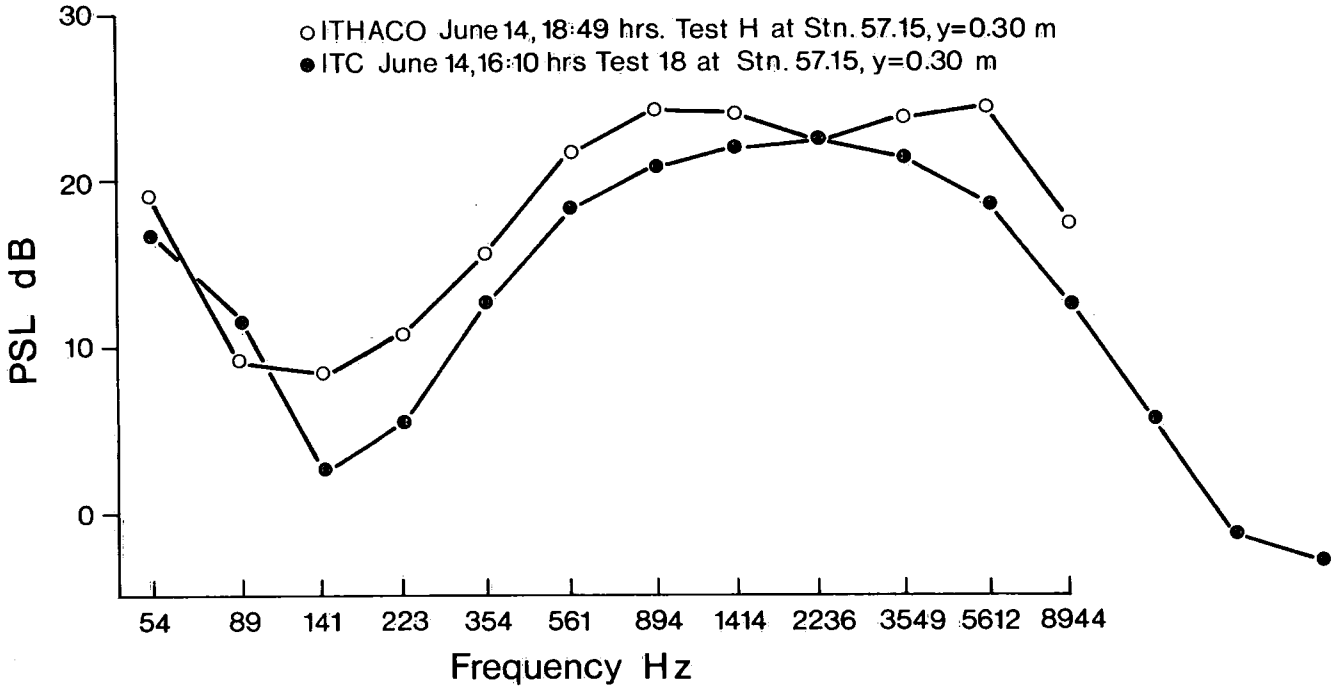

Figure 42. Frequency spectrograph comparison of tests 18 and H at station 57.15 m.

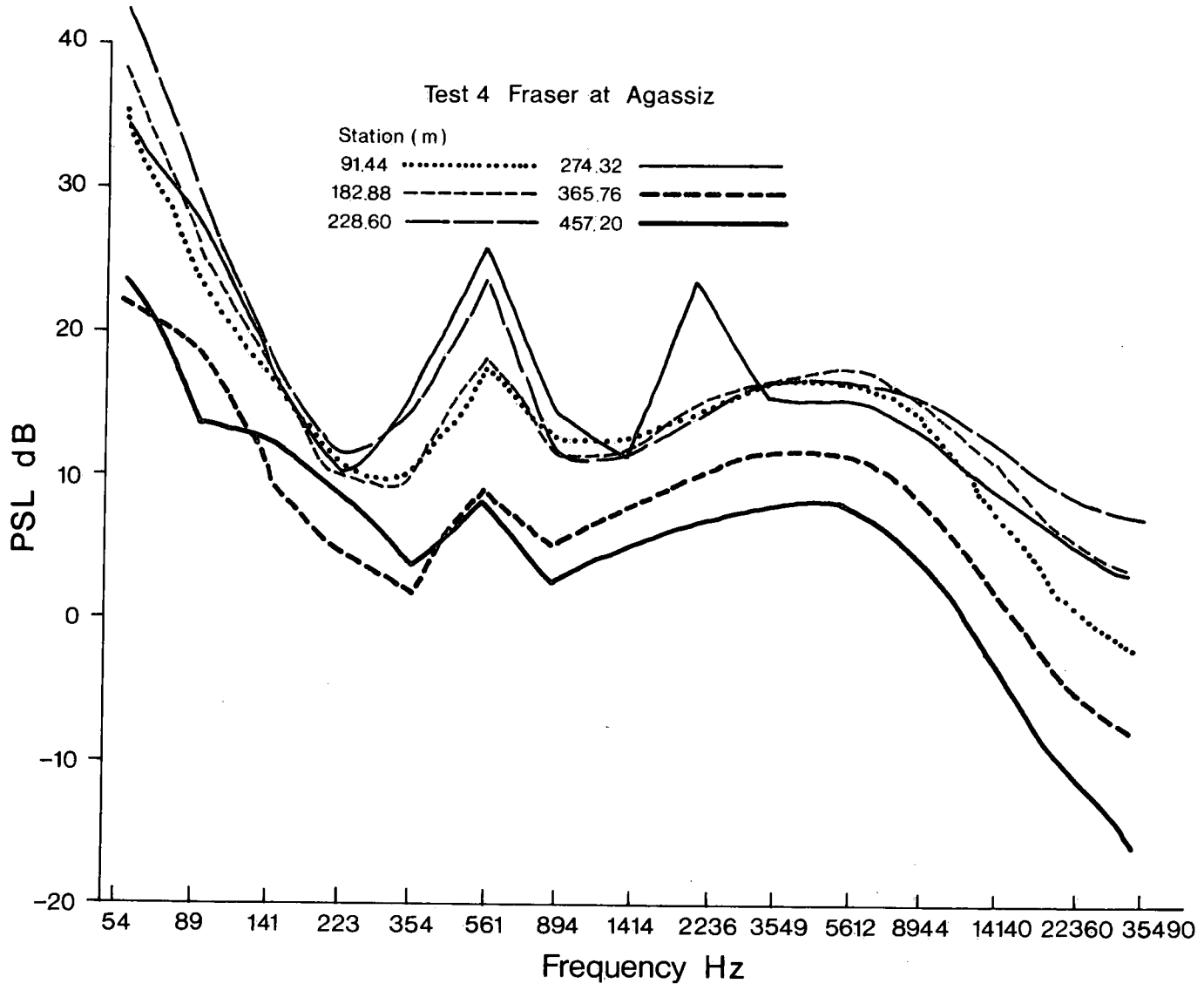

Figure 43. Frequency spectrograph, test 4, Fraser site.

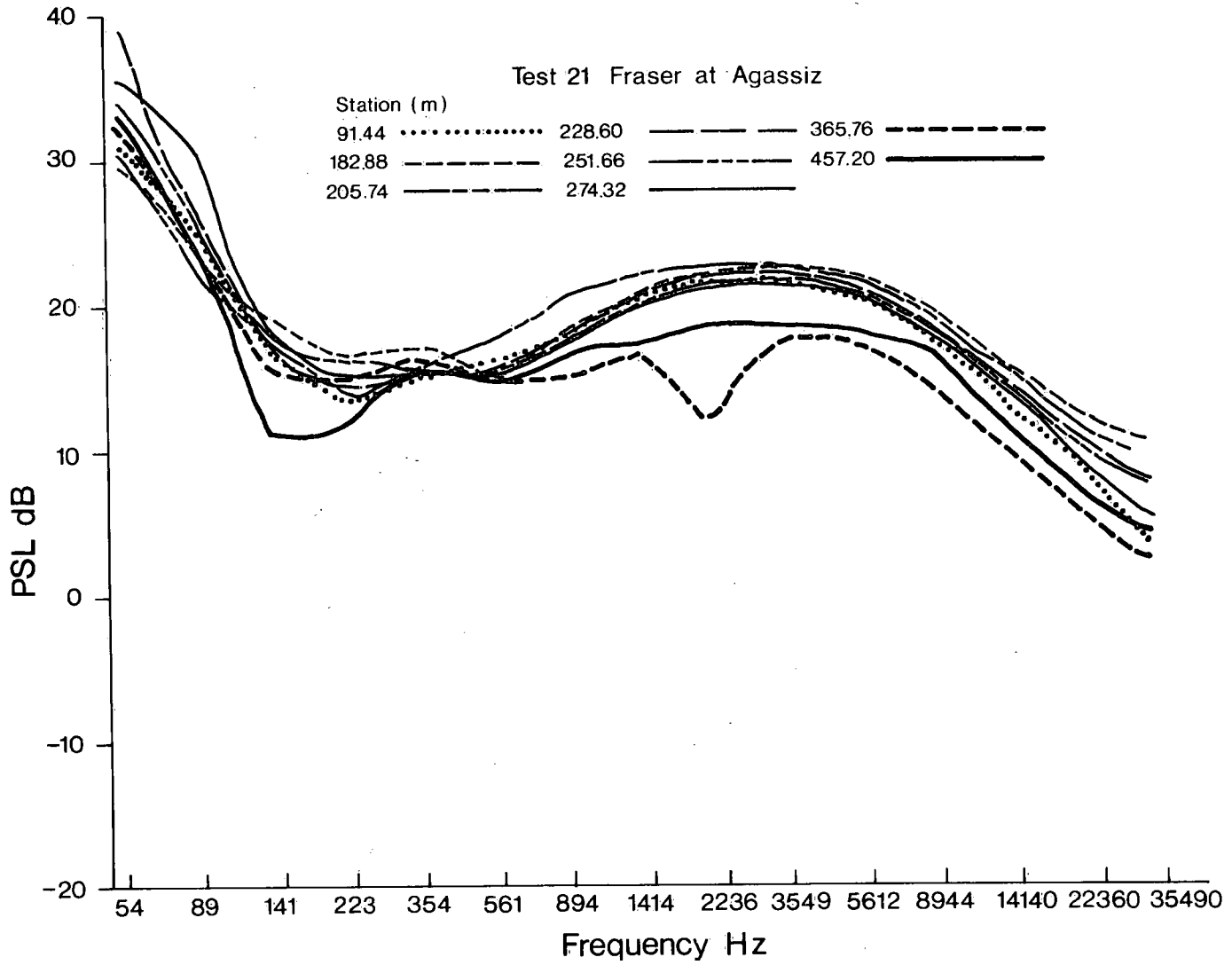

Figure 44. Frequency spectrograph, test 21, Fraser site.

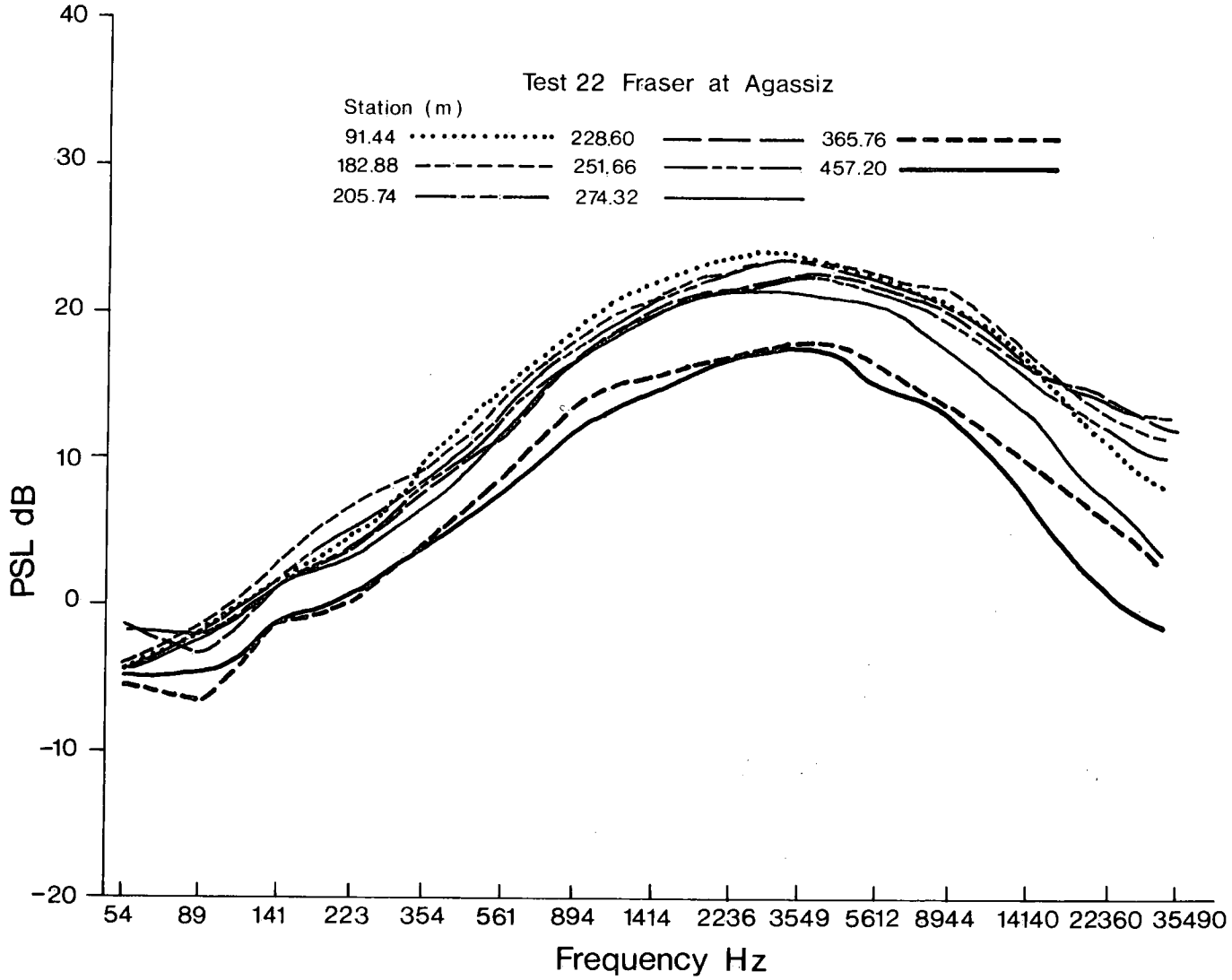

Figure 45. Frequency spectrograph, test 22, Fraser site.

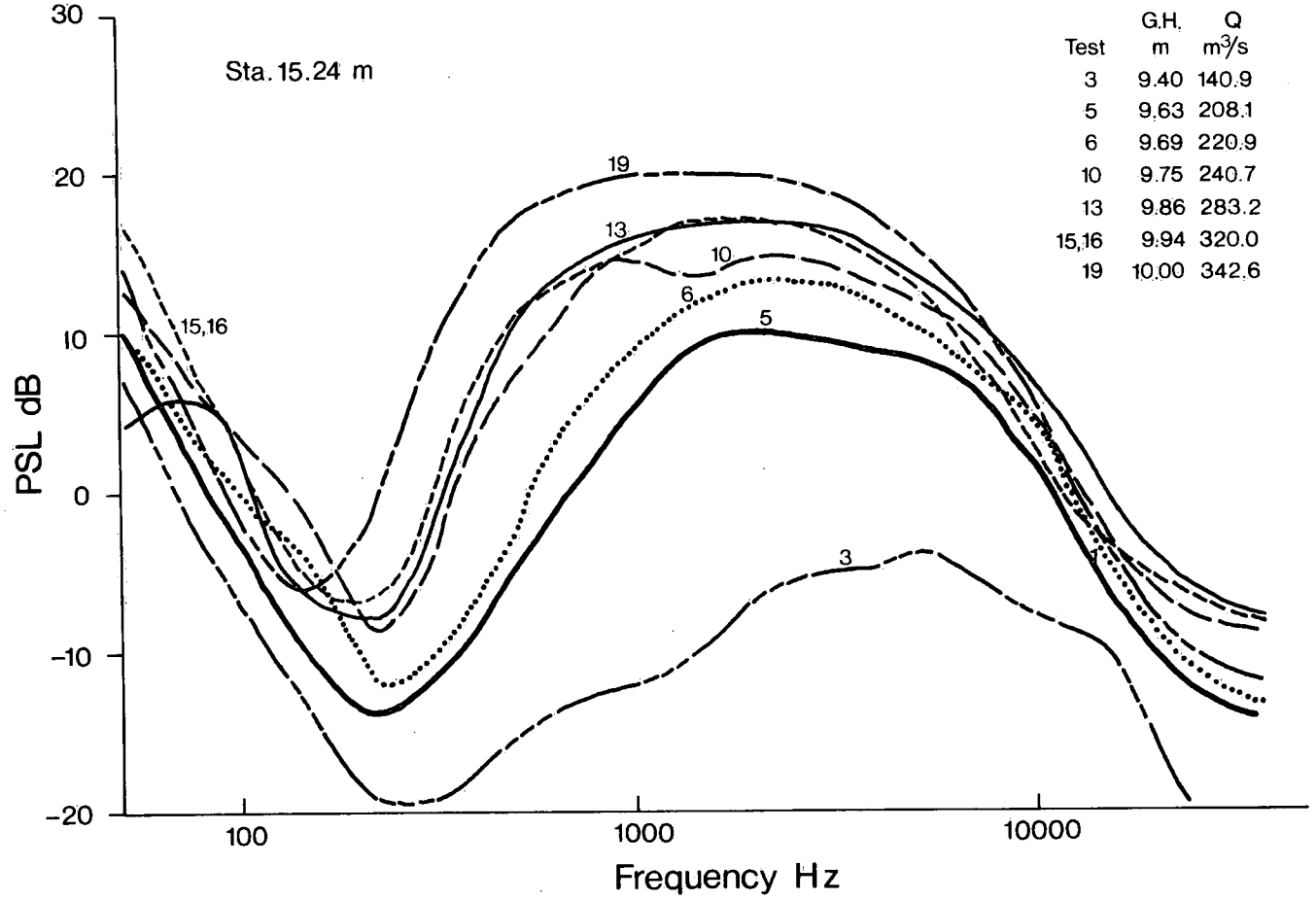

Figure 46. Frequency spectrograph, station 15.24 m, Vedder site.

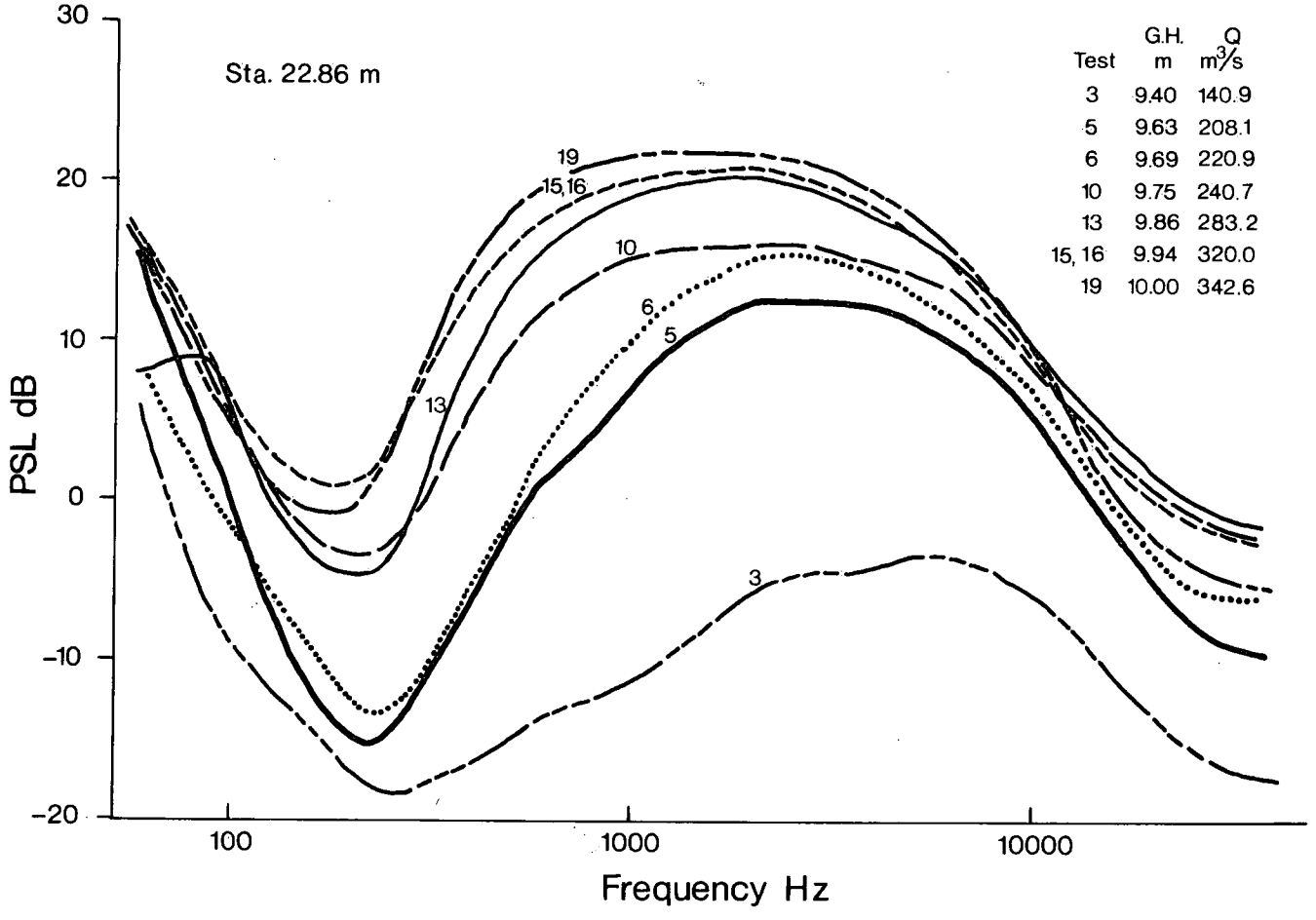

Figure 47. Frequency spectrograph, station 22.86 m, Vedder site.

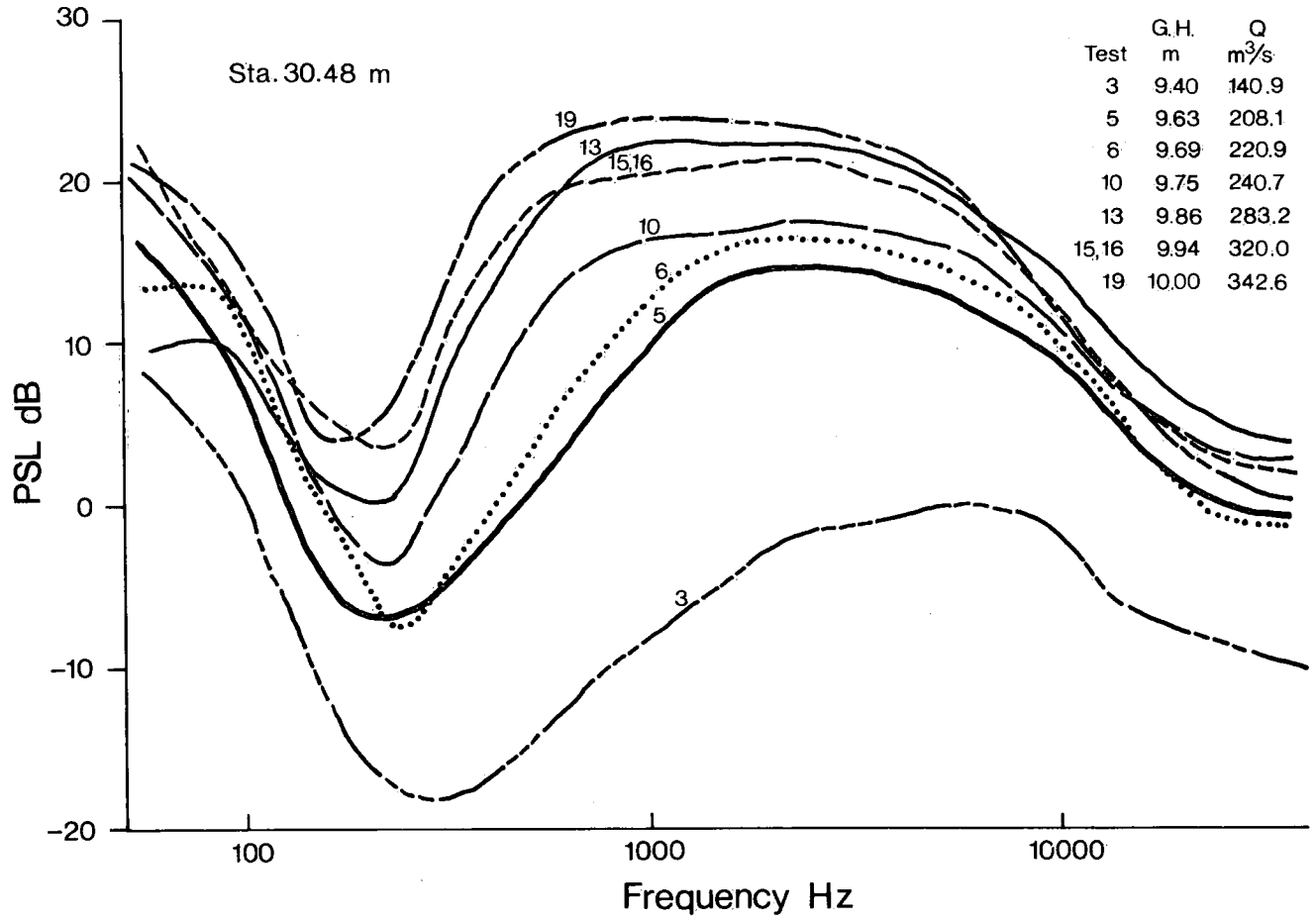

Figure 48. Frequency spectrograph, station 30.48 m, Vedder site.

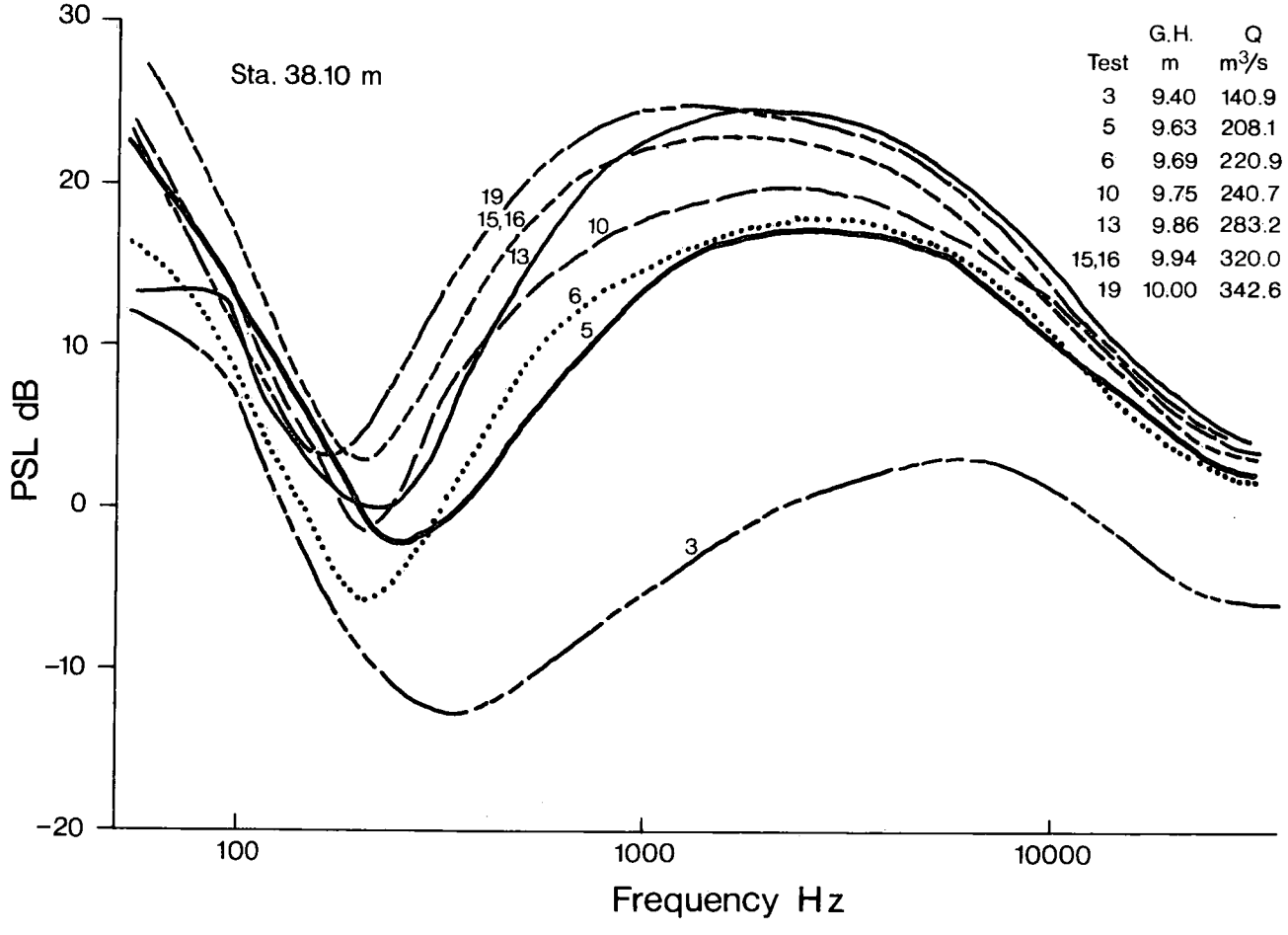

Figure 49. Frequency spectrograph, station 38.10 m, Vedder site.

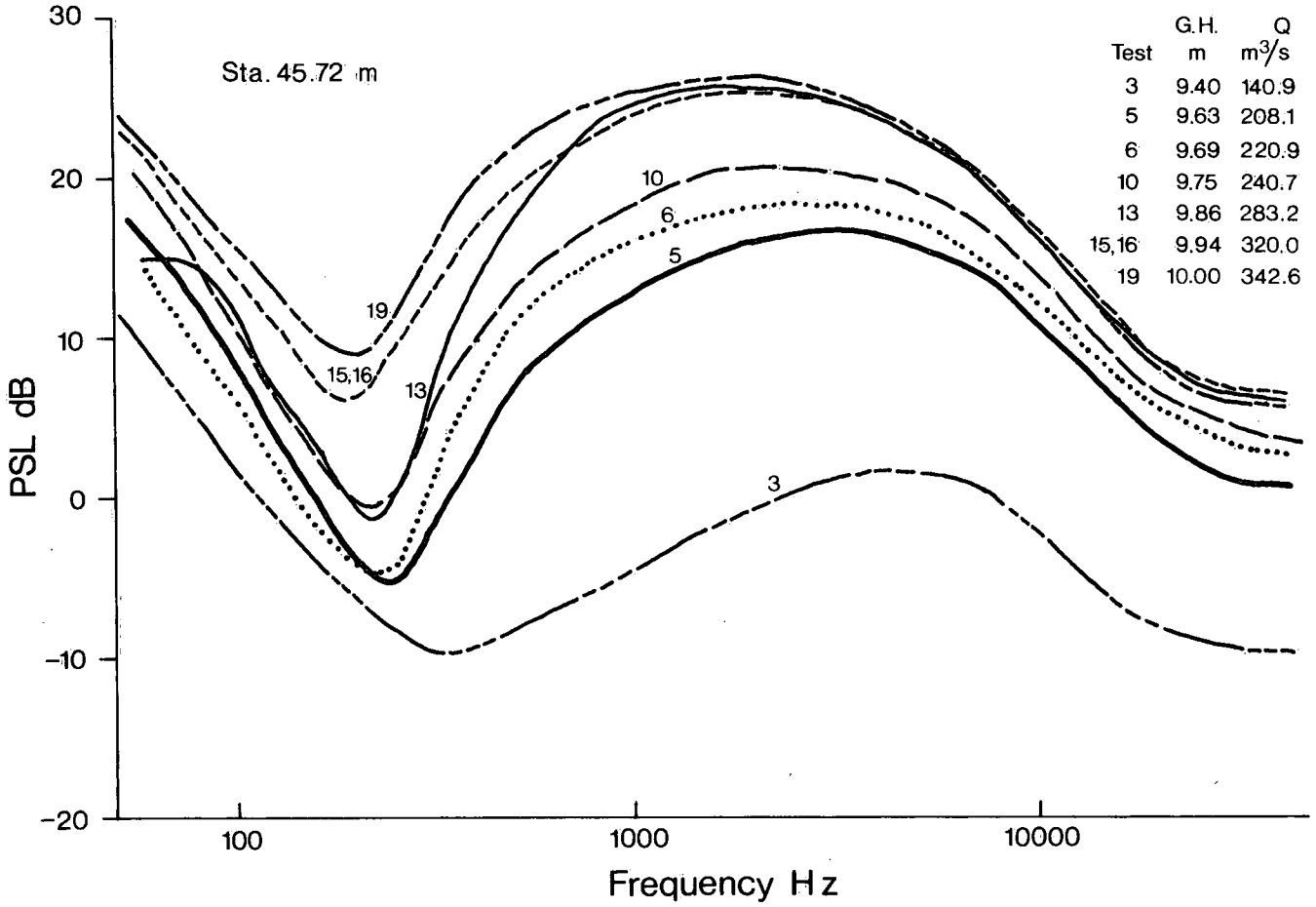

Figure 50. Frequency spectrograph, station 45.72 m, Vedder site.

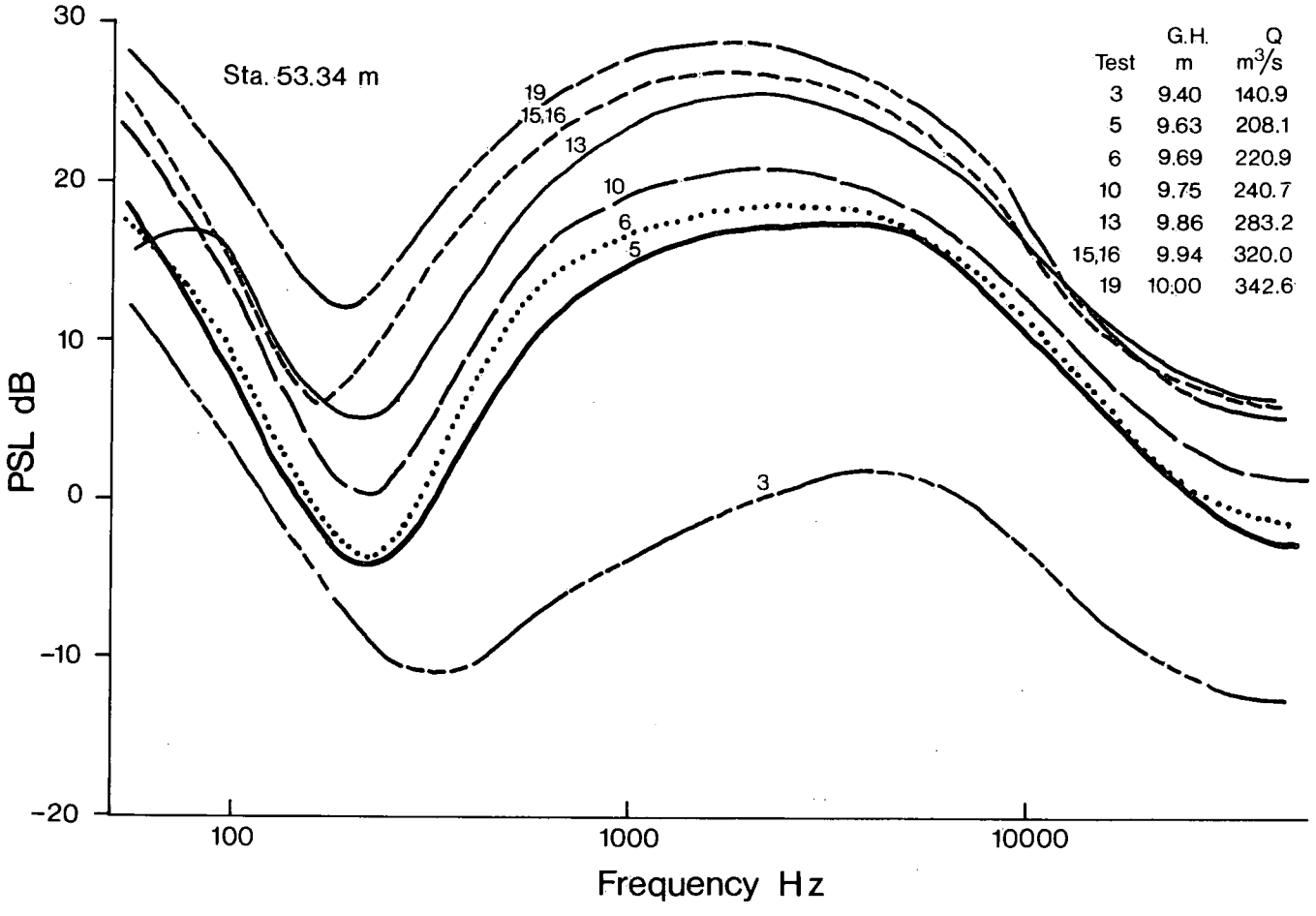

Figure 51. Frequency spectrograph, station 53.34 m, Vedder site.

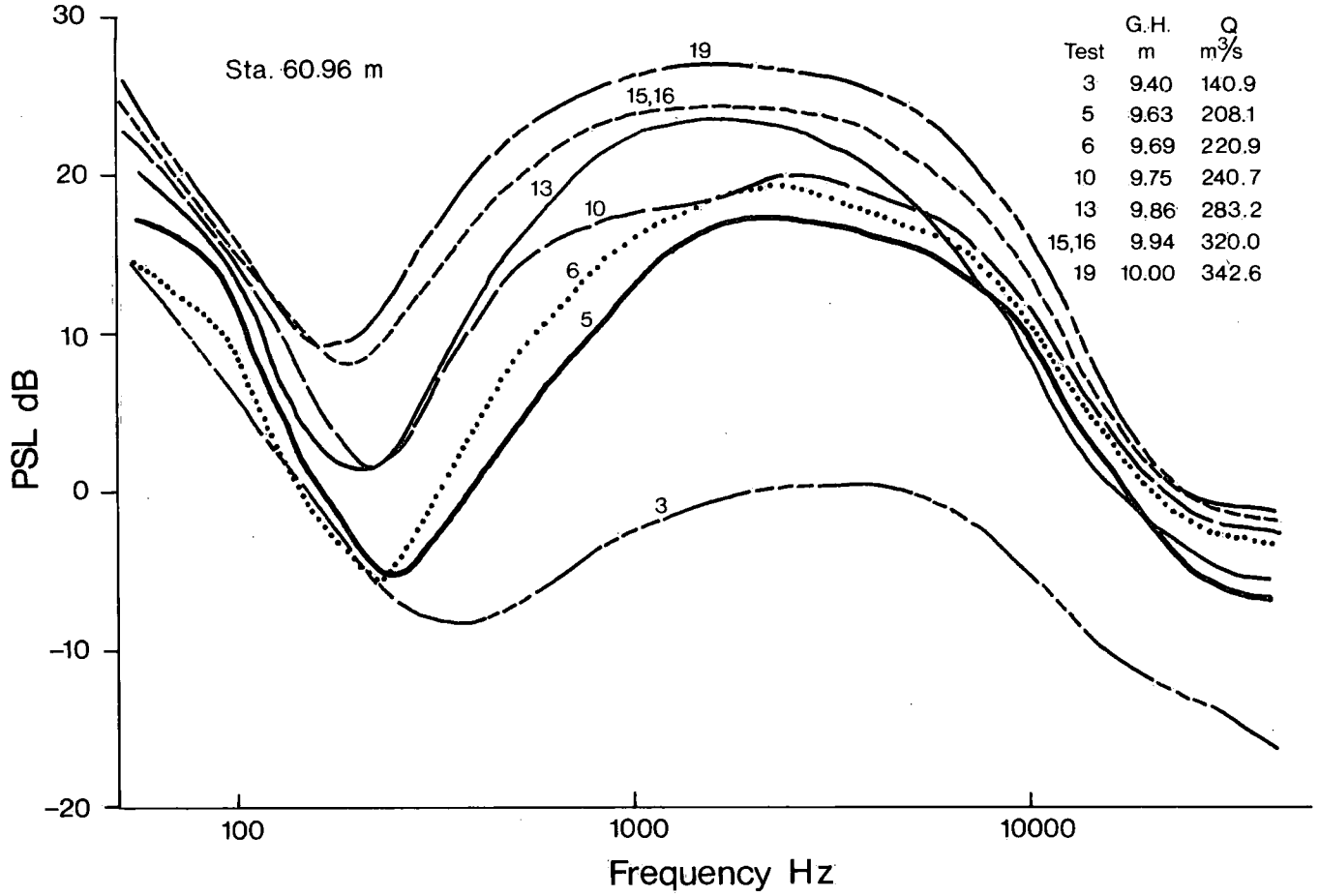

Figure 52. Frequency spectrograph, station 60.96 m, Vedder site.

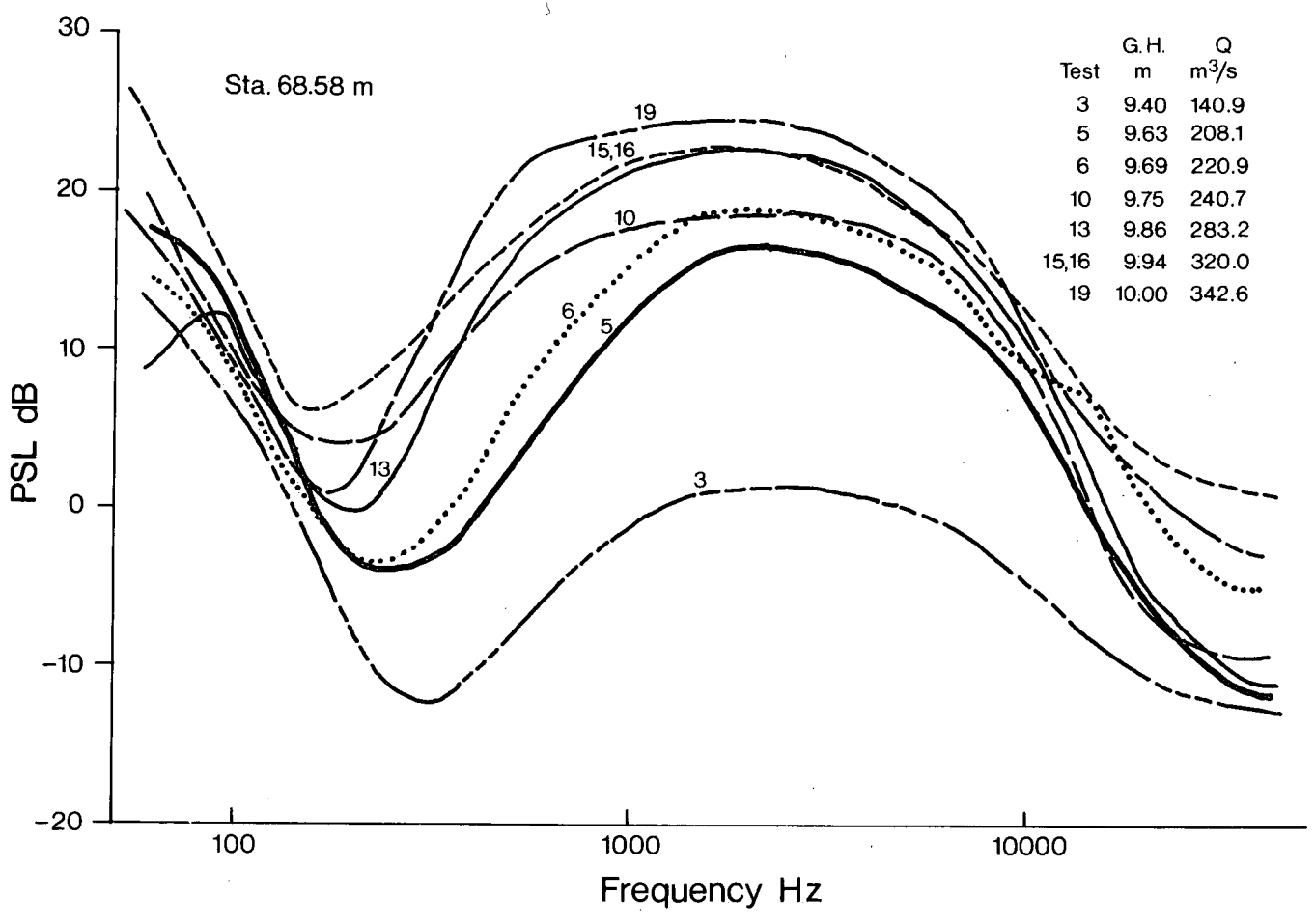

Figure 53. Frequency spectrograph, station 68.58 m, Vedder site.

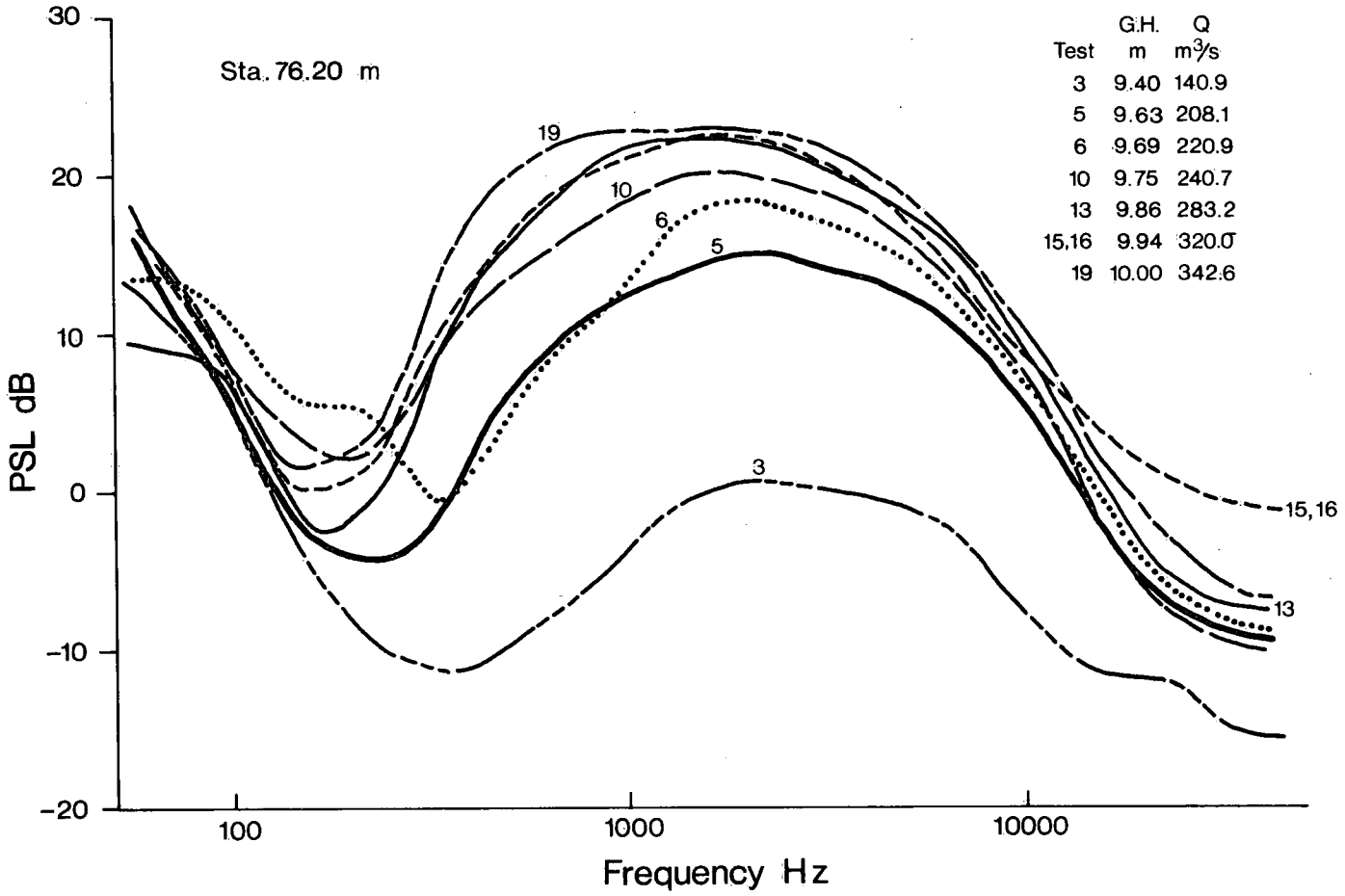

Figure 54. Frequency spectrograph, station 76.20 m, Vedder site.

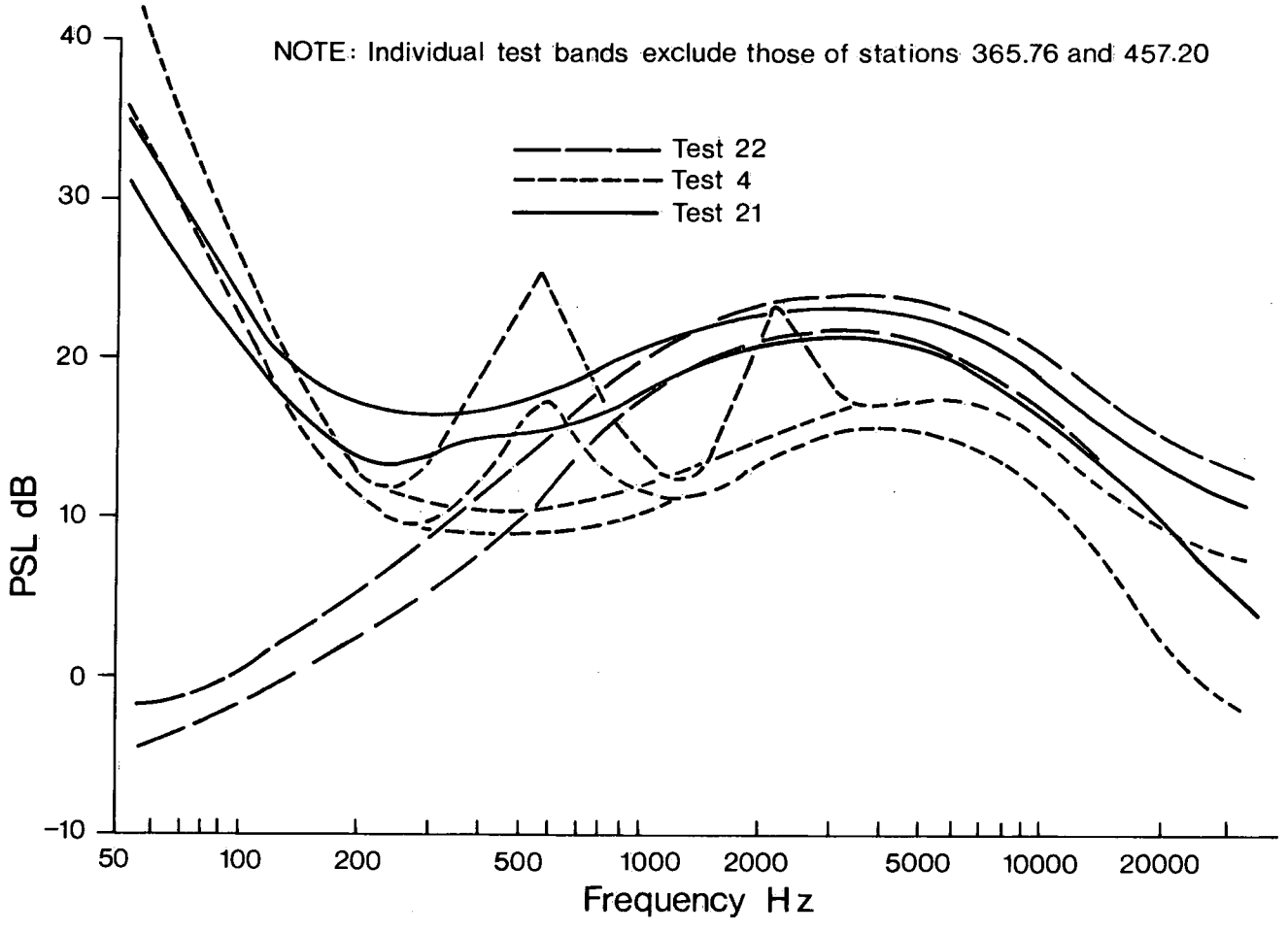

Figure 55. Frequency spectrograph comparison of tests 4, 21 and 22, Fraser site.

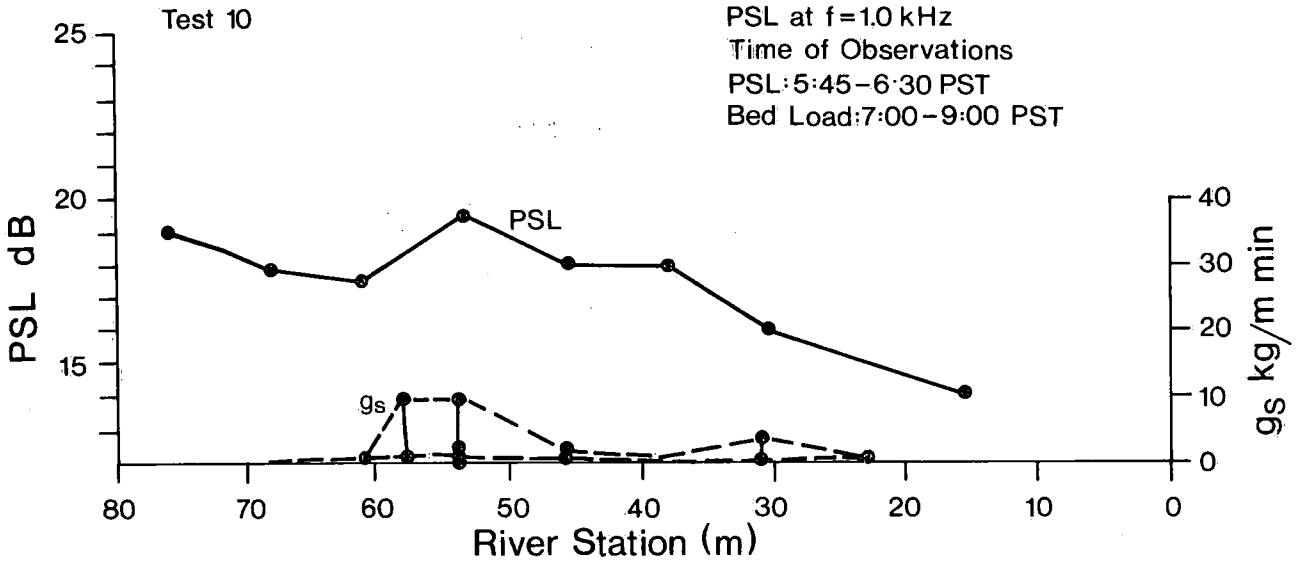

Figure 56. Bed-load transport and PSL distribution, Vedder site, test 10.

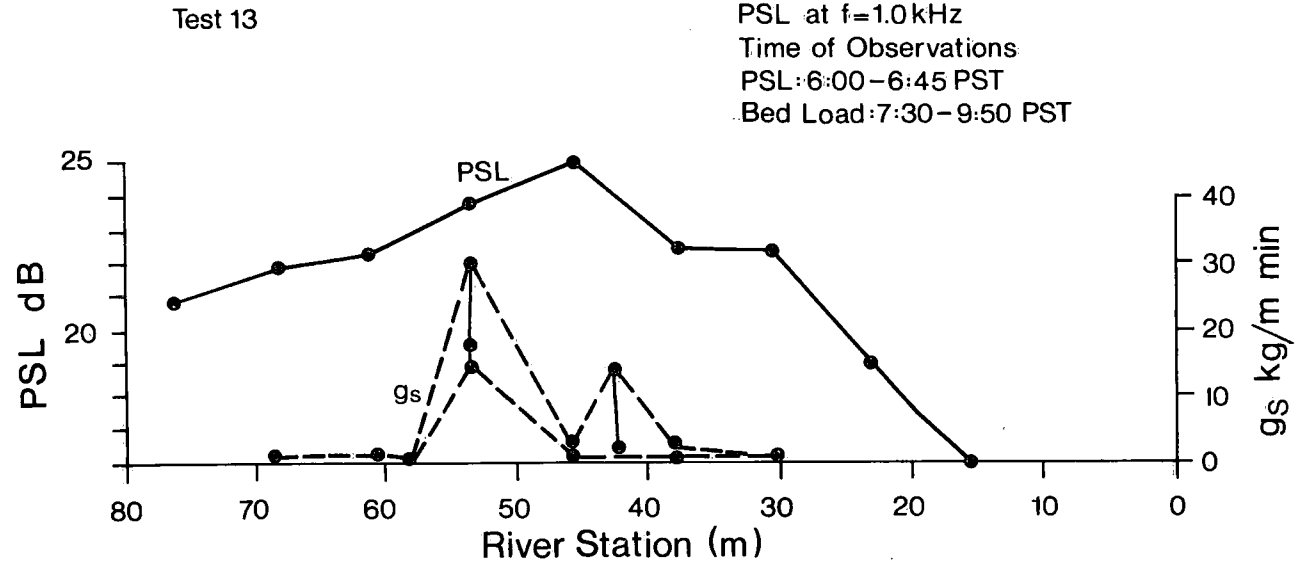

Figure 57. Bed-load transport and PSL distribution, Vedder site, test 13.

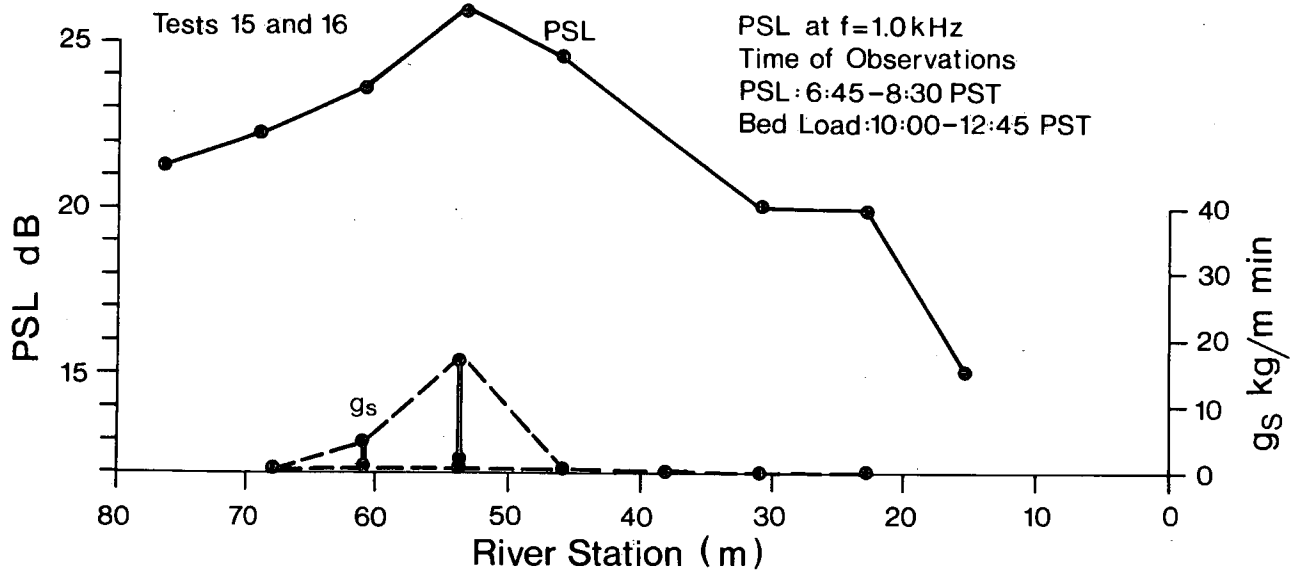

Figure 58. Bed-load transport and PSL distribution, Vedder site, tests 15 and 16.

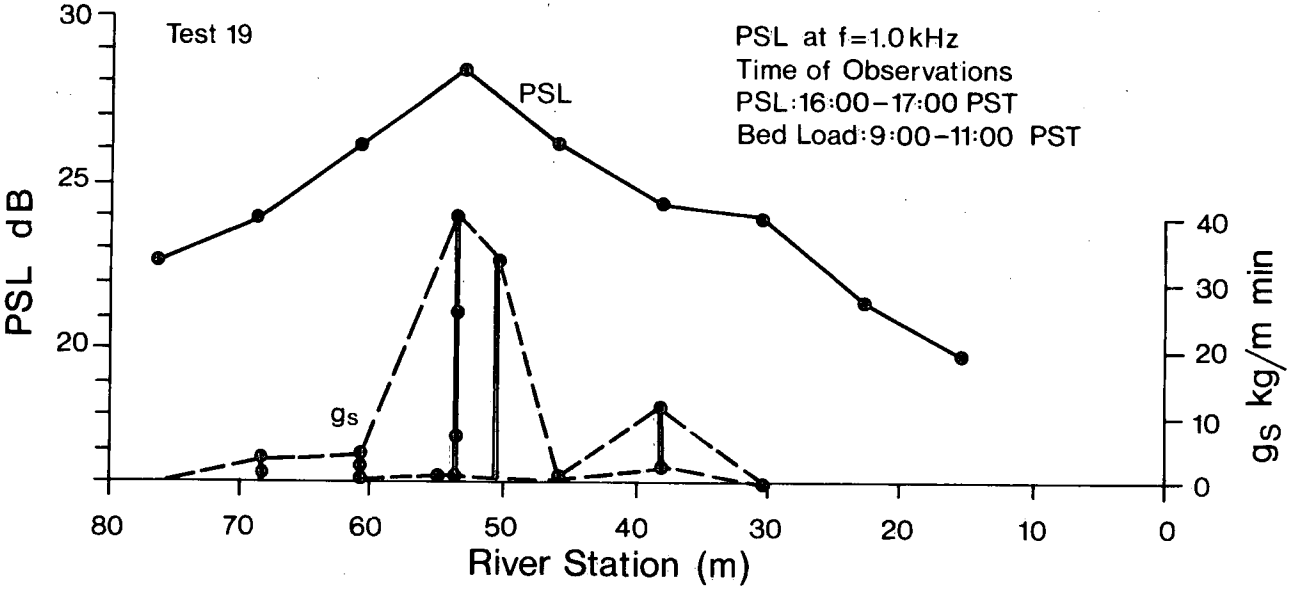

Figure 59. Bed-load transport and PSL distribution, Vedder site, test 19.

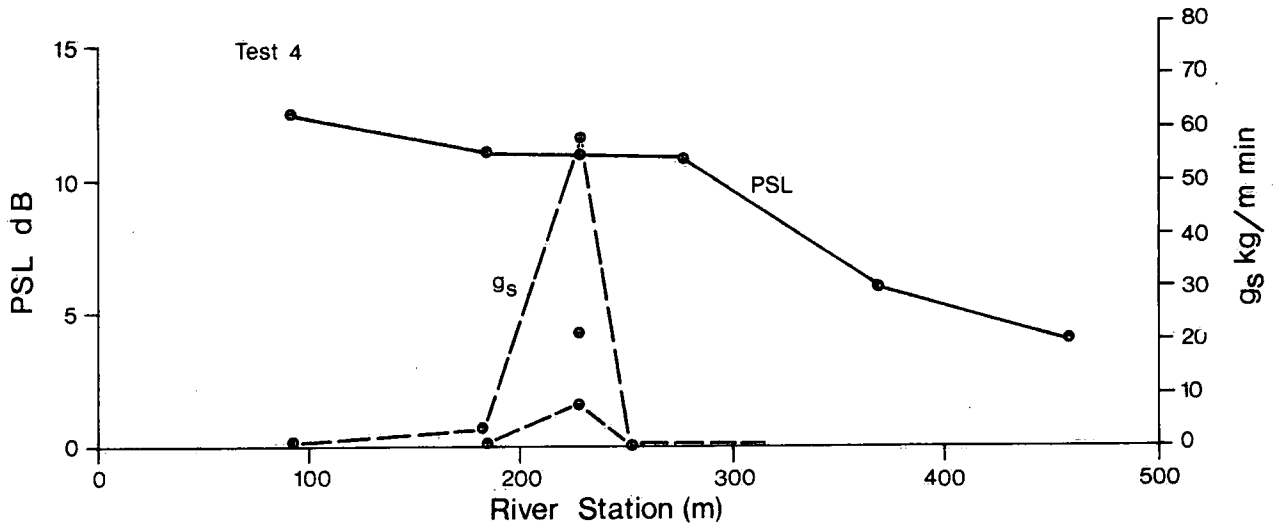

Figure 60. Bed-load transport and PSL distribution, Fraser site, test 4.

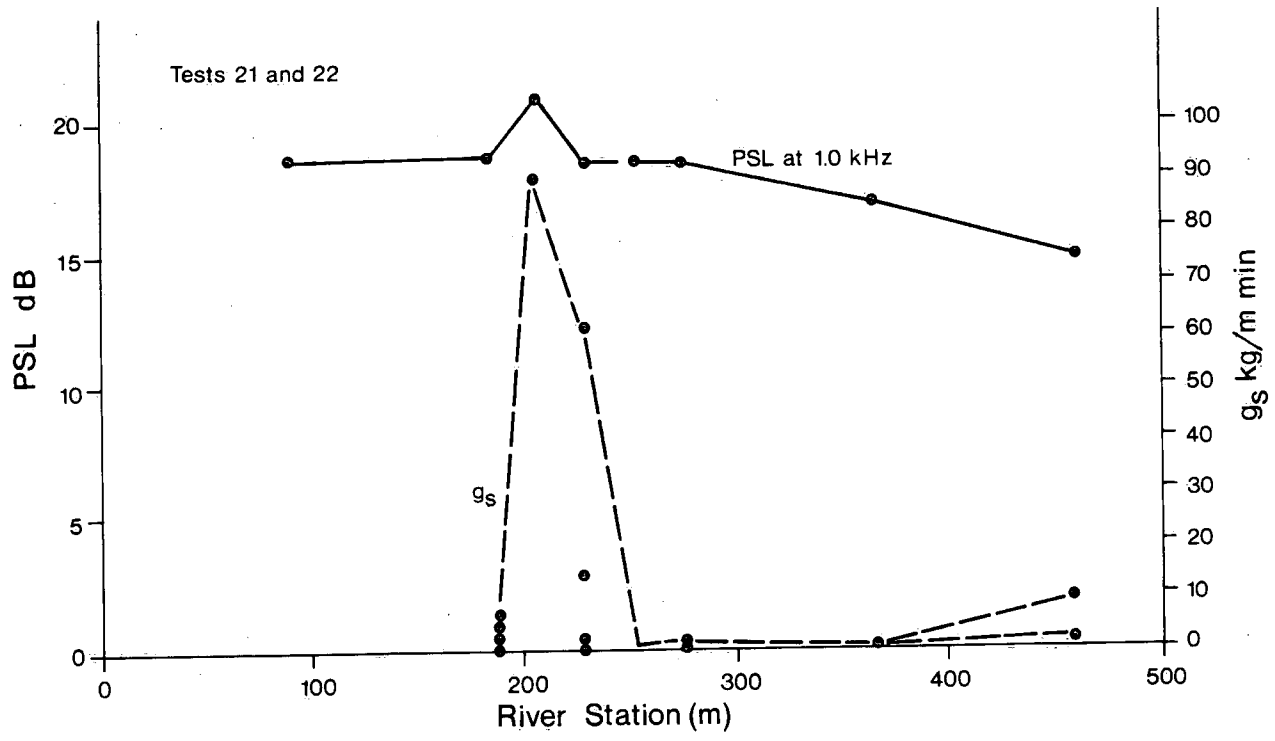

Figure 61. Bed-load transport and PSL distribution, Fraser site, tests 21 and 22.

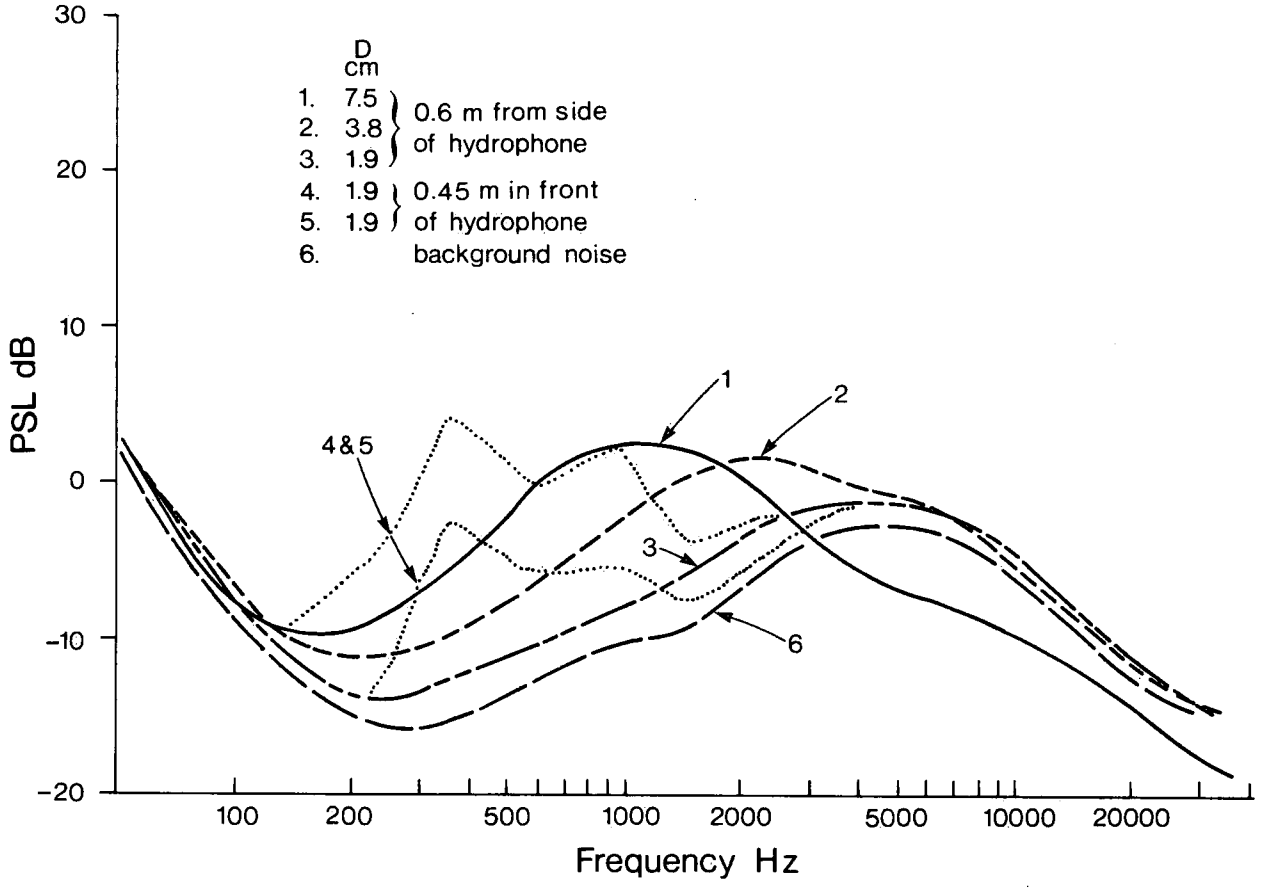

Figure 62. Frequency spectrograph owing to different pebble sizes.

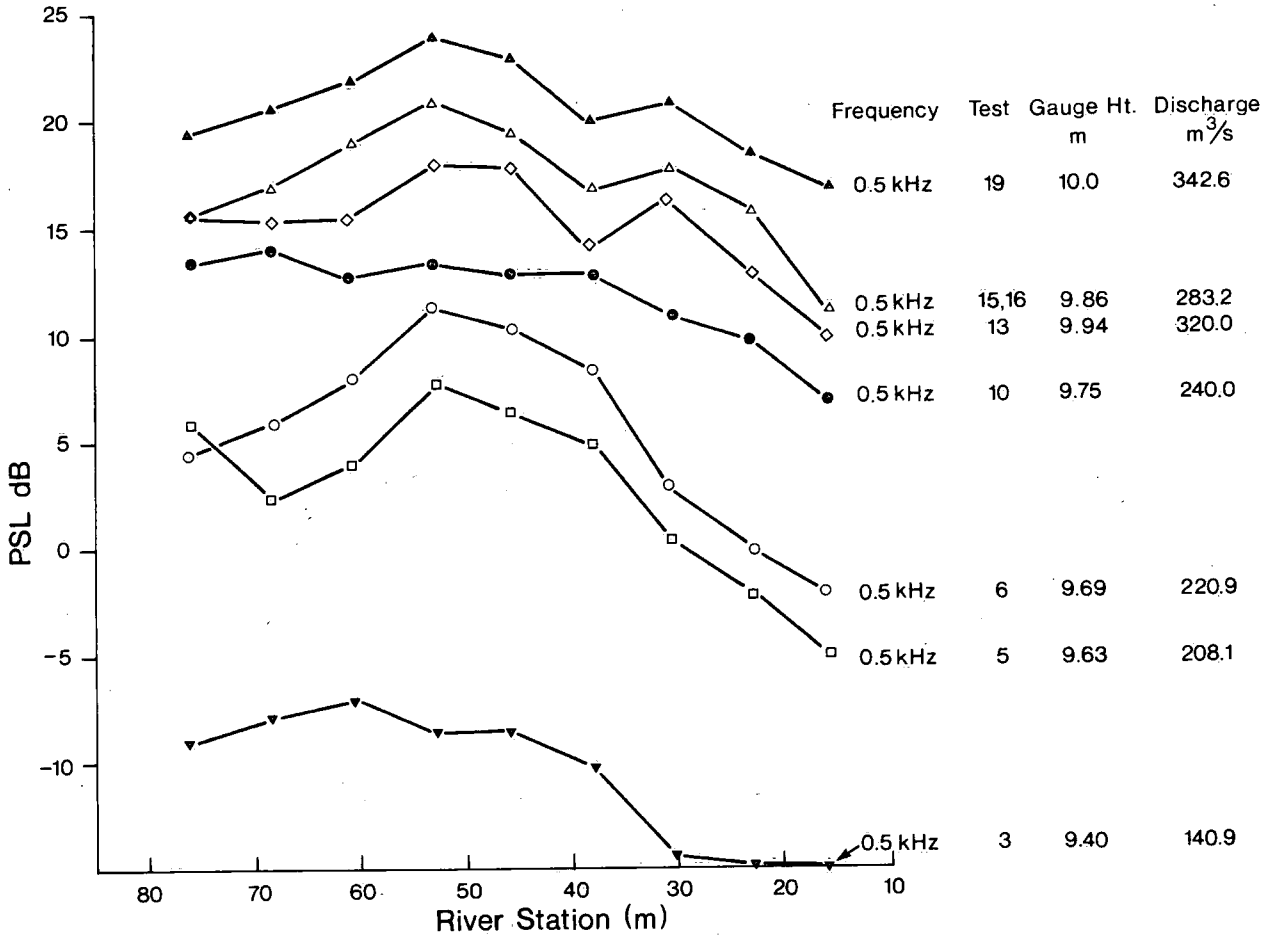

Figure 63. PSL distribution at 0.5 kHz along Vedder site cross section.

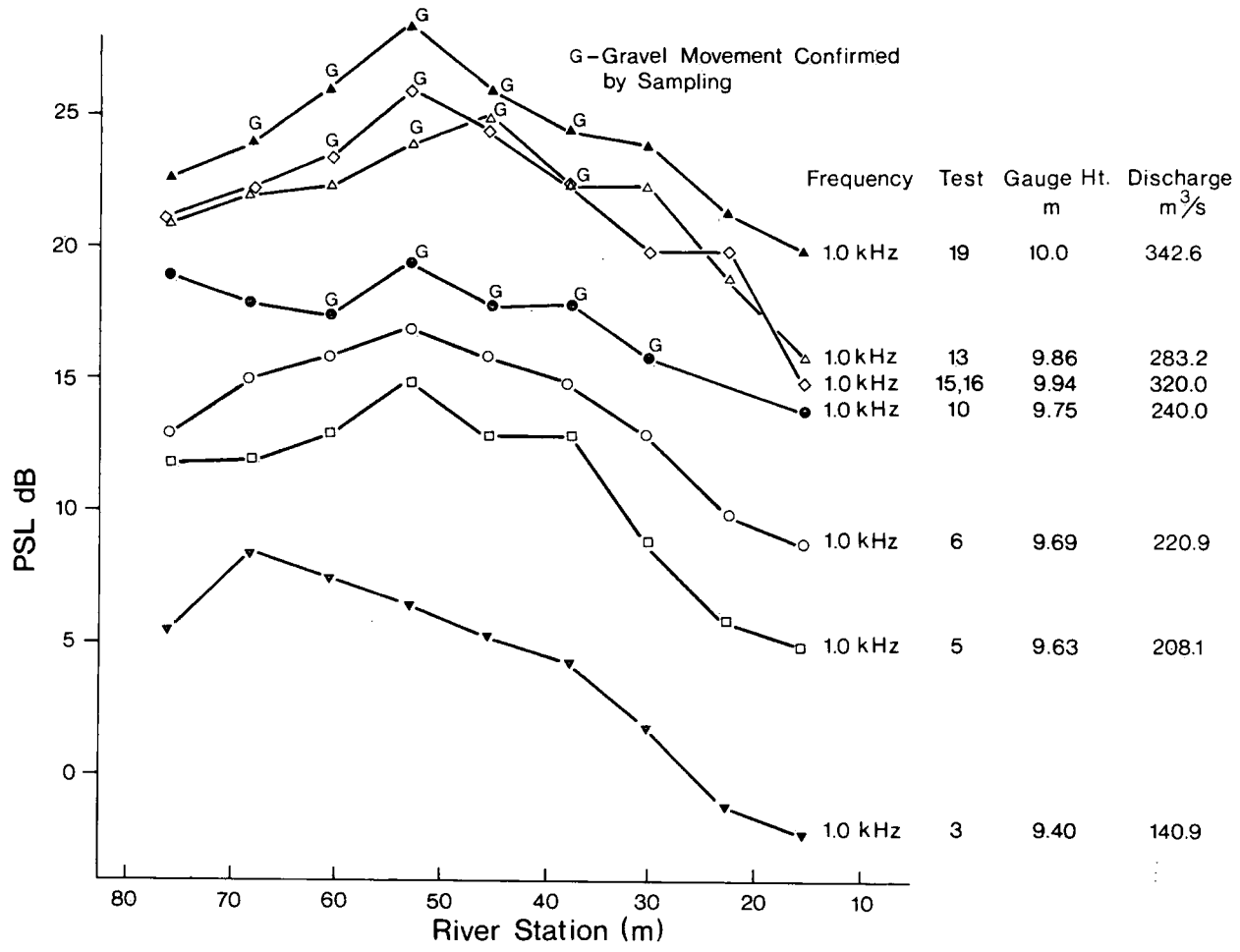

Figure 64. PSL distribution at 1.0 kHz along Vedder site cross section.

Appendix A

Ithaco Hydrophone System Information

Ithaco Hydrophone System Information

ITHACO SYSTEM COMPONENTS AND USAGE MODES

The following is a list of Ithaco system components and usage modes:

a) Ithaco 605M101 hydrophone with preamplifier (manufacturer's quoted sensitivity of -64 dB re 1 V/μbar attenuated by sensor placement in hollow of lead body by 16 dB),
b) Ithaco 411M102 variable bandpass filter,
c) Ithaco 3161 logarithmic amplifier,
d) Ithaco 450R power supply,
e) Esterline Angus T171B graphic recorder, and
f) Uher 4400 tape recorder.

Data acquisition and analysis modes are illustrated in Figures A-1 and A-2. The measured voltage relationships with sound pressure level are explained in Figure A-3.

UHER TAPE RECORDER PERFORMANCE

Performance Tests

Objective: To determine playback reproducibility of controlled input signals.

Procedure: A series of rms voltage signals (e_t) were generated at various frequencies corresponding to one-octave or one-third octave mid-band frequencies, passed through wide-band filter with high and low cutoff frequencies set at 50 Hz and 10 kHz and recorded on Uher tape recorder. (The recording schematic is illustrated in Figure A-4.) The signal was also processed through the log amplifier to obtain output signal level in decibels on the chart recorder. The recorded signal was played back through the Ithaco filter and log amplifier and was filtered through one-octave or one-third octave passbands. (The playback schematic is shown in Figure A-5.)

Results: Results are given in Figures A-6 and A-7. The playback signal values at each frequency represent signal values obtained through the one-octave or one-third octave filters centred on the frequencies of the original signal.

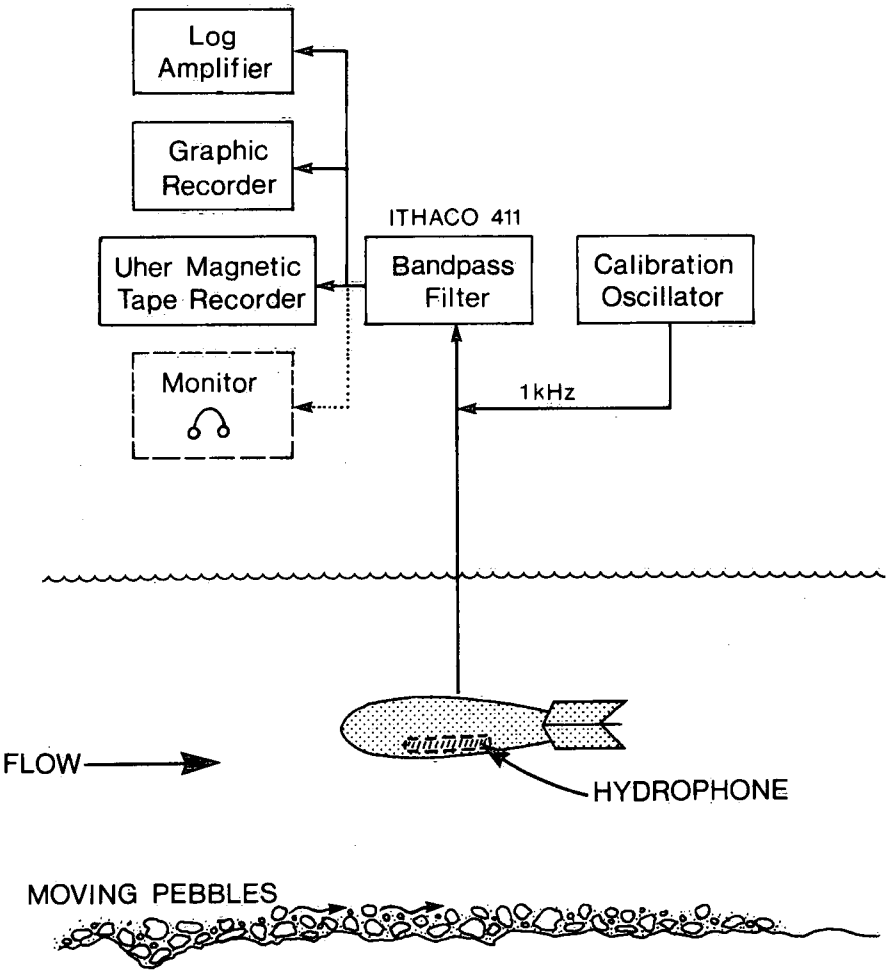

Figure A-1. Ithaco system data acquisition mode.

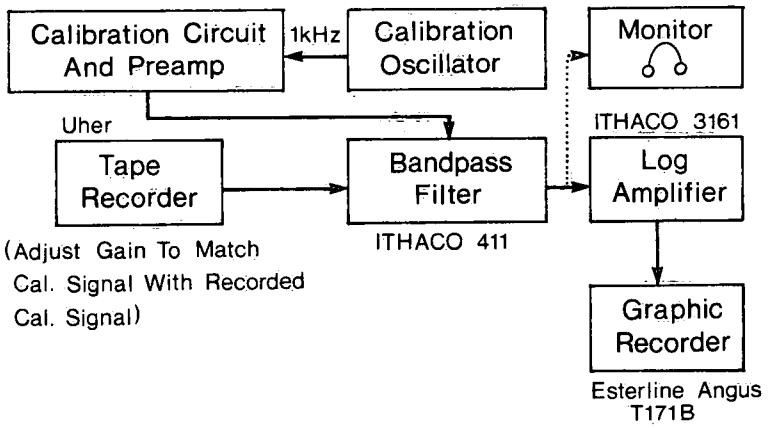

Figure A-2. Ithaco system data analysis mode.

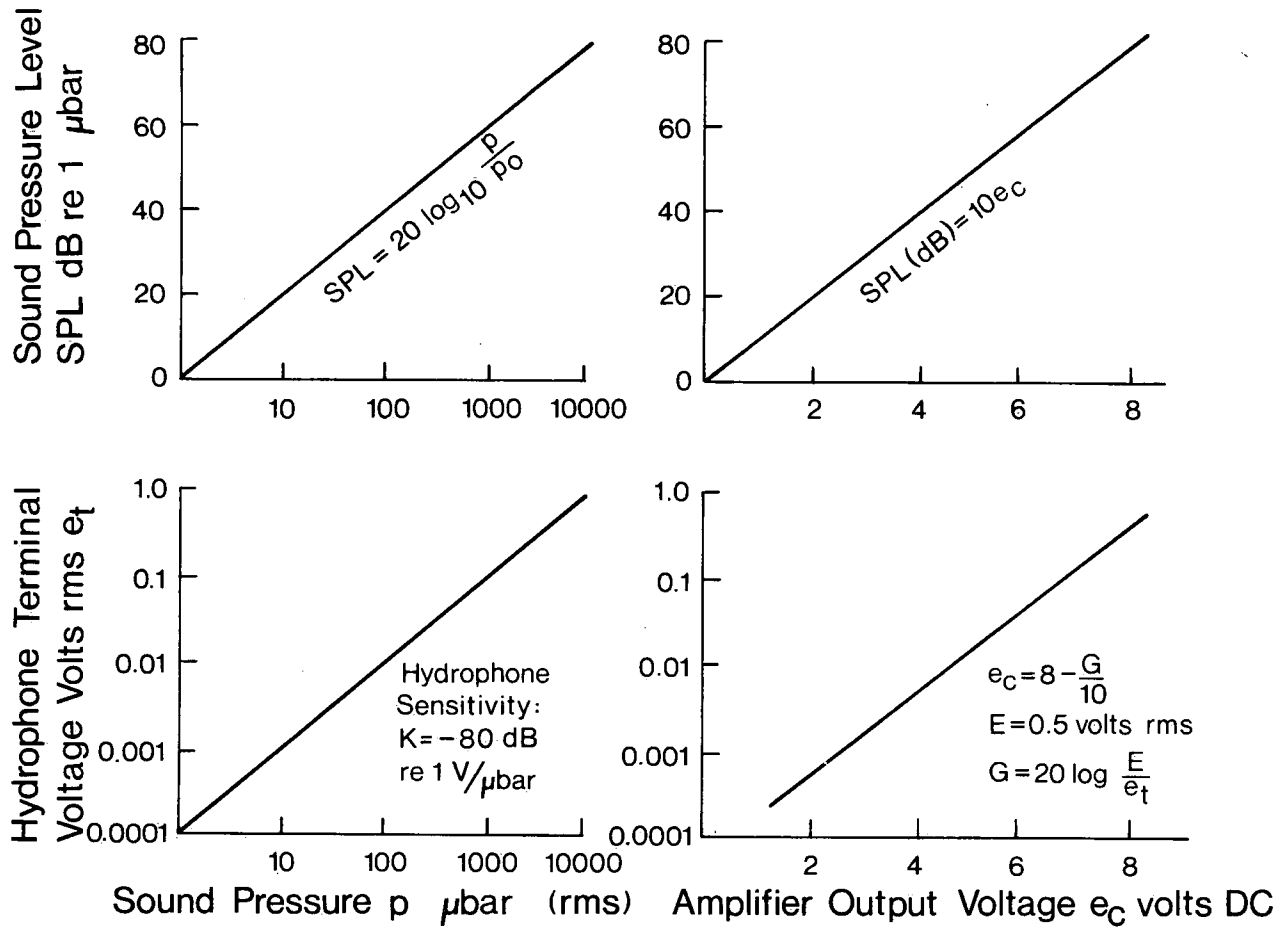

Figure A-3. Voltage relationships with sound pressure level.

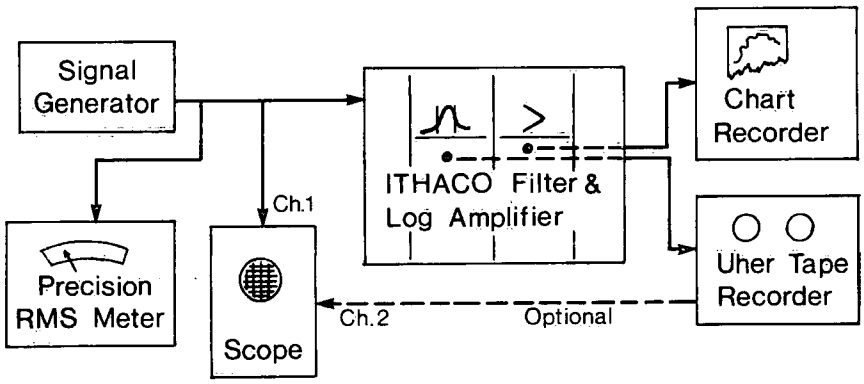

Figure A-4. Test recording mode.

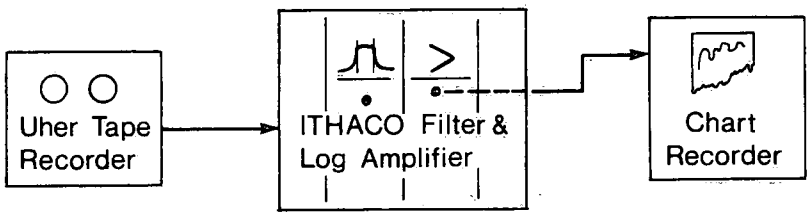

Figure A-5. Test playback mode.

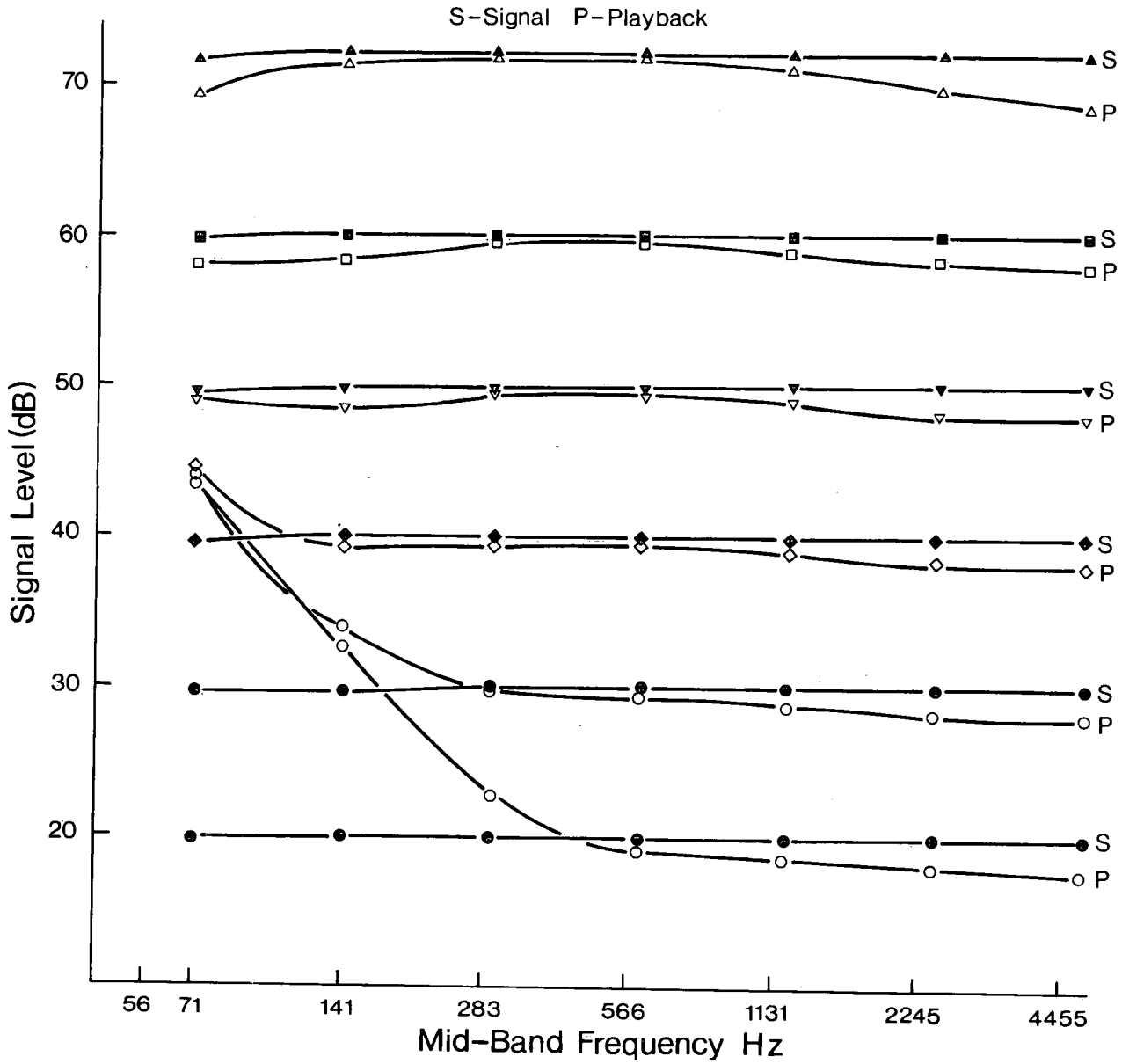

Figure A-6. Uher tape recorder playback performance (one-octave passbands).

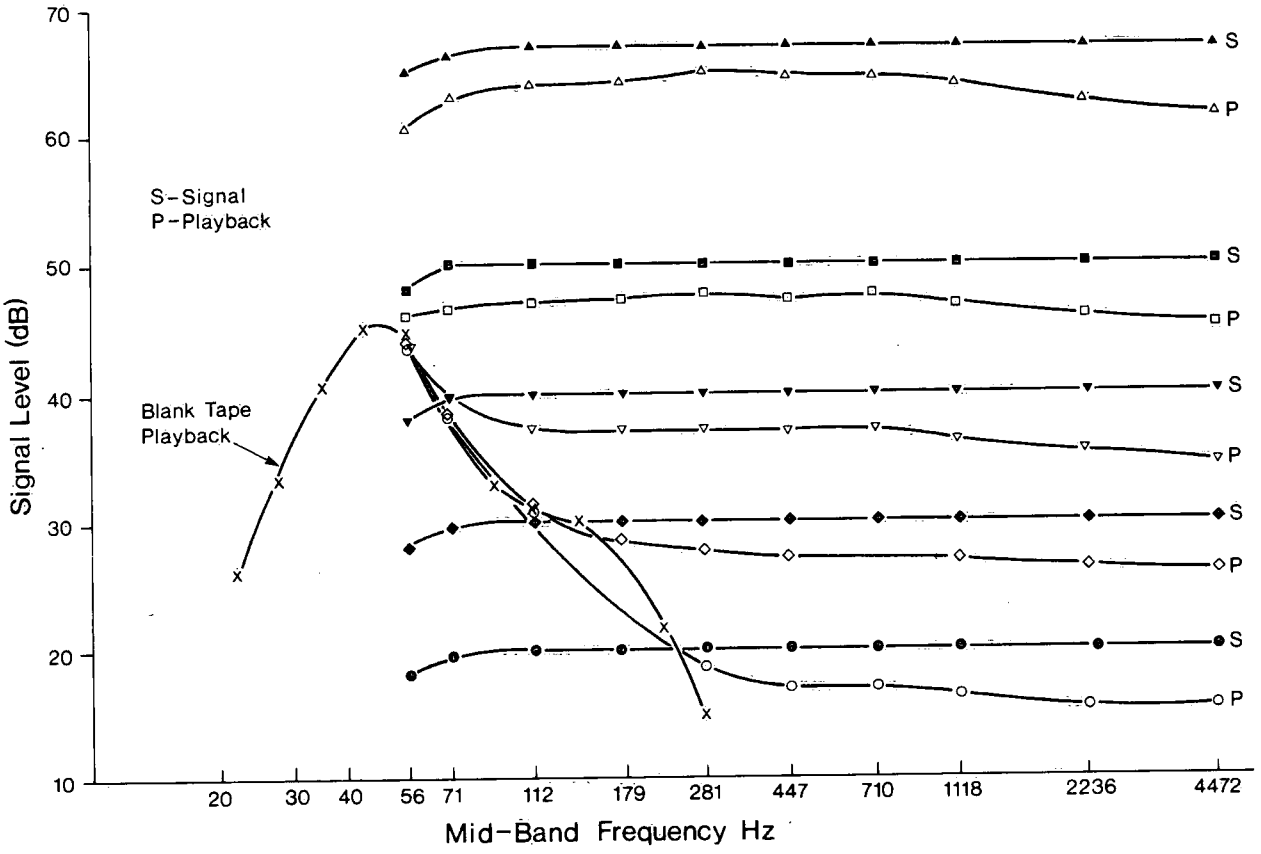

Figure A-7. Uher tape recorder playback performance (one-third octave passbands).

Appendix B

Bed-Load Measurement Data

Table B-1. Basket Sampler Data, Vedder River, 1974

Station (m)	June 3 Time (PST)	June 3 g_s (kg/m min)	June 4 Time (PST)	June 4 g_s (kg/m min)	June 12 Time (PST)	June 12 g_s (kg/m min)	June 13 Time (PST)	June 13 g_s (kg/m min)	June 14 Time (PST)	June 14 g_s (kg/m min)	June 15 Time (PST)	June 15 g_s (kg/m min)
15.24			9:32	0	9:17	0					11:10	0
22.86	9:00	0	8:45		9:12	0	9:37	0			11:05	0
30.48	9:10	0	9:55	trace	7:00	0.23	9:30	0			11:00	0
			10:03	trace	7:07	3.71						
					7:15	0.74						
38.10	9:18	0	10:11	0.60	7:23	0.45	8:48	2.67				
			10:19	trace	7:31	0.59	8:56	0.15			10:52	11.52
							9:22	1.78			10:56	2.97
42.67							9:03	14.11				
							9:08	0.25				
							9:15	1.24				
45.72	9:37	trace	10:28	0.60	7:39	0.15	8:13	2.72	12:47	0.37	10:15	0.59
	9:45	trace	10:36	0	7:56	1.04	8:17	1.19	12:50	0	10:26	0
					8:03	0.59						
48.76							8:22	0			10:33	0.25
							8:40	0			10:38	33.19
											10:46	0.13
53.34	9:54	3.27	10:43	0	8:03	1.48	7:47	30.84	10:05	1.85	8:50	40.13
	10:13	0	10:51	trace	8:10	2.97	7:52	14.86	10:15	17.33	9:05	26.00
	10:20	0			8:17	9.20	7:59	17.83	10:20	0.37	9:09	3.47
									10:25	0.13		
					8:32	9.66	8:06	0.25				
					8:40	1.48						
60.96	10:28	0	10:59	0	8:25	0	7:32	trace	10:37	5.05	9:14	0
					8:49	0.22	7:40	0.54	10:45	0.59	9:20	2.97
											9:25	3.47
68.58	10:38	0	11:08	2.67	8:57	0	9:47	0			9:33	3.86
			11:31	trace							9:36	1.85
			11:39	0							9:50	0.01
76.20	10:46	0			9:30	0	9:55	0			9:57	0
Test	5		6		10, 11, 12		13, 14		15,16,17,18		19	

Table B-2. Basket Sampler Data, Fraser River, 1974

	May 30		June 19	
Station (m)	Time (PST)	g_s (kg/m min)	Time (PST)	g_s (kg/m min)
91.44	11:37	0.01		
	11:45	0.04		
182.88	11:50	0.00	13:27	4.59
	11:55	3.78	13:32	0.00
	12:00	0.00	13:38	0.60
			13:41	0.21
209.74			14:41	89.87
228.60	12:09	7.71	13:49	1.73
	12:19	58.67	13:49	61.30
	12:27	21.61	13:56	14.64
251.46			14.32	0.00
274.32	12:34	0.00	14.02	0.00
	12:37	0.00	14:07	1.21
369.76	12:45	0.00	14:13	0.00
			14:20	1.61
			14:27	9.08
457.20	12:50	0.00		